Two-Layer, Planar, Superconducting Multichip Module Technology

W. A. Luo, H. J. Yao, G. Zhang, F. T. Chan, S. S. Ang, W. D. Brown, G. J. Salamo, and J. W. Cooksey
High Density Electronics Center (HiDEC)
The University of Arkansas
Fayetteville, AR 72701, U.S.A.
Phone: 501-575-6045
Fax: 501-575-7967
wdb@engr.uark.edu

ABSTRACT

Given that the speed of integrated circuits (ICs) is projected to continue to increase at its present rate, the packaging of ICs may become a formidable task not too distant into the future. In fact, as circuit integration and IC switching speeds continue to increase, chip-to-chip interconnection becomes the limiting factor in realizing the system performance benefits of using faster ICs. Multichip modules (MCMs) offer a high performance alternative to conventional printed wiring boards (PWBs), and one of the more promising applications for high temperature superconductors (HTSCs) is as signal interconnects between bare ICs in MCMs. We report on the successful development and fabrication of a superconducting MCM packaging technology using a novel yttrium-barium-copper-oxide (YBCO)/yttrium-stabilized zirconia (YSZ)/silicon dioxide (SiO_2)/yttrium-stabilized zirconia (YSZ)/yttrium-barium-copper-oxide (YBCO) multilayer substrate using either a chemical-mechanical planarization technique or a conventional lift-off process on a single-crystal YSZ substrate. To reduce the complexity of the processing required, the two-layer Interconnected Mesh Power System (IMPS) MCM topology was used. For demonstration purposes, a 100 MHZ ring oscillator multichip module using gallium arsenide technology was successfully fabricated.

Key Words: multichip module, high-temperature superconductor

Introduction

One of the fundamental challenges to reducing the linewidth of interconnects in both integrated circuits (ICs) and multichip modules (MCMs) is the resulting increase in parasitic resistance. The increased parasitic resistance increases the propagation delay of signals traveling along the interconnect. High-temperature superconductors offer an attractive solution to this parasitic resistance problem since they exhibit a negligible resistance when operated in their superconducting state. Consequently, the propagation delay of signals is reduced significantly. Furthermore, high interconnect bandwidths (up to 100 GHz) are possible without sacrificing packaging density. Other advantages of superconducting interconnects are that faster device switching and lower voltage operation for CMOS and GaAs are possible when operating at the liquid nitrogen temperature of 77K. The liquid nitrogen operating environment also reduces heat dissipation problems and increases MCM reliability. In this paper, we report on two approaches to the successful fabrication of a superconducting MCM using a novel yttrium-barium-copper-oxide (YBCO)/yttrium-stabilized zirconia (YSZ)/silicon dioxide (SiO_2)/yttrium-stabilized zirconia (YSZ)/yttrium-barium-copper-oxide (YBCO) multilayer substrate. A chemical-mechanical planarization technique, as well as a conventional lift-off process, were used to fabricate superconducting MCMs on a single-crystal YSZ substrate.

Device Design and Fabrication

Typically, conventional MCM-D technologies require at least a four-layer metallization system to provide power, ground, and signal distribution for the ICs they contain [1]. However, it is very difficult to fabricate more than two layers of superconducting interconnects on a substrate due to the necessity for maintaining critical structural alignment of the superconducting thin film in a multilayer structure. The surface onto which the superconductor is deposited must be planar since any

Effect of Planarization of the Bottom Superconducting Yttrium-Barium-Copper-Oxide Layer in the Multilayer Structure

W. A. Luo, H. J. Yao, S. Afonso, S. J. Qin*, S. H. Yoo, S. Ang,
W. D. Brown, G. J. Salamo, and F. T. Chan
University of Arkansas, Fayetteville, AR 72701

ABSTRACT — **YBCO/YSZ/SiO_2/YSZ/YBCO multi-layer structures have been successfully grown on single crystal YSZ substrates. The YBCO superconducting layers (300 nm thick) were deposited using pulsed laser deposition (PLD). The YSZ layers (300 nm thick) which are biaxially aligned were deposited using PLD and the ion beam assisted deposition (IBAD). A thick silicon dioxide layer (2-4 microns) was sandwiched between the YSZ layers to meet the low dielectric constant requirement for multi-chip module applications. However, if the bottom superconducting layer was patterned into interconnecting lines as required in device applications, the surface of the YSZ/SiO_2/YSZ on top of the patterned bottom superconducting layer had a roughness of about 500 nm. As a result, the top YBCO was no longer superconducting. Thus, planarization of the patterned bottom superconducting layer becomes a key issue. We have developed a "fill-in and lift-off" process to fill the gap between the patterned bottom superconducting lines with YSZ. As a result, we were able to reduce the surface roughness of the bottom YBCO layer to about 10 nm so the top layer was superconducting with a critical temperature of 87 K.**

I. Introduction

One potential application of high temperature superconducting (HTS) films is for signal interconnects between integrated circuit chips on a multi-chip module (MCM) substrate. A typical HTS MCM needs at least four layers: power plane, ground plane, and two or more signal planes [1]. Using a new approach, called the Interconnected Mesh Power System (IMPS) [2], a superconducting MCM can be realized with only two superconducting layers. This reduction makes the IMPS approach to fabricating a superconducting MCM very attractive since it significantly reduces material and technological demands as well as cost. Even with only two superconducting layers required, however, several problems have prevented the realization of a practical MCM. For example, using Yttrium-Barium-Copper-Oxide (YBCO) as the superconducting material, S. Afonso et al. have successfully fabricated YBCO/YSZ/SiO_2/YSZ/YBCO multi- layer structures [3]. In order to keep the distributed capacitance low, a thick SiO_2 layer (1-2μm) whose dielectric constant is less than four was chosen to isolate the two superconducting interconnects, and two biaxially aligned Yttrium Stabilized Zirconia (YSZ) layers were deposited on top and underneath the SiO_2 as buffer layers to prevent diffusion of the amorphous SiO_2 into the YBCO layers. However, when the bottom YBCO layer is patterned into interconnecting lines, the surface of the YSZ/SiO_2/YSZ is no longer flat. The roughness of the surface is usually greater than the thickness of the bottom YBCO layer due to over etching in the patterning process. Since the top YBCO layer is found not to be superconducting when fabricated on a rough surface, the planarization of such a rough surface becomes a key issue. In this paper we report on a "fill-in and lift-off" planarization procedure and the effect of planarization of the bottom superconducting YBCO layer on the performance of the top YBCO layer superconducting layer in the multi-layer structure.

Manuscript received September 15, 1998.
This work was supported in part by DARPA (Contract No. 972-93-I-0036) through HiDEC at the University of Arkansas, U.S. Army research Office DAAH04-96-1-0455, and NSF DMR 9318946.

*Permanent address: Guizhou University, Guiyang 550025, P. R. China. Work partially supported by the Science and Technology Council of Guizhou Province, P. R. China.

II. Experimental Details and Results

A. Patterned Multilayer Structure

We fabricated a YBCO/YSZ/SiO_2/YSZ/YBCO/YSZ (substrate) multi-layer structure via a procedure described in [3]. Both the top and bottom YBCO layers were patterned into meander lines which were 19 cm long. The line widths of the bottom and top YBCO interconnect lines were 20μm and 30μm, respectively, as shown in Fig. 1. The resistance

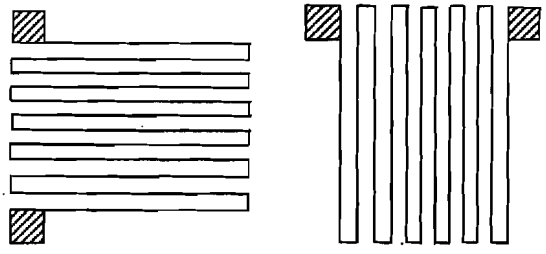

(a) Bottom YBCO pattern (b) Top YBCO pattern

Fig. 1. Schematic diagram of the meander line patterns in YBCO/YSZ/SiO_2/YSZ/YBCO multi-layers: (a) bottom YBCO; (b) top YBCO. (The diagram is not drawn to scale, line widths in (a) and (b) are 20μm and 30μm respectively, each 19 cm long).

ELSEVIER

19 October 1998

PHYSICS LETTERS A

Physics Letters A 247 (1998) 267–272

Normally ordered unitary operator for multimode squeezed fermion states

Hong-yi Fan [a,b,1], Yue Fan [c], F.T. Chan [c]

[a] *China Center of Advanced Science and Technology (World Laboratory), P.O. Box 8730, Beijing 100080, China*

[b] *Department of Material Science and Engineering, University of Science and Technology of China, Hefei, Anhui 230026, China* [2]

[c] *Department of Physics, University of Arkansas, Fayetteville, AR 72701, USA*

Received 30 April 1998; accepted for publication 12 August 1998

Communicated by P.R. Holland

Abstract

We derive normally ordered unitary operators for generalizing multimode squeezed fermion states. The operators are considered as images corresponding to a pseudo-classical Grassmann numbers' $SO(2n)$ orthogonal transformation in the n-mode fermionic coherent state representation. The derivation can be facilitated by the newly developed technique of integration within an ordered product of operators for the fermionic system. © 1998 Elsevier Science B.V.

1. Introduction

Recently, squeezed photon states have attracted much attention of physicists due to their potential use in optical communication and interferometer measurements [1]. Contrary to the general expectation that Fermi–Dirac statistics limit fermion clustering behaviour to that of antibunching, the characteristic features of fermionic squeezing were predicted [2,3] and squeezed fermion states have been introduced [4]. Formally, a general n-mode fermion squeezing is presented by a unitary transformation of the field operators,

$$f_i \to L_{ij}(s) f_j - K_{ij}(s) f_j^\dagger , \tag{1.1}$$

where s stands for the squeezing parameters (repeated indices in a term imply summation), and the L and K satisfy

$$LL^\dagger + KK^\dagger = I_n , \qquad L\tilde{K} + K\tilde{L} = 0 \tag{1.2}$$

[1] E-mail: fhym@dmse.mse.ustc.edu.cn.

[2] Mailing address.

PII S0375-9601(98)00621-5

ELSEVIER

Physica C 280 (1997) 17–20

PHYSICA C

$Tl_2Ba_2CaCu_2O_y$ superconducting thin films on polycrystalline Al_2O_3 substrates with textured YSZ buffer layers

Q. Xiong *, S. Afonso, K.Y. Chen, G. Salamo, F.T. Chan

Department of Physics / High Density Electronics Center, University of Arkansas, Fayetteville, AR 72701, USA

Received 19 November 1996; revised 11 April 1997; accepted 15 April 1997

Abstract

We report for the first time the successful fabrication of $Tl_2Ba_2CaCu_2O_y$ superconducting thin films on polycrystalline Al_2O_3 substrates using yttria-stabilized-zirconia (YSZ) buffer layers. Ion beam-assisted laser deposition was used to obtain the textured YSZ buffer layers. The $Tl_2Ba_2CaCu_2O_y$ thin films were shiny, highly *c*-axis oriented with respect to the film surface and strongly in plane textured. The zero resistance temperature of these films was as high as 108 K with a critical current density of $\sim 10^5$ A/cm^2 at 77 K. © 1997 Elsevier Science B.V.

PACS: 74.76.Bz; 74.72.Fq
Keywords: $Tl_2Ba_2CaCu_2O_y$ thin film; Ion beam-assisted deposition

1. Introduction

Since the discovery of high temperature superconductors (HTS), many possible applications of HTS thin films have been conceived and demonstrated. Space communications, radar and microwave filters for both the current cellular and tomorrow's PCS communications systems would each benefit from the use of HTS thin films. One of the biggest impediments to the application of HTS is that HTS carry only a limited amount of current without resistance. This problem arises from their two-dimensional layered structure. According to earlier studies [1,2], if the layers do not line up properly, the critical current density will decrease dramatically in the misaligned region. One way to overcome this problem is by growing epitaxially, micron-thin layers of the material on well organized substrates. The process has the effect of lining up the superconducting layers more accurately. For example, HTS thin films grown on single crystal $LaAlO_3$ [3–5] or $SrTiO_3$ [6] substrates have a good lattice match between the HTS and the substrates and have a correspondingly critical current density of about $\sim 10^6$ A/cm^2. In fact, the current density is large enough for most HTS thin film applications. While this effort is impressive, it is far from useful. The single crystal substrates are both expensive and extremely difficult to make with the large surface area required. One challenge to HTS thin film growth research is to find new substrates that can be produced in adequate size at lower cost. Recent studies [7–12] have shown that a highly bi-axially aligned YSZ layer can be grown on inexpensive non-crystalline substrates, and that the YSZ-layer can then act as a template for HTS

* Corresponding author. Tel.: +1 501 5754313; fax +1501 5754580.

PII S0921-4534(97)00169-X

ELSEVIER

Physica C 282-287 (1997) 683-684

PHYSICA C

Fabrication and characterization of vias for contacting $YBa_2Cu_3O_{7-x}$ multilayers

J. W. Cooksey, S. Afonso, W. D. Brown, L. W. Schaper, S. S. Ang, R. K. Ulrich, G. J. Salamo, and F. T. Chan

High Density Electronics Center, University of Arkansas, 600 W. 20th Street, Fayetteville, AR 72701 USA

In order to connect multiple layers of high temperature superconductor (HTS) interconnects, low contact resistance vias must be used to maintain high signal propagation speeds and to minimize signal losses. In this work, 40 μm via contacts through $YBa_2Cu_3O_{7-x}$ /$SrTiO_3$/SiO_2/YSZ/$YBa_2Cu_3O_{7-x}$ multilayers utilizing dry etching techniques and sputter deposited Au for contacting through the vias have been successfully fabricated and characterized. The vias connect two laser ablated $YBa_2Cu_3O_{7-x}$ (YBCO) signal lines through thick (4-5 μm) SiO_2 insulating layers. This approach to making multilayer superconductor vias provides a low resistance contact between the YBCO layers while maintaining space efficiency and fabrication compatibility with the superconductor.

1. INTRODUCTION

Since the discovery of high temperature superconductivity (HTS), researchers have utilized their low resistance behavior in many applications. One such application is that of multichip modules (MCMs.) Unlike that of VLSI technologies where smaller feature sizes in successive generations allow interconnect lengths and power dissipation to be reduced, MCMs will not have that same luxury. As the complexity of ICs advances, pinout count per IC increases, and operating frequencies increase, MCM normal metal interconnections will have to grow in length and will not be allowed to reduce in cross-sectional area. On MCM-D substrates, typical copper or aluminum interconnection dimensions are about 2 to 5 μm in thickness and between 15 and 30 μm wide with corresponding via sizes. By cooling the metal to 77 K (liquid nitrogen temperature), the resistivity of copper decreases by a factor of about 7 which allows a corresponding decrease in the interconnect's cross-sectional area. In order to increase the wiring density beyond that of cryo-cooled MCMs and improve the chip-to-chip bottleneck at high frequencies, alternatives to conventional metal interconnects must be considered [1].

HTS interconnections, with negligible resistivity at operating frequencies of several tens of GHz and lower, have great potential to reduce an interconnect's cross-sectional area with typical thicknesses of less than 1 μm and widths of less than 2 μm for MCM applications with similar spacings. The main challenge for attaining multiple layers of high density, high performance HTS interconnects appears to be in fabricating compact, low resistance vias.

The work presented here focuses on this problem and describes a method of fabricating noble metal vias for use in an HTS MCM prototype.

2. EXPERIMENTAL DETAILS AND RESULTS

A cross-section of our multilayer YBCO structure utilizing Au vias is shown in Figure 1.

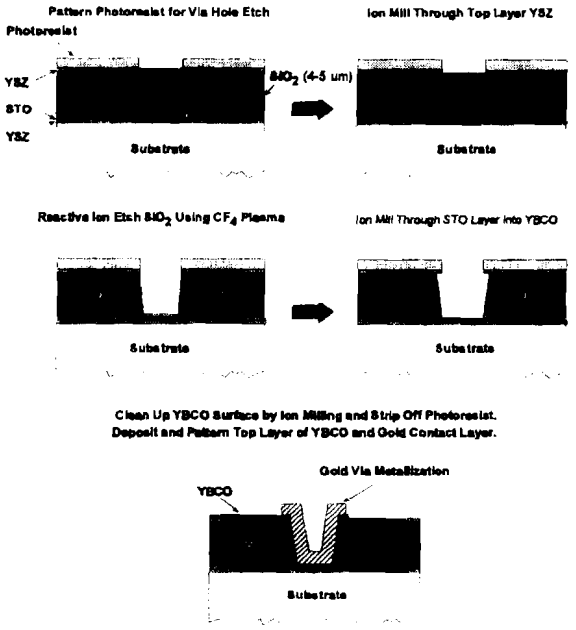

Figure 1. HTS via process.

PII S0921-4534(97)00495-4

ELSEVIER

Physica C 282-287 (1997) 613-614

PHYSICA C

Improvement of in-plane alignment of $YBa_2Cu_3O_{7-x}$ films on polycrystalline alumina substrates using biaxially aligned CeO_2/YSZ buffer layers

K. Y. Chen, S. Afonso, Q. Xiong, G. J. Salamo, and F. T. Chan

Department of Physics/High Density Electronics Center, University of Arkansas, Fayetteville, AR 72701, USA

Biaxially aligned superconducting $YBa_2Cu_3O_{7-x}$ thin films have been fabricated on ceramic alumina substrates. Yttria-stabilized zirconia buffer layers were first deposited on alumina using ion-beam assisted pulsed laser deposition. CeO_2 and YBCO films were subsequently deposited on the YSZ layer using pulsed laser deposition (PLD). All three layers were (001) oriented and biaxially textured. The YBCO films have T_c values of 89 K and J_c of $1x10^6$ A/cm^2 at 77 K.

1. INTRODUCTION

The successful deposition of biaxially aligned $YBa_2Cu_3O_{7-x}$ (YBCO) films on polycrystalline metal alloy substrates [1-2] has prompted an interest in polycrystalline or amorphous dielectric substrates such as glass [3] and alumina. Polycrystalline ceramic alumina (Al_2O_3) has a dielectric constant and loss tangent lower than that of most single-crystal substrates suitable for YBCO film growth. This dielectric property is desirable for high frequency applications. The use of ceramic alumina also brings the advantages of isotropic dielectric properties, as well as lower cost. In this paper, we report the preparation of YBCO films on polycrystalline alumina substrates with biaxially aligned CeO_2/YSZ buffer layers.

2. EXPERIMENTS

Biaxially aligned (001) YSZ films were first deposited on one side polished alumina substrates (Superstrate®996, Coors) using ion-beam assisted pulsed laser deposition. Deposition conditions have been given elsewhere [3]. In brief, about 5000-Å-thick YSZ films were deposited at room temperature in $3x10^{-4}$ Torr oxygen partial pressure. An argon ion beam bombarded the substrate at an incident angle of 55° from the substrate normal, while a 193 nm excimer laser ablated a YSZ target.

It was observed that a thin CeO_2 layer (<1000 Å) can eliminate ϕ =0° and $\phi \sim \pm 9°$ grains for the *c*-axis oriented YBCO films on YSZ substrates, and can thus improve the in-plane alignment of YBCO on YSZ [4]. In this study, we deposited a relatively thick CeO_2 layer (1000 ~ 4000 Å) as the second buffer layer. Finally, YBCO films (3000 ~ 4000 Å) were deposited on CeO_2/YSZ/alumina. Both CeO_2 and YBCO were deposited at an O_2 pressure of 200 mTorr and substrate temperature of 750°C using PLD.

3. RESULTS

The YBCO films were highly *c*-axis oriented as shown in Fig. 1. XRD ϕ scans of YSZ (111), CeO_2 (111) and YBCO (103) peaks are shown in Fig. 2. The texture relationship is YBCO[110]∥CeO_2[100]∥YSZ[100]. It can be seen that the full width at half-maximum (FWHM) of CeO_2 peaks is smaller than the FWHM of YSZ peaks, and the FWHM of the YBCO ϕ scan is smaller than that of the CeO_2 ϕ scan. It has been pointed out by Iijima et al. [1] that during IBAD the in-plane alignment of the YSZ surface is gradually improved with the increasing thickness of YSZ layers. Therefore, films grown on the top of YSZ layers are expected

PII S0921-4534(97)00435-8

ELSEVIER

Physica C 282–287 (1997) 685–686

PHYSICA C

Fabrication techniques and electrical properties of $YBa_2Cu_3O_{7-x}$ multilayers with rf sputtered amorphous SiO_2 interlayers

[a]S. Afonso, [a]K. Y. Chen, [a]Q. Xiong, [a]F. T. Chan, [a]G. J. Salamo, [b]J. W. Cooksey, [b]S. Scott, [b]S. Ang, [b]W. D. Brown, and [b]L. W. Schaper.

[a]Department of Physics and [b]Department of Electrical Enginneering/High Density Electronics Center, University of Arkansas, Fayetteville, AR 72701, USA

We have successfully fabricated $YBa_2Cu_3O_{7-x}$/YSZ/SiO_2/YSZ/$YBa_2Cu_3O_{7-x}$ multilayer structures on single crystal $LaAlO_3$ (100), substrates. The $YBa_2Cu_3O_{7-x}$(YBCO) layers were deposited using pulsed laser ablation (PLD), the biaxially aligned YSZ (250 nm thick) layers were deposited using ion beam assisted PLD (IBAD-PLD), and an amorphous SiO_2 (1-2μm) layer fabricated via rf sputtering was sandwiched between the YSZ layers. Fabrication techniques and characterization results are reported for patterned layers in this work.

1. INTRODUCTION

For high temperature superconductor multichip module(HTS-MCM) applications the basic building block is the HTS/Insulator (thickness >1μm)/HTS structure. A HTS-MCM can be defined as a miniaturized version of a multilayered printed wiring board with superconducting interconnects. Previously such a HTS-MCM prototype using a YBCO/$SrTiO_3$(500nm)/YBCO has been successfully fabricated by Burns et al [1]. Recently the use of ion beam assisted deposition to deposit biaxially aligned YSZ buffer layers on polycrystalline or amorphous substrates allowed for good quality YBCO films on these substrates [2-5]. Reade et al [6] were able to demonstrate using the ion beam assisted pulsed deposition (IBAD-PLD) technique that it was possible to fabricate the YBCO/YSZ-/amorphousYSZ(5μm)/YSZ/YBCO multilayers on oriented YSZ substrates with the top YBCO T_c ~ 87 K. They also fabricated the same structure using amorphous SiO_2, but cracks in the top YBCO layer did not permit electrical measurements of the top layer. The main advantage of SiO_2 is its low dielectric constant (~ 3.89), which makes it an ideal insulator material for MCMs.

In this paper we briefly describe the method to fabricate and the results obtained from the characterization of the YBCO/YSZ-/SiO_2/YSZ/YBCO multilayers.

2. EXPERIMENTS

The first YBCO layer (300nm thick) was fabricated by pulsed laser deposition using standard conditions. After patterning, part of the pads were masked to allow for transport measurements later. Next a 250 nm thick YSZ layer was deposited via IBAD PLD using conditions described in [5]. After this a 1-2 μm thick SiO_2 layer was deposited by reactively sputtering a Si target in oxygen ambient (the details of this process are described in [4]). Following the SiO_2 deposition another 250 nm thick biaxially aligned YSZ buffer/capping layer was deposited via IBAD PLD. Finally the masks were taken off and the top YBCO was deposited using the same conditions as the first YBCO except that the deposition temperature was kept ~ 20-30° lower. For the first set of multilayers the top YBCO layer was patterned into bridges over the underlying bridge patterns but shifted a little to the side so that the top bridge goes over step edges. The patterning was carried out by using photolithography and ion milling. For the second set of multilayers the top YBCO layer was patterned into

PII S0921-4534(97)00497-8

Magnetic field and temperature dependence of critical current densities in multilayer $YBa_2Cu_3O_{7-\delta}$ films

S. Afonso, F. T. Chan, K. Y. Chen, G. J. Salamo, Y. Q. Tang, R. C. Wang,[a] X. L. Xu,[b] and Q. Xiong
Physics Department/High Density Electronics Center, University of Arkansas, Fayetteville, Arkansas 72701

G. Florence, S. Scott, S. Ang, W. D. Brown, and L. W. Schaper
Electrical Engineering Department/High Density Electronics Center, University of Arkansas, Fayetteville, Arkansas 72701

In order to build high-temperature superconductor (HTS) multichip modules (MCMs), it is necessary to grow several epitaxial layers of YBCO that are separated by thick dielectric layers without seriously affecting the quality of the YBCO layers. In this work, we have successfully fabricated YBCO/YSZ/SiO_2/YSZ/YBCO structures on single-crystal $LaAlO_3$ substrates using a combination of pulsed laser deposition for the YBCO layers and ion-beam-assisted rf sputtering to obtain biaxially aligned YSZ intermediate layers. The bottom YBCO layer had a $T_c \sim 89$ K, $J_c \sim 7.2\times10^5$ A/cm^2 at 77 K, whereas the top YBCO layer had a $T_c \sim 86$ K, $J_c \sim 6\times10^5$ A/cm^2 at 77 K. The magnetic field and temperature dependence of J_c for the YBCO films in the multilayer have been obtained. The results for each of the YBCO layers within the YBCO/YSZ/SiO_2/YSZ/YBCO structure are quite similar to those for a good quality single-layer YBCO film. © *1996 American Institute of Physics.* [S0021-8979(96)03308-9]

I. INTRODUCTION

In electronic applications of high-temperature superconductor (HTS) thin films, the critical current density (J_c) is an important characteristic. One of the potential applications of high-temperature superconducting films is as electronic interconnects on a multichip module (MCM).[1] Since there are a minimum of two HTS thin films, separated by thick dielectric layers required, in HTS multichip modules (MCMs), it is necessary to know if the quality of the HTS layers is still maintained after the entire fabrication process is completed. In addition to the critical temperature (T_c) and critical current density at zero field, the dependence of J_c on an externally applied magnetic field and the temperature for the entire multilayer structure is crucial information for electronic applications. The YBCO/YSZ/SiO_2/YSZ/YBCO multilayer structure has been fabricated by Reade *et al.*[2] They reported cracking in the top YBCO layer, which limited their investigation of the properties of the multilayered structure.

In this article, we report a study of the temperature and magnetic field dependence of J_c for both YBCO layers in a YBCO/YSZ/SiO_2/YSZ/YBCO multilayer structure[3] performed by the magnetization method. Our results show that the temperature and magnetic field dependence of J_c of the YBCO layers of these samples are similar to those of high quality single-layer YBCO thin films.

II. EXPERIMENT

The YBCO/YSZ/SiO_2/YSZ/YBCO multilayer samples investigated here were prepared by using a combination of pulsed laser deposition and ion-beam-assisted magnetron sputtering. Details of the technique will be described elsewhere.[3] In short, a 200-nm-thick $YBa_2Cu_3O_{7-\delta}$ (bottom YBCO, layer 1) film was deposited on a single-crystal $LaAlO_3$ substrate (100 orientation and area 1×1 cm^2) by pulsed laser ablation at a substrate temperature of ~750 °C. Ion-beam-assisted rf sputtering was used to deposit biaxially aligned 200-nm-thick yttria-stabilized zirconia (YSZ) as a capping layer (layer 2). Next a 1-μm-thick, amorphous SiO_2 layer (layer 3) was deposited on layer 2 at room temperature by rf sputtering. The capping layer (YSZ) is used to prevent diffusion of the third SiO_2 layer into the top YBCO layer. A fourth layer (biaxially aligned YSZ) was then deposited on the SiO_2 layer to a thickness of 200 nm using the same method as for layer 2. This layer is very important. It not only functions as protection against the diffusion of the third SiO_2 layer into the YBCO layer, it also allows good epitaxial YBCO growth if it has a well-aligned structure. Finally, the top YBCO layer (layer 5) was deposited by laser ablation under the same conditions as was used for layer 1.

The orientation of the YSZ and YBCO layers was characterized by x-ray diffraction. The magnetization $M(H)$ loop was measured using a Quantum Design Magnetometer in fields up to 4 T, applied parallel to the c-axis direction and at a fixed temperature. This was repeated for different temperatures ranging from 5 to 77 K. The values of J_c were calculated using Bean's model. The electrical resistance was measured using the standard four-lead technique.

III. RESULTS AND DISCUSSION

X-ray diffraction data showed that all samples investigated here were single-phase highly c-axis oriented with very good in-plane epitaxy (Fig. 1). There were no cracks observed in the top YBCO layer. The resistance $R(T)$ and magnetization $M(T)$ of the samples were carefully measured for each YBCO layer. Figure 2 shows the typical resistance as a function of temperature for the top YBCO layer. The

[a]Permanent address: Department of Materials Science, Fudan University, Shanghai, People's Republic of China.
[b]Permanent address: Ion Beam Laboratory, Shanghai Institute of Metallurgy, Chinese Academy of Sciences, Shanghai, People's Republic of China.

 0021-8979/96/79(8)/6593/3/$10.00

Magnetization of $HgBa_2CuO_{4+\delta}$ with $0.03 \leqslant \delta \leqslant 0.4$

Q. Xiong, S. Afonso, Y. Q. Tang, F. T. Chan, and G. Salamo
Physics Department/High Density Electronics Center, University of Arkansas, Fayetteville, Arkansas 72701

Y. Y. Xue and C. W. Chu
Physics Department and Texas Center for Superconductivity, University of Houston, Houston, Texas 77204

$HgBa_2CuO_{4+\delta}$ (Hg1201) samples with $0.03 \leqslant \delta \leqslant 0.4$ have been obtained. The magnetization of the powdered Hg1201 samples was determined using a Quantum Design SQUID magnetometer. It was observed that while the magnetization of Hg1201 increased with δ in the underdoped region, the magnetization decreased with δ in the overdoped region. These results suggest an increase of n_s/m^* with oxidation in the underdoped region and a decrease in the overdoped region, similar to that reported in underdoped HTSs and overdoped Tl2201 and Tl1201. © *1996 American Institute of Physics.* [S0021-8979(96)03108-6]

I. INTRODUCTION

Soon after the discovery of high-temperature superconductivity (HTS), it was realized that the existence of CuO_2 layers in HTSs is very crucial and the charge carriers in the CuO_2 layers control the physical properties in both the superconducting state and the normal state. T_c is one of the properties that the charge carriers in the CuO_2 layers have a marked effect upon. On the one hand, it was found that there are three different regimes in the relationship of T_c to the number of charge carriers n in the CuO_2 layers (where n is determined from valence balance or thermoelectric).[1–3] The underdoped region is where the superconducting phase appears near the insulating magnetic phase. T_c increases with increased n in this region. The optimal doping region is where T_c approaches the highest values within the given series. Next, comes the overdoped region. In this region, T_c decreases with further increases in n. On the other hand, based on muon spin-rotation (μSR) measurements,[4–6] it was found that T_c vs n_s/m^* forms a double-valued relation in Tl2201 (where n_s is the superconducting condensate density, m^* is the effective mass). This means that as n increases, n_s/m^* increases in the underdoped region, and decreases in the overdoped region. Until now, most studies have concentrated on the underdoped and optimal region, probably because underdoped and optimally doped samples are fairly easy to synthesize for most HTS systems. On the contrary, the overdoped region has been observed in only a few systems. The $HgBa_2CuO_{4+\delta}$ compound (Hg1201) has been shown to be scientifically significant,[7] because it has the highest T_c among all HTS materials that have one CuO_2 plane, and has the widest doping range that can be achieved by changing oxygen content alone.[8] Thus it is a good candidate for studies on charge carrier and doping related properties in the overdoped region.

In this article, we report a study of T_c vs n_s/m^* done by measuring the magnetization volume fluctuation of Hg1201 when oxygen content is varied from 0.03 to 0.4, covering the entire range from $T_c = 0$ K (underdoping region) to $T_c = 20$ K (overdoping region). We observed that the magnetization of Hg1201 increases with δ in the underdoped region and decreases with δ in the overdoped region. The results suggest that a double-valued relation of T_c to n_s/m^* also exists in the Hg1201 compound.

II. EXPERIMENT

All samples were synthesized by a two-step method, i.e., by first forming a precursor of (Ba, Cu) oxides, then reacting HgO with the precursor inside an evacuated quartz tube. Precursor with an initial composition of Ba_2CuO_y was prepared by a solid-state reaction. High-purity powders of BaO (99.95%) were thoroughly mixed in appropriate proportions. The mixed powders were calcined in an alumina crucible at 930 °C for 24 h under a mixed gas of Ar:O=4:1. Three intermediate regrindings were carried out during this period. The composite Hg source used was a prereacted Hg1:2:0:1 pellet made by compacting the thoroughly mixed HgO (99.998%) and pulverized precursor powder. A reactant pellet was sealed in an evacuated quartz tube of fixed volume, together with an extra Ba_2CuO_y precursor pellet. Details were given in Ref. 9. A stainless-steel tube was used to contain the quartz tube as a safety precaution. The whole assembly was then heated to 800–830 °C for 8 h before slow cooling to room temperature. Samples with different oxygen content were obtained by heating as-synthesized samples at different temperatures and oxygen partial pressures for appropriate periods of time.[9] To reach the underdoped region, the sample was heated in a vacuum of $\sim 2 \times 10^{-6}$ Torr at a temperature between 200 and 450 °C for 20–100 h. For the overdoped samples, the as-synthesized compound was heated in a 1–500 bar O atmosphere between 240 and 400 °C for 10–300 h. Phase characterization was performed by x-ray powder diffraction on a Rigaku DMAX/BIII diffractometer. The magnetization was measured using a Quantum Design SQUID magnetometer. The oxygen content δ of the samples were measured by thermogravimetric analysis[8] and calibrated using neutron powder diffraction.[10]

III. RESULTS AND DISCUSSION

Figure 1 shows the x-ray diffraction pattern of one of our as-synthesized samples, which indicated that the Hg1201 sample was nearly single phase. Figure 2 shows the normal state susceptibility as a function of the temperature. The data fits the Curie law, $\chi = \chi_0 + C/T$, very well with $\chi_0 = 1.04 \times 10^{-6}$ emu/g and $C = 2.45 \times 10^{-4}$ emu/g. The magnetization in various magnetic fields H has also been measured. As shown in the inset of Fig. 2, the magnetization

 0021-8979/96/79(8)/6580/3/$10.00

Epitaxial $Tl_2Ba_2CaCu_2O_8$ superconducting thin film on $Sr_2(AlTa)O_6$ buffer layer

Y. Q. Tang, K. Y. Chen, S. Afonso, X. L. Xu,[a] Q. Xiong, G. Salamo, and F. T. Chan
Department of Physics/High Density Electronic Center, University of Arkansas, Fayetteville, Arkansas 72701

R. Guo and A. Bhalla
Materials Research Laboratory, Pennsylvania State University, University Park, Pennsylvania 16802

(Received 19 June 1995; accepted for publication 17 August 1995)

Epitaxial $Tl_2Ba_2CaCu_2O_8$ superconducting films have been successfully grown on the dielectric $Sr_2(AlTa)O_6$ (SAT) buffer layers. X-ray diffraction data showed that the films were highly c-axis oriented with a rocking curve full width half maximum as narrow as 0.3°. The films also had an excellent in-plane epitaxy with $Tl_2Ba_2CaCu_2O_8$[100] aligned with SAT[100] and MgO[100] of the substrate. The zero resistance temperature T_c of the superconducting films ranged from 95 to 103 K and the transport critical current density J_c in zero field was 3×10^5 A/cm^2 at 77 K. © *1995 American Institute of Physics.*

In the study of high-temperature superconducting films, buffer layers have been extensively used[1–6] because being interposed between the substrate and the film of interest, these layers can alleviate a variety of problems such as chemical incompatibility, thermal or lattice mismatch.[7] As a new dielectric compound, $Sr_2(AlTa)O_6$ (SAT) was synthesized to be one of the potential substrate materials for the growth of high T_c superconducting films.[8] Because of its relatively low dielectric constant[9,10] and good thermal expansion coefficient and lattice match with YBCO,[8–11] SAT was successfully used as a buffer layer material for the growth of YBCO thin films.[10,11] Recent studies have shown that by depositing an epitaxial SAT buffer layer on MgO, the lattice mismatch problem between a MgO substrate and a YBCO superconducting film was reduced, leading to an improvement of superconducting properties.[10]

$Tl_2Ba_2CaCu_2O_8$ superconducting films, while exhibiting higher T_c and lower surface resistance than YBCO,[12] are much more difficult to prepare with good qualities due to the high volatility and chemical reactivity of thallium and the high reaction temperature. Although best films with transport J_c of $1.06–5.3\times10^6$ A/cm^2 were obtained by carefully optimizing the thallination procedure and using suitable substrates such as $LaAlO_3$[13–15] or $SrTiO_3$,[16] the high cost and high dielectric constants of such substrates can limit further applications of $Tl_2Ba_2CaCu_2O_8$ films in microelectronics. Some other substrates of low cost and low dielectric constants such as sapphire, silica, and MgO suffer from the chemical incompatibility or large lattice mismatch with $Tl_2Ba_2CaCu_2O_8$ and consequently yield poor film quality and low J_c. To resolve these problems, a suitable buffer layer compatible both with the $Tl_2Ba_2CaCu_2O_8$ film and with the substrate should be used. By choosing CeO_2 as buffer layers, Holstein *et al.* were able to avoid the chemical reaction of the $Tl_2Ba_2CaCu_2O_8$ films with the sapphire substrates and produced epitaxial $Tl_2Ba_2CaCu_2O_8$ films with T_c of 97–98 K and transport J_c of 2.8×10^5 A/cm^2 at 75 K.[3]

The crystallographic phase of ordered SAT has a double cell cubic perovskite structure with a lattice constant a_0=7.777 Å[10] or $a_0/2$=3.888 Å, while a_0=3.895 Å in the disordered cubic perovskite.[9] These lattice constants are close to those of Tl-based superconductors (a_0=3.85–3.86 Å). In fact, SAT has better lattice match to the TlBaCaCuO superconductors than many other substrates such as MgO (a_0=4.213 Å), YSZ ($a_0/\sqrt{2}$=3.639 Å), $LaAlO_3$ (a_0=3.792 Å), and even $SrTiO_3$ (a_0=3.905 Å). Moreover, SAT is similar to $SrTiO_3$ in structure and was tested to be chemically stable at high temperature.[8,9] Therefore, it should also be a good candidate to act as a buffer layer in the fabrication of Tl-based superconducting films. In this communication, we report for the first time the preparation of epitaxial

FIG. 1. SEM photograph of a $Tl_2Ba_2CaCu_2O_8$ superconducting film on SAT/MgO.

[a]Permanent address: Ion Beam Laboratory, Shanghai Institute of Metallurgy, Chinese Academy of Sciences, Shanghai 200050, China.

 0021-8979/95/78(11)/6846/3/$6.00

Epitaxial $Sr_2(AlTa)O_6$ films as buffer layers on MgO for $YBa_2Cu_3O_{7-x}$ thin film growth

K. Y. Chen, S. Afonso, R. C. Wang,[a] Y. Q. Tang, G. Salamo, and F. T. Chan
Department of Physics/High Density Electronics Center, University of Arkansas, Fayetteville, Arkansas 72701

R. Guo and A. S. Bhalla
Material Research Laboratory, Pennsylvania State University, University Park, Pennsylvania 16802

(Received 27 March 1995; accepted for publication 19 April 1995)

$Sr_2(AlTa)O_6$ thin films (2000–3000 Å) have been deposited on MgO (001) substrates using pulsed laser deposition (PLD). X-ray-diffraction analysis shows that the $Sr_2(AlTa)O_6$ grows with the c axis highly oriented normal to the substrate plane and very good in-plane epitaxy. The subsequently deposited $YBa_2Cu_3O_{7-x}$ films using PLD on $Sr_2(AlTa)O_6$ buffered MgO substrates exhibit excellent epitaxial growth with a narrow rocking curve width and a small ϕ scan peak width. The critical temperature T_{c0} of 90–92 K has been achieved reproducibly and the critical current density is over 2.7×10^6 A/cm^2 at 77 K. © *1995 American Institute of Physics.*

High-T_c superconducting $YBa_2Cu_3O_{7-x}$ (YBCO) films have been successfully grown on a number of substrates, such as $SrTiO_3$, $LaAlO_3$, MgO, YSZ, and $LaGaO_3$. In many high-frequency electronic applications, such as superconducting multichip modules, one requires substrates and dielectric layer materials with a low dielectric constant and a low loss tangent. In recent years, great efforts have been made in searching for substrates and dielectric intermediate layer materials which can meet these requirements for specific electronic applications as well as the requirements for growth of superconducting films.[1-5] Several materials such as $SrTiO_3$,[2,4] MgO,[2,3] YSZ,[1] and CeO_2,[3,5] have been used as buffer layers for fabricating $YBa_2Cu_3O_{7-x}$ films on some substrates of application interest. The dielectric constant of $SrTiO_3$, however, is too high to be useful in some high-frequency devices, whereas MgO and YSZ have a relatively large lattice mismatch with superconducting materials. Another cubic perovskite material $Sr_2(AlTa)O_6$ (SAT) has recently become of interest as a buffer layer and dielectric interlayer for thin films of oxide superconductors[6,7] because it has a good lattice match with the high-T_c superconductors. Ordered SAT arises from the alternate ordered distribution of Al and Ta atoms on the octahedral site of the primitive perovskite unit cell, resulting in a doubling of the lattice constant. In disordered SAT, Al and Ta atoms randomly occupy the octahedral site. Both ordered and disordered structures are closely lattice matched to the a-b plane of YBCO. Another advantage of SAT is that it has a lower dielectric constant than that of $SrTiO_3$, YSZ, and CeO_2. Table I shows the dielectric properties of SAT ceramic samples measured at both room and liquid nitrogen temperatures. Moreover, the thermal expansion coefficient of SAT is 9.7×10^{-6} °C in the temperature range from room temperature to 600 °C, which is highly compatible with that of YBCO, and there are no structural phase transitions and twinning behavior observed. These properties indicate that SAT is suitable as a buffer layer material for high-T_c thin films in device applications.

In this communication, we report our experimental results on fabricating SAT buffer layers on MgO substrates and YBCO/SAT/MgO multilayers. We chose MgO as a substrate material in this work because it has a relatively low dielectric constant ($\epsilon=10$) and is inexpensive compared to other substrates such as $SrTiO_3$ and $LaAlO_3$. The main disadvantage of using MgO for making superconducting films is the large lattice mismatch between it and YBCO. As a result, the critical temperature of YBCO grown directly onto MgO is usually limited to 88 K.[4] The motivation of this study is to use SAT as a buffer layer to overcome the drawback of MgO. Furthermore, MgO has been successfully used as a first buffer layer on a few substrates such as MgF_2 and Si.[2,8] This suggests, therefore, that if SAT can be successfully deposited onto MgO, it can be used as a second buffer layer for growing YBCO films.

SAT and YBCO films were deposited using the pulsed laser deposition technique. A 193 nm laser beam generated by an excimer laser was focused to provide an energy density of ~1.3 J/cm^2. The laser repetition rate was 6 Hz. An oxygen pressure was maintained in the vacuum chamber at 200–250 mTorr during deposition of both the SAT and YBCO films. The quality of the SAT and YBCO films was examined by x-ray diffraction, and four-probe T_c and J_c measurements.

The SAT target used was a ceramic pellet of the ordered phase with a lattice constant $a_0=7.777$ Å prepared using

TABLE I. Dielectric properties of ceramic SAT with 97% theoretical density.

	Room temperature		Low temperature (77 K)	
	10 kHz	Microwave	10 kHz	Microwave
ϵ	11.8	10.7 (11.0 GHz)	11.8	···
tan δ ($\times10^{-4}$)	16.8	3.64 (7.64 GHz)	0.42	2.09 (7.64 GHz)

[a]Permanent address: Department of Materials Science, Fudan University, Shanghai, People's Republic of China.

 0021-8979/95/78(3)/2138/3/$6.00

ELSEVIER

Physica C 253 (1995) 329–333

PHYSICA C

Synthesis and start cation-composition of $HgBa_2CuO_{4+\delta}$

Q. Xiong [a,*], F.T. Chan [a], Y.Y. Xue [b], C.W. Chu [b]

[a] *Physics Department / High Density Electronics Center, University of Arkansas, Fayetteville, AR 72701, USA*
[b] *Physics Department and Texas Center for Superconductivity, University of Houston, Houston, TX 77204, USA*

Received 17 July 1995; revised manuscript received 11 August 1995

Abstract

The synthesis conditions of $HgBa_2CuO_{4+\delta}$ were studied. It was observed that the best phase purity was achieved at an apparent cation ratio of Hg:Ba:Cu = 0.7:2:1 that was obtained by either Hg deficient initial compositions or extra Hg absorbents, e.g. Au foil. No significant impurities or site mixing can be identified by X-ray/neutron powder diffraction investigations in these non-stoichiometric samples. However, their large paramagnetic background suggests the existence of (Ba, Cu) oxides. Our data also show that this apparent Hg deficiency is likely to be synthesis-reaction related.

1. Introduction

The actual cation stoichiometry and phase composition of $HgBa_2CuO_{4+\delta}$ (Hg-1201) samples obtained through solid-state reactions are still debatable. Hg rich impurities, e.g. $BaHgO_2$ [1] or metal Hg drops [2] were observed in nearly all cases where the stoichiometric initial composition of Hg:Ba:Cu = 1:2:1 was adopted. Hg-1201 samples with no significant (> 5%) impurity phases detectable by X-ray/neutron powder diffraction have been synthesized either with off-stoichiometric compositions [3], or by using extra Hg absorbing materials such as precursor pellets [4] or Au foil [5]. Such off-stoichiometric synthesis conditions have also been observed in Tl and Bi based families [6,7]. Both the severe site mixing [8] and the particular reaction conditions during synthesis [9] have been proposed as possible explanations for this. These two models present two different scenarios, and will suggest very different ways to improve the synthesis process. As part of our investigation of the Hg based high-temperature superconductors (HTS's), the effects of the initial composition are presented here. It was observed that an initial composition of Hg:Ba:Cu ~ 0.7:2:1 leads to the best result over a broad range of conditions. Although no significant (> 5%) impurity phases can be identified, our magnetization measurements suggest 20–30% impurities in the samples so obtained. Therefore, this cation ratio seems to be synthesis-reaction related. Our data also demonstrate that the Cu/Hg site mixing is not the main reason for this Hg deficiency. Therefore, further investigation on the formation reactions of Hg-1201 is called for.

2. Experimental

All samples were synthesized by a two-step method, i.e. by first forming a precursor of (Ba, Cu)

* Corresponding author.

SSDI 0921-4534(95)00525-0

Superconducting $TlSr_2(Ca,Cr)Cu_2O_7$ thin films with critical current density up to 10^6 A/cm^2

Y. Q. Tang, K. Y. Chen, I. N. Chan, Z. Y. Chen, Y. J. Shi, G. J. Salamo, F. T. Chan, and Z. Z. Sheng
Department of Physics, University of Arkansas, Fayetteville, Arkansas 72701

(Received 8 March 1993; accepted for publication 13 June 1993)

Superconducting $TlSr_2(Ca,Cr)Cu_2O_7$ thin films with zero resistance temperature T_c up to 102 K and critical current density J_c as high as 10^6 A/cm^2 at 77.7 K have been successfully prepared via laser ablation and thallium diffusion. Prolonged low temperature annealing in air was used for film processing. X-ray diffraction patterns indicated that the films were highly oriented 1212 phase with c axes normal to the $LaAlO_3(100)$ or $MgO(100)$ substrates.

Among the Tl-based high T_c superconductors,[1-4] the single Tl-O layered Tl-1212 and Tl-1223 compounds have drawn more and more attention in applied superconductivity.[5-7] Since the distance between Cu-O conducting planes in these compounds is shorter than in the compounds with two Tl-O layers (2212 and 2223), leading to stronger interlayer coupling, it is suggested that the thermally activated flux motion in Tl-1212 and Tl-1223 phases may not be as severe as that in double Tl-O layered compounds.[8] It is also believed that the single Tl-O layered compounds have higher critical current density J_c and their superconducting performances are less influenced by magnetic field.[5,8,9] These advantages make Tl-1223 and Tl-1212 phases good candidates for the fabrication of superconducting wires and thin films.

Based on the work of the 105 K $TlSr_2(Ca,Cr)Cu_2O_7$ bulk material in which Cr primarily takes the position of Ca,[10] we have recently prepared this kind of 1212 phase film by chemical deposition[11] and by laser ablation.[12] It was found that the new 1212 films were easy to prepare and could sustain a wide range of processing conditions. However, the superconducting properties of the films should be further improved in order to meet the requirements of practical application.

In this communication, we report the preparation of highly oriented Cr-substituted 1212 phase $TlSr_2(Ca,Cr)Cu_2O_7$ films of good quality. The films were produced by a two-step process via laser ablation and post-annealing in Tl vapor. By carefully controlling annealing conditions, we have successfully obtained superconducting $TlSr_2(Ca,Cr)Cu_2O_7$ films with T_c of 98–102 K and J_c of 1×10^6 A/cm^2 at 77.7 K. To our knowledge, the J_c value is among the highest values achieved in 1212 phase Tl-based thin films.

The precursor films with a fixed starting composition of $Sr_2CaCr_{0.2}Cu_2O_z$ were first deposited onto $MgO(100)$ or $LaAlO_3(100)$ substrates using an Ar-F excimer laser. This starting composition was chosen according to the optimum range of Cr amount in the nominal compositions $TlSr_2CaCr_yCu_2O_z$ (y=0.15–0.25) of bulk material.[10] The laser operated with a wavelength of 193 nm at 10 Hz. The pulse energy was 125 mJ. The oxygen pressure in the deposition chamber was 200 mTorr and the deposition time was 20–30 min. The substrate temperature was controlled in the range of 250–350 °C during ablation. It was found that the substrate temperature was not critical during deposition as long as it was lower than 600 °C. With a thickness of 0.3–0.8 μm, the precursor films had a dark brown color and looked mirror-like.

The as-deposited precursor films were then annealed in Tl vapor. One unfired pellet with the nominal composition $Tl_xSr_2CaCr_{0.2}Cu_2O_z$ (x=1 or 1.3) was used as the main Tl vapor source, and some fired pellets were used as supports and as an auxiliary Tl source. We determined that x=1 in the nominal composition corresponded to the ideal Tl amount for synthesizing the 105 K 1212-phase bulk material. This ratio did not seem adequate for prolonged film annealing. Therefore, x=1.3 was chosen to enhance the concentration of Tl vapor during the annealing process. Two kinds of slightly different configurations were used in the film annealing. One was the so-called "untouched method," in which the unfired pellet was placed about 1 mm above the precursor film in a covered alumina boat. The other was called the "touched method," where the film was sandwiched between two pellets vertically placed in a closed alumina cylinder with the film surface confined to the unfired pellet. Annealing was carried out in a programmable tube furnace at 860–870 °C, about 50 °C lower than the calcining temperature for bulk material.[10] A lower annealing temperature proved to be helpful in improving the properties of superconducting films.[13,14] A cooling rate as low as 2 °C/min was used to ensure the final film quality.[12] The T_c and J_c of the fabricated superconducting films were then measured either by the four-probe or by the self-inductance[15] method.

In previous work, annealing was carried out in a flowing oxygen atmosphere for less than 3 h and the nominal $TlSr_2CaCr_{0.2}Cu_2O_y$ pellets were used as a Tl vapor source.[11,12] In the present work, however, we annealed the films in air and prolonged the annealing time to 5–20 h. These modifications played an important role in improving the quality of the resulting films. Studies on the effect of oxygen pressure on the formation of Tl-based superconductors show that the decrease of oxygen pressure can reduce the temperature of phase formation and enable the reaction at lower temperature.[14,16] The oxygen pressure in air (0.2 atm) is much lower than the 1 atm flowing oxygen; thus, the formation of superconducting film at low anneal-

 0021-8979/93/74(6)/4259/3/$6.00

Thermoelectric power of the thallium-based superconductor $Tl_2Ba_2Ca_2Cu_3O_{10-\delta}$

Y. Xin, K. W. Wong, and C. X. Fan
Department of Physics and Astronomy, University of Kansas, Lawrence, Kansas 66045

Z. Z. Sheng and F. T. Chan
Department of Physics, University of Arkansas, Fayetteville, Arkansas 72701
(Received 9 November 1992; revised manuscript received 3 March 1993)

The temperature dependence of the thermoelectric power of the high-temperature superconductor $Tl_2Ba_2Ca_2Cu_3O_{10-\delta}$ is reported. The contribution of holes from the valence band satisfying a Fermi-liquid model gives the major part of the measured thermoelectric power. The results show that the conduction-band electrons also contribute to the total output of the thermoelectric power and the portion of the electron's contribution increases with temperature. An explicit expression for the thermolectric power of the 2:2:2:3 phase was derived based on a two-band model and the experimental data, which is given as $S(\mu V)=0.121T-(280-0.2T)e^{-550/T}$. A general formula, $S=AT+(B\lambda+CT)\exp(-\lambda/T)$, is found to give a close description of the thermoelectric power of various cuprate high-T_c superconductors.

The absolute thermoelectric power S in an excellent indicator of many fundamental aspects of charge transport in a conducting material. We can extract useful information from the characteristics of S-temperature dependency to reveal the normal-phase transport mechanism of a material. Furthermore, the sign of S can be used to distinguish the major charge carrier in the transport process. In certain regimes, S can also provide knowledge for the bandwidths and band gaps which govern the transport properties of the material.

Since the discovery of high-T_c superconductors, there have been a large number of experimental and theoretical efforts to understand the thermoelectric power of such a material. However, a satisfactory interpretation of experimental results are still lacking. $Tl_2Ba_2Ca_2Cu_3O_{10-\delta}$ is a very stable superconductor with a transition temperature above 120 K, which is the highest to date. Several groups[1-3] have studied the thermoelectric power of Tl-based compounds, including the 2:2:2:3 phase; but, unfortunately, a quantitative study is far from complete due to a lack of single phase samples. We carried out thermoelectric power study on a very pure 2:2:2:3 phase sample in a quantitative manner. Based on the experimental result, we propose a two-band (conduction CB, valence VB) conduction mechanism and give an explicit expression of the thermoelectric power of the Tl-based superconductor. This theoretical expression may also be applied to other high-T_c superconductors.

Samples used in this study were prepared by our recently developed method.[4] The sample $Tl_2Ba_2Ca_2Cu_3O_{10-\delta}$ is a pure 2:2:2:3 phase sample (no impurity being detected by powder x-ray diffraction). The thermoelectric power was measured with a modified differential method[5] in the temperature range from 300 to 100 K.

Figure 1 shows the S plot against temperature of the sample $Tl_2Ba_2Ca_2Cu_3O_{10-\delta}$. At room temperature, the value of S for this sample is 1.8 μV/K and S increases almost linearly with decreasing temperature. It has a maximum value of 12.3 μV/K at about 135 K and drops abruptly as T approaches T_c. These values are to be compared to those in Ref. 5 and will be discussed later.

The thermoelectric power-temperature dependency of $Tl_2Ba_2Ca_2Cu_3O_{10-\delta}$, as viewed from the overall behavior, is similar to those reported for $(La,Sr)_2CuO_{4-\delta}$, $RBa_2Cu_3O_{7-\delta}$ (R = rare earth), $Bi_2Sr_2CaCu_2O_{8-\delta}$, and $Tl_2Ba_2CaCu_2O_{8-\delta}$.[6-15] To explain the temperature dependence of S and the exhibition of a broad maximum above T_c for these high-T_c materials, some groups suggested a model of a strong phonon-drag effect,[16-18] while others expressed a strong doubt on this suggestion.[19,20] Based on our experimental data, there appears to be no evidence in support of phonon-drag contribution to the thermoelectric power. We found that the thermoelectric power can be simply explained from the diffusion of the charge carriers.

A specific formula for the thermoelectric power of a metal satisfying the Fermi liquid model, due to electron

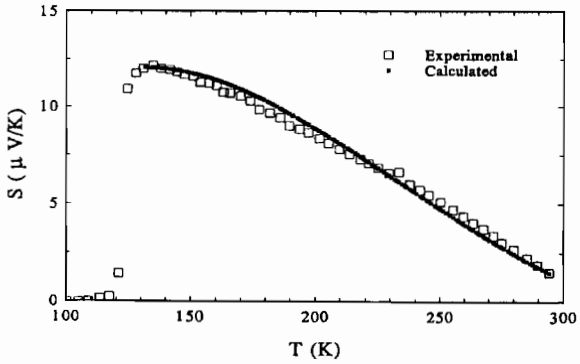

FIG. 1. Thermoelectric power vs temperature of $Tl_2Ba_2Ca_2Cu_3O_{10-\delta}$.

Supercond. Sci. Technol. 6 (1993) 173–175. Printed in the UK

Preparation of $Tl_2Ba_2Ca_2Cu_3O_{10}$ thin films via low-temperature Tl-diffusion

Y Q Tang†, Z Z Sheng†, W A Lou†, Z Y Chen†, Y N Chan†, Y F Li†, F T Chan†, G J Salamo†, D O Pederson†, T H Dhayagude‡, S S Ang‡ and W D Brown‡

† Department of Physics, University of Arkansas, Fayetteville, Arkansas 72701 USA
‡ Department of Electrical Engineering, University of Arkansas, Fayetteville, Arkansas 72701 USA

Received 24 November 1992

Abstract. Superconducting $Tl_2Ba_2Ca_2Cu_3O_{10}$ thin films with T_c ($\rho = 0$) up to 121 K were successfully prepared via the deposition of a BaCaCuO precursor (by laser ablation or sputtering) and thallium diffusion under 1 atmosphere of air. Instead of a short annealing time at high temperature, we use a prolonged annealing time (up to 60 hours) at lower temperature (800–815 °C). The films obtained with this procedure are generally good in morphology, highly oriented and exhibit a critical current density, J_c, of about 1–2 × 10^5 A cm^{-2} on MgO(100) and up to 1.5 × 10^6 A cm^{-2} on $LaAl_3$(100) at 77 K. Both T_c and J_c values reported here are comparable to the best Tl-2223 films prepared by the pseudo-one-step process.

1. Introduction

Since the discovery of Tl-based superconductors [1–2], the compound $Tl_2Ba_2Ca_2Cu_3O_{10}$ (Tl-2223 or 2223) has been found to have the highest T_c ($\rho = 0$) up to 127 K [3–4]. With high sintering temperature (>850 °C), it is usually not difficult to prepare and reproduce bulk 2223 materials with T_c about 120 K. However, to further improve the T_c, a sophisticated post-annealing procedure, involving low-temperature treatment and oxygen adjusting, must be introduced. By encapsulating the 2223 samples in evacuated quartz tubes and post annealing at low temperatures (750–760 °C) for about 10 days or more, the T_c can be increased to 127 K [3–4]. Moreover, reduced partial oxygen pressure has proved useful in decreasing the synthesis temperature of the 2223 phase [5] and in increasing its T_c [3].

In the fabrication of Tl-2223 thin films, where post annealing is still necessary for both pseudo-one-step or two-step processes [6], reduction of annealing temperature is of particular importance because it not only leads to the formation of high-quality films but is also a necessary step towards a real one-step process such as that for Tl-1212 film [7]. Previous annealing procedures for 2223 films generally use high temperatures (>850 °C) and short times (5–60 min), which usually generate relatively rough film surface and poor J_c. Lee *et al* recently reported the low temperature formation of 2223 films in reduced O_2 pressure [8]. With their pseudo-one-step procedure, the quality of the 2223 film was improved significantly. Their best films were shiny to the eye and showed a T_c as high as 121 K and a J_c of 1.6 × 10^6 A cm^{-2} at 77 K. However, their technique was somewhat complicated. Our recent work on spray pyrolysis also showed that, even under 1 atmosphere of oxygen, 2223 films with T_c up to 121 K can still form at relatively low annealing temperature if the annealing time is long enough [6].

In this paper, we report the two-step formation of 2223 films at low annealing temperature in 1 atmosphere of air. Under optimum conditions, the T_c ranged from 117 K to 121 K, and J_c is 1–2 × 10^5 A cm^{-2} for the films on MgO(100) substrates and up to 1.5 × 10^6 A cm^{-2} on $LaAlO_3$ at 77 K.

2. Experimental details

The substrates used for film production were MgO(100) and $LaAlO_3$(100). The BaCaCuO precursor films were deposited by laser ablation or sputtering. The details of the equipment for these methods are described elsewhere [9, 10]. The substrates were heated at 400–500 °C for the laser ablation but were kept at room temperature during sputtering. The precursor films deposited by laser were 0.4–0.5 μm thick while those by sputtering were about 0.8 μm. Thallium was then introduced by annealing the as-deposited BaCaCuO films with crude $Tl_{1.7}Ba_2Ca_{2.3}Cu_3O_x$ pellets in a closed alumina boat. The films were placed in a free-surface configuration with the pellet positioned about 1 mm above the film. The pellets were prepared using high purity Tl_2O_3, BaO_2, CaO and CuO powder [11]. The annealing temperature was 750–820 °C, 80–150 °C lower than the conventional temperature for bulk formation and at least 50 °C lower than the generally used

0953-2048/93/030173 + 03 $07.50

Jpn. J. Appl. Phys. Vol. 31 (1992) pp. 3851-3852
Part 1, No. 12A, December 1992

Short Note

Fabrication of Superconducting $TlSr_2(Ca, Cr)Cu_2O_7$ Thin Films by Laser Ablation and Thallium Diffusion

Yongqiu TANG, Weiang LUO, Zuyao CHEN, Seifollah NASRAZADANI*, Fui T. CHAN, Gregory SALAMO, Donald O. PEDERSON and Zhengzhi SHENG
Department of Physics, The University of Arkansas, Fayetteville, Arkansas 72701, USA

(Received June 29, 1992; accepted for publication September 19, 1992)

Superconducting $TlSr_2(Ca, Cr)Cu_2O_7$ thin films have been prepared on MgO(100) substrates via laser ablation and thallium diffusion. Precursor SrCaCrCuO films were first deposited by an excimer laser; thallium was then incorporated by annealing the precursor films between un-fired TlSrCaCrCuO bulk pellets. The product superconducting films are 1212 phase and exhibit $T_c(\rho=0)$ up to 90 K and J_c(transport) up to 10^4 A/cm^2.

KEYWORDS: superconducting thin film, high T_c superconductor, Tl-Sr-Ca-Cu-O system, "1212" phase, Cr addition, laser ablation

Among M-substituted (M=Pb, Bi, Cr or rare earth) 1212-type phase (Tl, M)Sr_2(Ca, M)Cu_2O_7 compounds,[1-7] the Cr-substituted $TlSr_2(Ca, Cr)Cu_2O_7$ exhibits a T_c as high as 110 K and is easy to synthesize.[7] Motivated by this easy formation and high T_c, we have successfully prepared 100 K $TlSr_2(Ca, Cr)Cu_2O_7$ superconducting films via spray pyrolysis and thallium diffusion.[8] However, the films obtained by the spray technique are generally thick and rough on surface which may not be suitable for certain electronic applications. In this paper, we report the preparation of $TlSr_2(Ca, Cr)Cu_2O_7$ superconducting films on MgO(100) substrates using laser ablation and thallium diffusion. Zero-resistance temperature $T_c(\rho=0)$ of the best films was 90 K, and the critical transport current J_c was about 10^4 A/cm^2 at 77 K.

The laser ablation target with nominal composition of $Cr_{0.2}Sr_2CaCu_2O_x$ was prepared by sintering a pellet of properly mixed powder of Cr_2O_3, SrO, CaO and CuO at 880°C for 24 h. Precursor films were deposited onto MgO(100) substrates at 260-280°C using a Kr-F excimer laser with a wavelength of 248 nm. The laser operated at 20 Hz with a power of 200 mJ. The oxygen pressure in the deposition chamber was 200 mTorr and the deposition time was 7-20 min. The as-deposited precursor films were then put between unfired $TlCr_{0.2}Sr_2CaCu_2O_x$ bulk pellets in a covered alumina cylinder, and were heated in a programmable tube-furnace at 860-880°C for 30-180 min in an oxygen atmosphere. A high temperature worked with a short annealing time while the lower temperature treatment took longer. In the cooling step, some films were cooled in argon while others were cooled in oxygen. Different cooling rates were used. The methods and instruments used for investigating the thickness, morphology, X-ray diffraction patterns as well as the T_c and J_c of films were all described in ref. 8.

The precursor films deposited by laser ablation were mirror-like with a shiny dark brown color and were not conducting. The thickness of the films varied from 0.3-0.8 μm depending on the deposition time. After the Tl-diffusion procedure, the films turned black, and were superconducting. Although the preparation conditions for TlSrCaCrCuO films were much less sensitive than that for TlBaCaCuO superconducting films,[8] the annealing procedure was still very crucial for the superconducting properties.

Table I lists the processing conditions and T_c and J_c for some films. It shows clearly that both annealing temperature and cooling rate play very important roles in the film properties. Film S1 was annealed at 880°C for 30 min in an oxygen flow. The X-ray diffraction pattern of this film (Fig. 1) shows that the film is single 1212 phase $TlSr_2(Ca, Cr)Cu_2O_7$ and exhibits a strong orientation with c-axis perpendicular to the surface of the MgO(100) substrate. However, $T_c(\rho=0)$ of the film is only 82 K and the J_c is also low ($<10^3$ A/cm^2). The SEM photograph (Fig. 2(a)) illustrates that the film consists of uniform crystalline grains with an average size of 2 μm, but the morphology is porous. Obviously, it is the porosity that causes the poor J_c of film. In contrast, films processed at lower temperature have random orientation but are more dense (Fig. 2(b)). These films exhibit higher $T_c(\rho=0)$ and J_c. By decreasing the temperature from 880°C to 865°C, T_c is increased from 82 K to 90 K (also see Fig. 3). A rapid cool-

Table I. Annealing condition and $T_c(\rho=0)$ and J_c for some films.

Sample	Annealing condition	T_c(K)	J_c(A/cm^2)
S1	880°C, 30 min (O_2), cooling rate: 50°C/min (Ar)	82	6×10^2
S2	875°C, 60 min (O_2), cooling rate: 50°C/min (Ar)	85	1×10^3
S3	870°C, 90 min (O_2), cooling rate: 50°C/min (Ar)	86	2×10^3
S4	870°C, 90 min (O_2), cooling rate: 50°C/min (O_2)	87	2×10^3
S5	865°C, 150 min (O_2), cooling rate: 2°C/min (O_2)	90	1×10^4
S6	860°C, 180 min (O_2), cooling rate: 2°C/min (O_2)	90	1×10^4

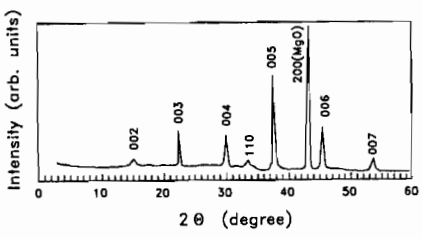

Fig. 1. X-ray diffraction pattern for the superconducting $TlSr_2(Ca, Cr)Cu_2O_7$ film S1 in Table I. It shows that this film is single 1212 phase and is highly oriented.

*Department of Mechanical Engineering, The University of Arkansas.

Analytic solution of a two-dimensional hydrogen atom. II. Relativistic theory

S. H. Guo,* X. L. Yang, and F. T. Chan
Department of Physics, University of Arkansas, Fayetteville, Arkansas 72701

K. W. Wong
Department of Physics and Astronomy, University of Kansas, Lawrence, Kansas 66045

W. Y. Ching
Department of Physics, University of Missouri–Kansas City, Kansas City, Missouri 64110
(Received 12 March 1990; revised manuscript received 20 September 1990)

In this paper, we derive the exact analytic solution for the relativistic $(2+1)$-dimensional hydrogen atom, both with and without the Chern-Simons field. The atomic spectra without the Chern-Simons field is expanded in powers of the fine-structure constant and compared to the nonrelativistic spectra with the fine-structure splitting, while the Chern-Simons spectrum is investigated in detail for different anomalous angular-momentum values. Fractional statistics and charge are a natural consequence of the Chern-Simons eigenfunctions. The semion (particle with exotic statistical phase factor $\pm i$) ground state for such a hydrogen atom collapses.

I. INTRODUCTION

In paper I (Ref. 1) we have studied the $(2+1)$-dimensional [$(2+1)$D] hydrogen problem in the nonrelativistic limit. We have also used the perturbation theory to calculate the fine-structure correction of the energy levels. It would be of great interest to see if these same results can be obtained from a relativistic theory. Recently, much interest has been generated on the particle dynamics of the $(2+1)$D problem. In particular, the $(2+1)$D gauge theory with the Chern-Simons action[2] is known to produce some very interesting physical phenomena, such as exotic angular momentum (fractional spin), fractional charge, and fractional statistics.[3] Recently the unique characteristics of the nonrelativistic $(2+1)$D theories have been proposed as the explanation for fractional quantum Hall effect,[4] and have been suggested as relevant to high-T_c superconductivity.[5]

In this paper, we will first present the exact analytic solution to the $(2+1)$D relativistic hydrogen atom without the Chern-Simons action. The exact eigenenergy solution is then expanded in powers of the fine-structure constant. The result is compared term by term to the nonrelativistic solution given in paper I. In the second half of this paper, we consider the effect of the Chern-Simons term. It is shown that, for a small anomalous angular-momentum correction, the analytic eigenenergy can again be expanded in an ascending power of the fine-structure constant. The result shows that the originally nonrelativistic portion of the spectra, which is degenerate in angular momentum, is now split into two separate parity spectra. On the other hand, for anomalous angular-momentum correction approaching the semion (particle with exotic statistical phase factor $\pm i$) state, such an expansion in the powers of the fine-structure constant is not possible. In fact, the atom basically collapses before reaching the semion state.

II. RELATIVISTIC SOLUTION OF A 2D HYDROGEN ATOM

A. Dirac equation for a 2D hydrogen atom

The 2D Dirac Hamiltonian for an electron placed in the potential $V(r)$ created by the proton is

$$H=c\boldsymbol{\alpha}\cdot\mathrm{p}+\beta m_e c^2+V(r)\ , \tag{2.1}$$

where matrices $\boldsymbol{\alpha}$ and β satisfy the relations

$$\alpha_x^2=\alpha_y^2=\beta^2=1\ , \tag{2.2}$$

$$\alpha_x\alpha_y+\alpha_y\alpha_x=\alpha_x\beta+\beta\alpha_x=\alpha_y\beta+\beta\alpha_y=0\ . \tag{2.3}$$

An explicit and familiar representation of $\boldsymbol{\alpha}$ and β is provided by

$$\alpha_i=\begin{bmatrix}0 & \sigma_i\\ \sigma_i & 0\end{bmatrix},\quad i=1 \text{ and } 2\ ,$$
$$\beta=\begin{bmatrix}I & 0\\ 0 & -I\end{bmatrix}\ , \tag{2.4}$$

in terms of the 2×2 unit I matrix and Pauli σ_i matrices. In the 2D polar coordinates, the corresponding Dirac equation is

First-Principles Calculation of Optical Properties of C_{60} in the fcc Lattice

W. Y. Ching, Ming-Zhu Huang, and Yong-Nian Xu
Department of Physics, University of Missouri-Kansas City, Kansas City, Missouri 64110

W. G. Harter and F. T. Chan
Department of Physics, University of Arkansas, Fayetteville, Arkansas 72701
(Received 12 July 1991)

The electronic and optical properties of C_{60} in the fcc lattice have been studied by a first-principles method. It is shown that C_{60} has a low dielectric constant and an optical spectrum rich in structures; this is drastically different from diamond and graphite. The spectrum shows five disconnected absorption bands in the 1.4 to 7.0 eV region with sharp structures in each band that can be attributed to critical-point transitions. This is a manifestation of the localized molecular structure coupled with long-range crystalline order.

PACS numbers: 78.20.Bh, 71.25.Tn

The recent discovery of the third form of carbon in the form of C_{60} fullerene [1] and its crystalline form with a fcc lattice [2] has prompted an upsurge of experimental and theoretical studies [3–11]. Research efforts were further accelerated by the announcement of the fact that when intercalated with alkali elements such as K [12–14] and Rb [15], the C_{60} crystal becomes superconducting with a T_c approaching 28 K [15]. Therefore, it is extremely important to understand the fundamental electronic properties of this fascinating material. In this paper we report a first-principles calculation of the electronic and optical properties of C_{60} in the fcc lattice. Although a number of theoretical calculations on isolated C_{60} clusters exist (see references cited in [4]), the study of the optical properties of the C_{60} crystal is especially important. The unique structure of C_{60} in the crystalline form raises the question of the proper interplay of the localized molecular structure and the long-range periodicity in the determination of the electron wave function.

We have used the first-principles, self-consistent, orthogonalized linear combination of atomic orbitals (OLCAO) method in the local-density approximation to calculate the electronic structure of fcc C_{60}. The Wigner interpolation formula was employed for the correlation correction. This method has been widely used in the study of band structures and optical properties of a large number of solids, especially those with complex structures [16]. The method is uniquely suited for C_{60} since even with a simple fcc structure, the unit cell contains 240 valence electrons and an economic expansion in the basis function is crucial [17]. The fcc lattice constant used was 14.20 Å with two types of C-C bonds (1.46 and 1.40 Å) in the icosahedral C_{60} cluster. The relative orientation of the C_{60} cluster with respect to the z axis was chosen to be the same as that in Ref. [7]. The basis functions were Bloch functions which are linear combinations of atomic C $1s$, $2s$, and $2p$ orbitals. The atomic orbitals were expressed as combinations of sixteen Gaussian-type orbitals with decaying exponents ranging from 50000 to 0.15. A high degree of accuracy in fitting the electron charge distribution as a sum of atom-centered Gaussian functionals has been achieved [16]. Because of the large unit cell, only two special k points were used in the self-consistent cycle, while for the density-of-states (DOS) calculation, 89 k points in the irreducible portion of the fcc Brillouin zone (BZ) were employed. The large degree of k-point sampling in the BZ in conjunction with the linear analytic tetrahedron method enabled us to evaluate the DOS with high precision without using the Gaussian broadening procedure which may wash out van Hove singularities. For the optical calculation, we have limited the transition frequency to within the 10 eV range, i.e., all interband transitions from 10 eV below the top of the occupied valence band (VB) to 10 eV above are included. All relevant dipole matrix elements associated with each pair of transitions at each k point were included using the wave functions obtained from the band calculation. Symmetry-forbidden transitions were automatically excluded by having zero transition matrix elements between the Bloch states.

Figure 1 shows the calculated band structure near the gap. This band structure is similar to the work of Ref.

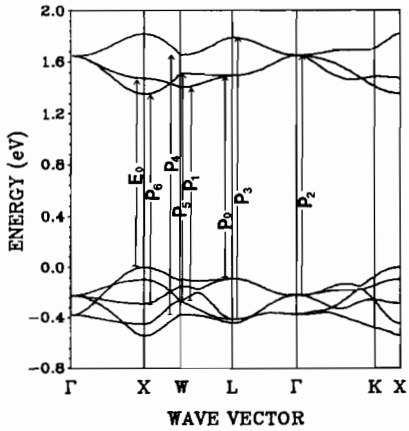

FIG. 1. Calculated band structure of C_{60} in the fcc lattice near the gap. Arrows show critical-point transitions.

Analytic solution of a two-dimensional hydrogen atom. I. Nonrelativistic theory

X. L. Yang, S. H. Guo,* and F. T. Chan
Department of Physics, University of Arkansas, Fayetteville, Arkansas 72701

K. W. Wong
Department of Physics and Astronomy, University of Kansas, Lawrence, Kansas 66045

W. Y. Ching
Department of Physics, University of Missouri–Kansas City, Kansas City, Missouri 64110
(Received 12 March 1990; revised manuscript received 20 September 1990)

The two-dimensional hydrogen problem is solved analytically. In the nonrelativistic case, exact formulas for energy eigenvalues and eigenfunctions for both the discrete and continuous parts of the spectrum, dipole matrix elements, dc Stark effect, single- and two-photon transition rates, and fine and hyperfine structures are obtained. Comparison is made between the two- and the three-dimensional cases. Some interesting aspects of the solution unique to the two-dimensional case are discussed.

I. INTRODUCTION TO TWO-DIMENSIONAL HYDROGEN ATOM

The hydrogen atom is the name given to the system composed of an electron with mass m_e and charge $-e$ and a positively charged nucleus (Ze) located at the origin of the coordinate system. The central force between the electron and the nucleus is determined by the attractive Coulomb potential function,

$$V(r)=-\frac{Ze^2}{r} . \tag{1.1}$$

The three-dimensional (3D) hydrogen atom played a central role in the early formulation and development of quantum mechanics and is now part of the standard curriculum in modern undergraduate physics.

If the motion of the electron around the nucleus is constrained in a plane by certain boundary conditions, then such a system is called the two-dimensional hydrogen atom. We would like to point out that "2D" in the name "2D hydrogen atom" only emphasizes that the motion of the electron around a positive point charge (not a line charge) is constrained in a plane. This system is not 2D in a strict sense that all fields including electromagnetic fields, photon emission, angular momentum, and spin are not confined to a plane.

The quantum-mechanical properties of the 2D hydrogen atom are the subject of this investigation. In this paper, paper I, we give a full account of the nonrelativistic description of a two-dimensional hydrogen atom. A detailed presentation[1] of the complete theory including the relativistic case and the Chern-Simons term will appear in paper II (we will refer to it as II) of this series. In the following section, we will present the solutions to the nonrelativistic case while in Sec. III some concluding remarks are made. Possible implications and potential applications to other branches of physics are pointed out.

Atomic units will be used unless otherwise stated.

II. NONRELATIVISTIC THEORY

The eigenstates of a 2D hydrogen atom are described by the Schrödinger equation, in polar coordinates,

$$\left[-\frac{\hbar^2}{2m_e}\left[\frac{\partial^2}{\partial r^2}+\frac{1}{r}\frac{\partial}{\partial r}+\frac{1}{r^2}\frac{\partial^2}{\partial\varphi^2}\right]-\frac{Ze^2}{r}\right]\psi(r,\varphi) =E\psi(r,\varphi) . \tag{2.1}$$

Using separation of variables

$$\psi(r,\varphi)=R(r)\Phi(\varphi) , \tag{2.2}$$

we obtain

$$\Phi(\varphi)=\frac{1}{(2\pi)^{1/2}}e^{il\varphi}, \quad l=0,\pm1,\pm2,\ldots \tag{2.3}$$

and

$$\frac{d^2}{dr^2}R(r)+\frac{1}{r}\frac{d}{dr}R(r) +\left[\frac{2m_e}{\hbar^2}\left[E+\frac{Ze^2}{r}\right]-\frac{l^2}{r^2}\right]R(r)=0 . \tag{2.4}$$

Equation (2.4) is the 2D radial Schrödinger equation; its solution $R(r)$, depends only on $|l|$. Solution (2.3) is also the eigenfunction of the angular momentum along the z direction

$$\hat{L}_z=-i\hbar\frac{\partial}{\partial\varphi} , \tag{2.5}$$

which commutes with the Hamiltonian. Hence l is a good quantum number.

Solid State Communications, Vol. 76, No. 12, pp. 1351–1356, 1990.
Printed in Great Britain.

0038-1098/90 $3.00 + .00
Pergamon Press plc

VANADIUM–LEAD SUBSTITUTED 2223 Bi–Sr–Ca–Cu–O SUPERCONDUCTORS

Ying Xin, Z. Z. Sheng and F. T. Chan

Physics Department, University of Arkansas, AR, USA

and

P. C. W. Fung and K. W. Wong*

Physics Department, University of Hong Kong, Hong Kong

(*Received* 20 *August* 1990 *by W. Y. Kuan*)

Following up our previous work [24] on the fabrication of the $Bi_{2-x}V_xSr_2Ca_2Cu_3O_y$ and $Bi_{2-x}V_xSr_2CaCu_2O_8$ superconductors with x ranging from a fraction to unity we report here the fabrication of double-substituted superconducting ceramics satisfying the nominal stoichiometric ratio of $Bi_{2-(x+y)}V_xPb_ySr_2Ca_2Cu_3O_q$, where x, y run from small fractions to 0.7. For most of the samples, the lower T_c = 80 K phase disappears, leaving the higher T_c = 110 K phase. Since a wide range of combinations of x, y can lead to similar superconductors and that the pure T_c = 110 K phase samples are associated with larger values of $(x + y)$, we believe that the V–Pb substitution is significantly different from the Pb-doped or Pb–Sb-doped cases in the basic crystal structure. Our samples are found to pass through the paramagnetic to the diamagnetic state as the temperature is decreased across the critical temperature region.

1. INTRODUCTION

IT HAS been found that there are quite a large number of crystal structures or phases that can co-exist or exist under separate conditions in the class of Bi–Sr–Ca–Cu–O superconductors [1–5]. For examples, there are nominal compositions satisfying Bi : Sr : Ca : Cu = 2:2:0:1 ($T_c \sim$ 10 K), 1:1:1:2 ($T_c <$ 80 K), 2:2:1:2 ($T_c \sim$ 80 K) and 2:2:2:3 ($T_c \sim$ 110 K). While the lowest order phase (2201) is mono-clinic, the other phases so far reported seem to have average orthorhombic structures with different crystal parameters. The (2201), (2212) and (2223) phases have single, double, and triple layers of CuO_2 plane in the sub-unit cell respectively, and more CuO_2 planes are believed to be associated with higher values of T_c. It is therefore important to enhance the (2223) 110 K phase by using various methods of preparation [e.g. 6, 7] or by doping. In fact, Al, La, Sb and Pb doped in the Bi-type superconductors [8–21] have been reported and the last member Pb has been found to be a rather good dopant in enhancing the 110 K phase. The double doping with Pb–Sb has aroused interest along this line [22, 23]. However, only a very limited amount of the dopant can replace Bi, in the nominal composition (< 40%).

In order to understand more fully about the role played by dopants of the high T_c phases of the Bi-type superconductors, it is crucial to find out whether other dopant(s), apart from Pb, could also enhance the formation of the high T_c phase(s). Even more important it is crucial to find out whether any other element can have an equal standing as Bi; at the end, we hope that Bi can be replaced completely such that a new superconductor class can be found. The recent band structure calculations [24] on a hypothetical structure same as the bismuth structure but with the composition $V_2Sr_2Ca_1Cu_2O_8$ produce a band structure favouring the formation of condensed charged excitons. According to the EEM theory [25, 26] a superconductor would result if such a condition is satisfied. Thus such an estimation suggests that vanadium might be used to replace Bi, at least partially. With this motivation in mind, we have attempted and have succeeded in replacing Bi by V in the predetermined (2212) and (2223) superconductors up to at least a ration of r = V/Bi = 1. We have demonstrated that the R–T curves show clear sudden drops at about 110 K, though the T_c (R = 0) value is only several degrees above that of the pure Bi-type superconductor prepared under same conditions. The readiness in the formation of the

* Permanent address: Physics Department, University of Kansas, KS 66045, USA.

The Runge–Lenz vector for the two-dimensional hydrogen atom

X. L. Yang, M. Lieber, and F. T. Chan
Physics Department, University of Arkansas, Fayetteville, Arkansas 72701

(Received 21 February 1990; accepted for publication 30 June 1990)

The recent discovery of novel properties possessed by two-dimensional systems has led to the investigation of properties of the hydrogen atom in two dimensions. With proper definition of the system, the so-called Runge–Lenz vector may be defined for this system, and shown to be related to the underlying $O(3)$ symmetry, just as for the three-dimensional system, although some interesting aspects are revealed.

I. INTRODUCTION

Much interest has been developing in the properties of two-dimensional systems. The existence of Chern–Simons terms[1] and the existence of anyons[2] that violate the theorem on spin and statistics are but two examples. There are also examples where two-dimensional behavior has been exhibited experimentally, such as the propagation of electrons in high-T_c superconductors, where the two-dimensionality is apparently imposed by the planes of copper atoms.[3] For the latter systems in particular the analysis of the two-dimensional hydrogen atom may be particularly relevant.

It is by now well known that the hydrogen atom in three dimensions exhibits an "accidental degeneracy" due to a "hidden" four-dimensional rotational group [$O(4)$] symmetry and the presence of an additional conserved vector, most commonly called the Runge–Lenz vector although actually much older than these two authors.[4] Indeed, in 1935 Fock[5] showed how to cast the momentum-space form of the Schrödinger integral equation into the equation for $O(4)$ hyperspherical harmonics. The connection of this approach with the older Runge–Lenz vector approach utilized by Pauli[6] in his solution of the hydrogen atom problem was exhibited by Bargmann,[7] who showed that linear combinations of the components of the Runge–Lenz vector and the angular momentum vector obeyed the commutation relations of the Lie algebra of $O(4)$ [or, more precisely, of $O(3)\times O(3)$ which is isomorphic to $O(4)$].

The approach of Fock was generalized to d dimensions by Alliluev.[8] In particular, he showed that the hydrogen atom in d dimensions exhibits the symmetry of the $(d+1)$-dimensional rotation group when expressed in momentum space, and the wave functions are nothing more than hyperspherical harmonics. His solution also pertains for the case $d=2$. In this case he finds for the energy levels in atomic units:[9]

$$E_n = -1/2(n-\tfrac{1}{2})^2, \tag{1}$$

where $n = 1,2,3,...$, and the momentum space wave functions are the ordinary $O(3)$ spherical harmonics Y_{nm}. However, the analogous $d=2$ generalization of the Runge–Lenz vector does not appear to have been previously discussed, so that is the gap that we feel it is now opportune to fill.

Before turning to the main body of this work, it is perhaps worth mentioning that there is some controversy as to the "correct" generalization of the Coulomb potential. Our approach is based on a potential proportional $1/r$, where r is the distance from the origin in d-dimensional space. An alternative definition, which coincides in the case $d=3$, arises from the desire to preserve Maxwell's equations, and particularly Gauss' law: The electric flux through a spherical hypersurface should be proportional only to the total charge enclosed, and be independent of the radius of the sphere. For $d=2$ this gives rise to a potential proportional to $\ln(r)$. For a recent paper on this potential see Ref. 10. However, it is our view that the $1/r$ potential is the more natural for $d=2$ since there are cases in which the motion of the electron around the nucleus is constrained in a plane by certain boundary conditions. The planar confinement to such a system can be a result of extreme anisotropy.

II. THE 2-D HYDROGEN ATOM

In two dimensions the Hamiltonian of our system may be written (using atomic units):

$$H = \tfrac{1}{2}(p_x^2 + p_y^2) - 1/r. \tag{2}$$

The angular momentum vector degenerates to a single component $L = L_z$:

$$L = xp_y - yp_x. \tag{3}$$

The Runge–Lenz vector $\mathbf{A}$, which in three dimensions is defined by

$$\mathbf{A} = \mathbf{r}/r - \tfrac{1}{2}(\mathbf{p}\times\mathbf{L} - \mathbf{L}\times\mathbf{p}) \tag{4}$$

degenerates to a two-dimensional vector:

$$A_x = x/r - \tfrac{1}{2}(p_yL + Lp_y),$$
$$A_y = y/r + \tfrac{1}{2}(p_xL + Lp_x). \tag{5}$$

The three quantities L, A_x, and A_y all commute with H and so are conserved. Their mutual commutation relations can be shown to be

$$[L, A_x] = iA_y, \tag{6}$$

$$[L, A_y] = -iA_x, \tag{7}$$

and

$$[A_x, A_y] = -2iHL. \tag{8}$$

Now, let us assume that the operators are operating on states that are all eigenstates of H with eigenvalue E, which we take to be negative, since we are interested in bound states. If we define new operators on this manifold:

$$\mathbf{u} = \mathbf{A}/\sqrt{(-2E)}, \tag{9}$$

then we may define a *three*-dimensional vector operator $\mathbf{N}$, with components $N_x = u_x$, $N_y = u_y$, and $N_z = L$ that satisfy the commutation relations characteristic of the components of an ordinary angular momentum operator in three dimensions. That is, using $H \to E$ in Eq. (8):

$$[N_i, N_j] = i\epsilon_{ijk}N_k. \tag{10}$$

These define the Lie algebra su(2), and familiar arguments

Solid State Communications, Vol. 76, No. 12, pp. 1357–1360, 1990.
Printed in Great Britain.

0038–1098/90 $3.00 + .00
Pergamon Press plc

DOUBLE TRANSITION IN CALCIUM-123 ($CaSr_2Cu_3O_y$) SUPERCONDUCTOR

Xin Fei, D.F. Lu, G.F. Sun and K.W. Wong

Physics Department, University of Kansas, KS 66045, USA

F.T. Chan, Z.Z. Sheng and Ying Xin

Physics Department, University of Arkansas, AR, USA

P.C.W. Fung and C.C. Lam*

Physics Department, University of Hong Kong, Hong Kong

and

W.Y. Ching and Y. Xu

University of Missouri, Kansas City, MO, USA

(*Received* 20 *August* 1990 *by W.Y. Kuan*)

The Ca^{2+} is successfully substituted for the 3+ rare earth element in the 123 ceramic structure. A double phase transition is observed in oxygen deficient samples. A superconducting transition onset occurs at 90 K, and all resistivity vanishes at 73 K. However, at a lower temperature of 50 K the sample exhibits a superconducting to insulating transition. The double transition in R–T is accompanied by a corresponding double magnetic transition in χ–T.

1. INTRODUCTION

THE Y-123 superconducting ceramic appears to be the only cuprate so far found that is stoichiometric [1], which makes the study of its electronic structure [2–5] less complicated. However, it is also well known that oxygen deficiency can occur in this material, and as oxygen molar ratio in the compound reduces below 6.5, the compound goes through an antiferromagnetic phase transition at a temperature close to the original non oxygen deficient superconducting critical temperature, and no superconducting phase is realized in this sample. This apparent antiferromagnetic phase transition near the superconducting critical temperature under oxygen deficient condition has drawn theorists to speculate that there is a coupling between the spin–spin interaction and the superconducting mechanism [6]. Since most high temperature superconductors contain copper, which has a d-orbital electron, it is difficult to delineate the magnetic moment interaction from charge electronic interactions which is responsible for the BCS [7] low T_c superconducting mechanism. We have proposed a purely charge electronic model [8] which has ignored the magnetic moment interacting terms for the explanation of the high T_c mechanism. This theory has been received with skepticism by others and is rightly so because of the above mentioned presence of an antiferromagnetic phase in some of the ceramic cuprate superconductors. Another rather puzzling fact also dealing with the Y-123 compound, is that there exists a tetragonal phase with 6 oxygen in the unit cell. This phase has similar lattice parameters and rather close electronic structures. Except that the copper oxide chain is replaced by a pure copper plane, thus in the electronic structure intrinsic hole states due to the copper oxide chain is missing [9]. The tetragonal Y-123 phase is not a superconductor. In the earlier days, people speculated the importance of the copper oxygen chain structure. Unfortunately, other experimental investigations, such as μ-spin relaxation, internal friction experiments [10] etc., all points to the contribution of the copper oxygen plane instead. Thus it appears to us that the oxygen deficiency in the copper oxygen chain serves more in enhancing the formation of the antiferromagnetic phase rather than the superconducting phase. In fact, since the presence of the antiferromagnetic phase in the oxygen deficient compound also precludes the existence of superconductivity in these

* Permanent address: Department of Applied Science, City Polytechnic of Hong Kong.

Solid State Communications, Vol. 76, No. 12, pp. 1347–1350, 1990.
Printed in Great Britain.

0038–1098/90 $3.00 + .00
Pergamon Press plc

OPTIMUM FABRICATION PROCESS AND SOME RELEVANT ANALYSIS FOR THE VANADIUM–LEAD DOUBLY SUBSTITUTED 2223 SUPERCONDUCTING CERAMICS

Ying Xin, Z.Z. Sheng, F.T. Chan

Physics Department, University of Arkansas, AR, USA

and

P.C.W. Fung and K.W. Wong*

Physics Department, University of Hong Kong, Pokfulam Road, Hong Kong

(*Received* 20 *August* 1990 *by W.Y. Kuan*)

In a previous investigation [2], we have fabricated the superconductor satisfying the nominal stoichiometric composition $Bi_{2-(x+y)}V_xPb_ySr_2Ca_2Cu_3O_q$, where x, y cover wide ranges of combinations, based on a particular preheating and sintering procedure. We follow up such work by exploring other solid state sintering processes and have found an optimum method via which we can fabricate very good superconductors with $T_c^s = 118\,K$ and $T_c\ (R = 0) = 108\,K$. X-ray analysis indicates that more than 95% of the typical sample belongs to the 2223 structure. All our samples show a paramagnetic – diamagnetic transition within a very small temperature range which is greater than T_c $(R = 0)$ and smaller than T_c^s.

1. INTRODUCTION

IN OUR series of work on the fabrication and related analysis of substituted Bi–Sr–Ca–Cu–O superconducting ceramics, we have shown that when Bi is partially replaced by vanadium, the 110 K phase can be significantly enhanced. Moreover, we have found that vanadium behaves more than a dopant in the sense that V and Bi can have equal weighting in their nominal atomic ratios [1]. Such a study is supported by band structure analysis. Following, we have remarked that if there is one type of doping or substitution, the resulting crystal structure may not be balanced. Rather, double substitution could allow for a balance of atomic sizes and Coulombic forces in the atomic arrangement within a superconducting unit cell. Consequently, we have fabricated the doubly substituted superconducting ceramics with the predetermined stoichiometric composition $Bi_{2-(x+y)}V_xPb_ySr_2Ca_2Cu_3O_q$ using one particular sintering process; here x and y ran for a range of fractions [2]. We have discovered that for a wide range of combinations of V and Pb, the critical temperature $T_c\ (R = 0)$ can be raised from typically $\sim 80\,K$ (due to the presence of the 2212 phase) to $T_c\ (R = 0)$ over 100 K. From such a result, we believe that the double substitution process represents an ordered one, preserving the 2223 structure. It would naturally be fruitful to explore some other sintering processes to improve the qualities of the samples. It would also be meaningful to carry out a careful analysis to find out the ratio of the 2223 and 2212 structures in the sample directly. These ideas provide the motivation of the investigation reported here.

2. EXPERIMENTATION

As before, appropriate AR grade powders of Bi_2O_3, SrO, CaO and CuO were mixed and ground in the nominal stoichiometric composition of $BiSr_2Ca_2Cu_3O_5$, the precursor. The resulting material was heated in a tube furnace at 820°C for 20 h with both ends of the tube open. After cooling in air, the precursor was ground again; then appropriate amounts of Bi_2O_3 and V_2O_3, PbO_2 powders of AR grade were mixed to prepare the sample according to the predetermined atomic proportion $Bi_{2-(x+y)}V_xPb_ySr_2Ca_2Cu_3O_q$. The preparation and the first stage of the sintering process is that as reported earlier, called sintering process A[2]. These samples further received different heating and cooling treatments as specified in Table 1. If we do not state the atmospheric gas like Ar or O_2, the samples were heated in air with both ends of the tube

* Permanent address: Physics Department, University of Kansas, KS 66045, U.S.A.

Solid State Communications, Vol. 75, No. 3, pp. 211-216, 1990.
Printed in Great Britain.

0038-1098/90$3.00+.00
Pergamon Press plc

VANADIUM SUBSTITUTED 2212 AND 2223 SUPERCONDUCTING CERAMICS

P.C.W. Fung, Z.C. Lin, Z.M. Liu
University of Hong Kong

Ying Xin, Z.Z. Sheng, F.T. Chan
University of Arkansas

K.W. Wong
University of Kansas

Yong-Nian Xu, W.Y. Ching
University of Missouri-Kansas City

(Received March 31, 1990 by W.Y. Kuan)

We report the successful fabrication of the ceramic superconductor $Bi_{2-x}V_xSr_2Ca_2Cu_3O_y$ and $Bi_{2-x}V_xSr_2CaCu_2O_8$, with x ranging from a fraction to at least unity, showing that Vanadium behaves more than a dopent. The critical temperatures of these phases remain a few degrees higher than that of the pure bismuth case subject to similar fabrication processes. The 110 K phase in the predetermined superconductor (2223) is significantly enhanced when V is mixed in. Relevant results of band structure calculations are also presented to provide physical explanation of choosing the element Vanadium according to the EEM theory.

I. INTRODUCTION

Since the discovery of the high Tc ceramic Bi-Sr-Ca-Cu-O system [1-4], it has been found that there are quite a large number of crystal structures or phases that can co-exist in the resulting superconductors. Crystal structure analysis reveals that the superconducting phases of the crystals (2201), (2212) and (2223) have single double, and triple layers of the CuO_2 plane in the sub-unit cell respectively.

During the past two years, a lot of effort has been devoted to the study of various properties and phase structure of this class of superconductor. For example, in [5], a study of higher order structures (4334), (4424) was carried out, together with an oxygen content analysis result using thermogravimetric experimentation. Anomaly and hysteresis in ultrasonic velocity in $BiSrCaCu_2Oy$ was reported [6]. Preparation of single structure (2212) ceramic was shown to be achieved by "melt and annealing" process. A rather detailed analysis of the electronic structure of the (2332) crystal using the photoemission and electron-energy-loss spectroscopy techniques was reported in [8]. In order to study the ordering of crystal composition in a wide range of temperature (88-623K) for the predetermined (1112) ceramic, the internal friction and shear modulus measurements were carried out in [9]. Specific heat study of the (1112) crystal was reported [10] in the range (2.5 to 300K). In [11], magneto-electrical measurements of the predetermined (2213) superconductor was carried out; the result of Hall coefficient measurement suggests that superconducting grains are interconnected by Josephson-like junctions (a kind of "weak-link"). Elastic anisotropy property and lattice instability study for the single crystal of (2212) was carried out at various temperature [12]. Critical current density of the (1112) superconductor was measured to be 8.6 * 105 A cm-2 at a few thousand Oe [13].

While effort like using different thermal treatment, pressure has been devoted to the study of the pure Bi-Sr-Ca-Cu-O ceramic in order to enhance the (2223) 110K phase, much study has been reported on attempting to achieve the same goal by doping. For example, Al and La were included in the bismuth type superconductor [14,15]. It has been reported by various sources that Pb is a good dopent [15-20]; internal friction study of double doping like (Pb,Fe) on the Bi-type superconductor appeared [21]. It is thought that the (2223) phase can be enhanced by choosing the right dopent. The resulting rise in Tc, or improvement of Jc etc. is very sensitive to the various methods of treatment in the fabrication of the sample (see e.g.[22]). We would also note that the dopent (like Pb) has replaced only a certain amount, up to at most about 40%, of Bi.

In order to understand better the Bi-type superconductors, or more general, the none-rare earth type of superconductors, it is crucial to find out whether Bi can be replaced completely, or that any element can have an equal standing as Bi. Based on the EEM theory [e.g. 23, 24] band structure analysis of some compounds has been carried out and it is found that by assuming the same lattice parameters

Brief Reports

Brief Reports are short papers which report on completed research which, while meeting the usual **Physical Review** *standards of scientific quality, does not warrant a regular article. (Addenda to papers previously published in the* **Physical Review** *by the same authors are included in Brief Reports.) A Brief Report may be no longer than 3½ printed pages and must be accompanied by an abstract. The same publication schedule as for regular articles is followed, and page proofs are sent to authors.*

Retardation in two-photon absorption

X. L. Yang, F. T. Chan, and M. Lieber
Department of Physics, University of Arkansas, Fayetteville, Arkansas 72701
(Received 27 January 1989)

Previous calculations of two-photon absorption and emission in hydrogen have revealed frequencies at which the transition is forbidden, at least within the approximations made. Here we show that if retardation is taken into account these so-called "transparency frequencies" are slightly shifted, but the zero transition amplitude persists.

INTRODUCTION

In recent papers on two-photon absorption and emission processes in atomic hydrogen,[1] it was discovered that certain photon frequencies were forbidden. Considering emission, for example, in the $3s$- $1s$ transition, there are two photons emitted of frequencies ω_A and ω_B such that the total energy of the two photons equals the energy difference between the $3s$ and $1s$ levels, i.e., 12 eV. However, the amplitude for this process passes through two zeros, symmetrically placed on either side of the equal frequency point $\omega_A=\omega_B$. (There are no zeros in the two-photon decay of the $2s$ metastable state.) The same amplitude governs the two-photon absorption process $1s$-$3s$, and so there exist two frequencies at which this absorption cannot take place; we call these the "transparency frequencies"[2] for either emission or absorption. Thus, since there is no corresponding amplitude zero at these transparency frequencies for the $1s$-$3d$ process, there is suggested a means for selective excitation of the $3d$ level. Transparency frequencies were found[1] for transitions between the $1s$ and ns levels for $n=3$, 4, 5, and 6, between the $1s$ and nd levels for $n=4$, 5, and 6, between the $2s$ and ns levels for $n=4$, 5, and 6, and between the $2s$ and nd levels for $n=5$ and 6.

The above remarks are based on calculations which use second-order perturbation theory and the dipole (long-wavelength) approximation.[1] It has recently been suggested to the authors[3] that the transparency phenomenon might disappear when retardation effects are taken into account. The reason for this expectation is that the amplitude as previously calculated is the sum of two terms, each representing one ordering of the emission of the two photons. In the dipole approximation these two terms are *real* for the $1s$-$3s$ case, and at the transparency frequencies they exactly cancel (in other cases the two terms are sometimes purely imaginary, with the same result). However, when retardation is included the relevant matrix elements would appear to be complex, and the cancellation thus much more unlikely. The purpose of this Brief Report is to show that simple parity arguments indicate that the terms remain real (or pure imaginary if the conventions of Ref. 1 are followed), but shift their value slightly. Thus the transparency condition persists, albeit at slightly shifted frequencies.

CALCULATION

When retardation is taken into account, the ns-$1s$ transition rate is proportional to the square of the modulus of the second-order perturbation theory expression

$$A_{ns\text{-}1s} \propto \left| \sum_I \left[\frac{M_I^{(1)}}{E_I-E_1-\hbar\omega_B} + \frac{M_I^{(2)}}{E_I-E_1-\hbar\omega_A} \right] \right|^2 , \quad (1)$$

where $M_I^{(1)}$ is

$$M_I^{(1)} = \langle ns | e^{i\mathbf{k}_A\cdot\mathbf{r}} \hat{\epsilon}_A\cdot\mathbf{p} | I \rangle \langle I | e^{i\mathbf{k}_B\cdot\mathbf{r}} \hat{\epsilon}_B\cdot\mathbf{p} | 1s \rangle , \quad (2)$$

and where I represents an arbitrary intermediate hydrogenic state including the continuum. In this expression $\hat{\epsilon}_A$ and $\hat{\epsilon}_B$ are the polarization vectors of the two photons. We have used the Coulomb gauge interaction Hamiltonian $-e\,\mathbf{A}\cdot\mathbf{p}/mc$, dropping the A^2 term which can never contribute to processes in which the electron changes energy levels. We note that this Hamiltonian differs from the $\mathbf{r}\cdot\mathbf{E}$ form used in our previous work[1] because the latter is equivalent to the $\mathbf{A}\cdot\mathbf{p}$ form only in the dipole approximation, whereas the $\mathbf{A}\cdot\mathbf{p}$ form is generally valid to all orders, according to the principle of minimal coupling. $M_I^{(2)}$ in Eq. (1) is the same as $M_I^{(1)}$ in Eq. (2) except for the exchange of the two photons, $A\leftrightarrow B$. Let us look at a typical matrix element of the form occurring in the M_I:

$$\langle nlm | e^{i\mathbf{k}\cdot\mathbf{r}} \hat{\epsilon}\cdot\mathbf{p} | n'l'm' \rangle . \quad (3)$$

Using De Moivre's theorem we may write the operator

Shifted $1/N$ expansion for the Hulthén potential

A. Z. Tang and F. T. Chan
Physics Department, University of Arkansas, Fayetteville, Arkansas 72701
(Received 19 June 1986)

The shifted $1/N$ expansion method is applied to the Hulthén potential. Numerical results for the energy values for $n=1-5$ states are presented. For $l=0$ states, the agreement between our results and the exact analytical solution is excellent.

Large-N expansion approximations have recently received much attention[1,2] because they offer the possibility of analytically handling interactions which need not be small. In the context of the nonrelativistic Schrödinger equation, it is interesting to note that for spherically symmetric potentials N and l always appear together in the form $k \equiv N+2l$, N being the number of spatial dimensions and l the eigenvalue of the N-dimensional orbital angular momentum. For the power-law potential $V(r)=Ar^{\nu}$, systematic and analytic procedures for finding the energy eigenvalue have been developed to successive orders in the parameter $1/k$. At the end of the calculation N is set equal to the physical value 3. Since $1/k \simeq \frac{1}{3}$ is not a very small expansion parameter, to obtain accurate results with perturbation theory one must calculate many orders, each order getting progressively much more complicated.

To improve series convergence, Sukhatme, Imbo, and Pagnamenta[3,4] have recently constructed a modified version of the $1/N$ expansion for the Schrödinger equation. This method, called the shifted $1/N$ expansion, uses the quantity $1/\bar{k}$ as an expansion parameter, where $\bar{k}=k-a=N+2l-a$, and a is a suitable shift and a negative number. In a subsequent paper,[5] they applied the method to the Yukawa potential $V(r)=-Ae^{-\beta r}/r$. In comparison with the "exact" numerical results, the shifted $1/N$ expansion scheme indeed surpasses all other currently available approximation procedures "for its simplicity, accuracy, and wide range of applicability."

In this paper we study the Hulthén potential via the shifted $1/N$ expansion technique. The Hulthén potential is exactly solvable only for the $l=0$ states, thereby providing an excellent check for the method; such checks are important because they give us confidence in the results of $l \neq 0$ states. Atomic units will be used unless otherwise stated.

The Hulthén potential[6]

$$V(r)=-\frac{\delta e^{-\delta r}}{1-e^{-\delta r}} \tag{1}$$

is of considerable interest and importance in atomic physics. In Eq. (1) δ, a constant, is called the screening parameter. To the best of our knowledge, the exact analytic energy eigenvalues are available only for $l=0$ states[6-8] and are given by

$$E_{n0}^{\text{exact}}=-\frac{\delta^2}{2}\left[\frac{2/\delta-n^2}{2n}\right]^2, \tag{2}$$

with

$$n^2<\frac{2}{\delta}, \tag{3}$$

which means that the number of bound states is limited. For very small screening parameter δ, the Hulthén potential reduces to the Coulomb potential $1/r$, and the corresponding energy eigenvalues, Eq. (2), reduce to

$$E_n^{\text{Coulomb}}=-\frac{1}{2n^2}, \tag{4}$$

which is the Coulomb energy level, as expected.

We refer the reader to Refs. 4 and 5 for the detailed derivation of the formulas needed in this work. (Our notation follows that of these two references which will be referred to as IPS1 (Ref. 4) and IPS2,[5] respectively; IPS1 Eq. (4) means Eq. (4) of IPS1.)

The energy eigenvalues are given by IPS2 Eq. (3) as an expression in powers of $1/\bar{k}$,

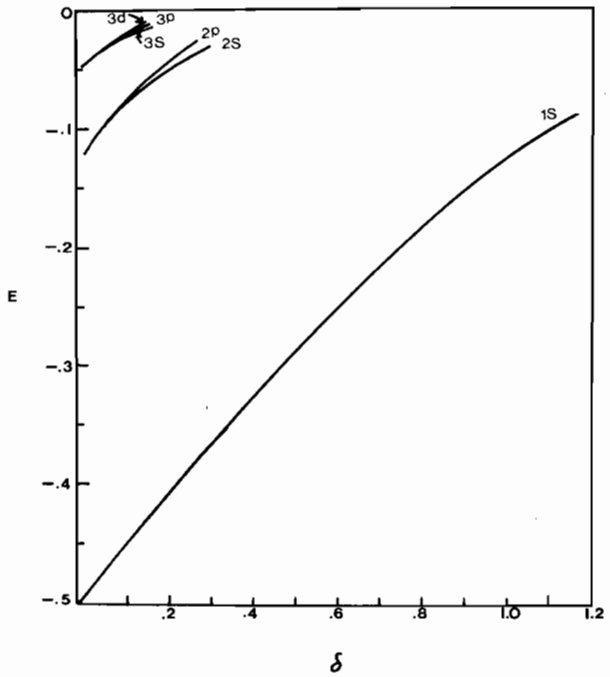

FIG. 1. Energy eigenvalues for $n=1-3$ Hulthén states as a function of δ. As $\delta \to 0$, curves for different l states (same n) approach each other owing to the accidental symmetry of the Coulomb potential.

J. Phys. A: Math. Gen. 20 (1987) 3771-3775. Printed in the UK

An exact propagator for a time-dependent harmonic oscillator with a time-dependent inverse square potential

Bin Kang Cheng† and F T Chan‡

† Departamento de Física, Universidade Federal do Paraná, Caixa Postal 19.081, 81.504 Curitiba, Brazil

‡ Department of Physics, University of Arkansas, Fayetteville, Arkansas 72701, USA

Received 30 April 1986, in final form 27 October 1986

Abstract. Using Feynman's polygonal paths for path integrals, the exact evaluation of the propagator for a time-dependent harmonic oscillator with a time-dependent inverse square potential becomes possible. The propagator at and beyond caustics is then evaluated by including the Maslov correction factor. Finally, we obtain the wavefunctions from the propagator obtained.

In this paper we consider a harmonic oscillator with time-dependent mass $M(t)$ and frequency $\omega(t)$ moving in one dimension under a time-dependent inverse square potential. The Lagrangian is given by

$$L(\dot{x}, x, t) = \tfrac{1}{2}M(t)(\dot{x}^2 - \omega^2(t)x^2) - g(t)/x^2 \tag{1}$$

where $M(t)g(t) > -\hbar^2/8$ to avoid 'the fall to the centre' (Landau and Lifshitz 1958). We shall restrict ourselves to studying the region $x \geq 0$ only since the solution in this region can be extended to $x < 0$ by using analytic continuation. For later convenience, we set $r' = r(t')$, $r'' = r(t'')$ and $r_j = r(t' + j\varepsilon)$ $(\varepsilon = (t'' - t')/N)$ for any function $r(t)$ of time t.

Using Feynman's polygonal paths (Feynman and Hibbs 1965), the short-time action can be written as

$$\begin{aligned} S_j(x_{j-1}, x_j) &= \frac{M_j}{2\varepsilon}(x_j - x_{j-1})^2 - \frac{\varepsilon}{2}M_j\omega_j^2 x_j^2 - \frac{\varepsilon g_j}{x_j x_{j-1}} \\ &= \frac{M_j}{2}\left(\frac{x_j^2 + x_{j-1}^2}{\varepsilon} - \varepsilon\omega_j^2 x_j^2\right) - \left(\frac{M_j x_j x_{j-1}}{\varepsilon} + \frac{\hbar^2(\nu_j^2 - \frac{1}{4})}{2M_j x_j x_{j-1}}\right) \end{aligned} \tag{2}$$

with $\nu_j = \frac{1}{2}(1 + 8M_j g_j/\hbar^2)^{1/2}$. Applying the asymptotic form of the modified Bessel function

$$I_{\nu_j}(u/\varepsilon) = (\varepsilon/2\pi u)^{1/2}\exp\left(\frac{u}{\varepsilon} - \frac{\varepsilon}{2u}(\nu_j^2 - \tfrac{1}{4}) + O(\varepsilon^2)\right) \tag{3}$$

for small ε, we have

$$\begin{aligned} \exp\left(\frac{\mathrm{i}}{\hbar}\sum_{j=1}^{N} S_j(x_{j-1}, x_j)\right) &= \prod_{j=1}^{N}\left(\frac{2\pi M_j x_j x_{j-1}}{\mathrm{i}\hbar\varepsilon}\right)^{1/2} I_{\nu_j}\left(\frac{M_j x_j x_{j-1}}{\mathrm{i}\hbar\varepsilon}\right) \\ &\quad \times \exp\left[\frac{\mathrm{i}M_j}{2\hbar}\left(\frac{x_j^2 + x_{j-1}^2}{\varepsilon} - \varepsilon\omega_j^2 x_j^2\right)\right]. \end{aligned} \tag{4}$$

0305-4470/87/123771+05$02.50

On the Second-Order Terms of Perturbation Theory

P. Froelich

Department of Quantum Chemistry, Uppsala University, Box 518, S-751 20 Uppsala, Sweden

F. T. Chan

Physics Department, University of Arkansas, Fayetteville, Arkansas 72701, USA.

Received 11 May 1987; 17 November 1987

The calculation of the higher-order transition amplitudes presents an old and well known problem of computational quantum mechanics. The origin of the problem is that the application of perturbation theory to the scattering theory formulas for transition amplitudes leads to expressions which are singular mathematically, and therefore difficult to handle numerically. Another difficulty is connected to the presence of infinite summations over the continuum of intermediate states. As an example we can mention the well known Born series for the transition amplitude.[1] The higher-order contributions contain the expectation values with respect to the resolvent operator

$$\begin{aligned} T_{fi} &= \langle \varphi_f | V_f | \varphi_i \rangle \\ &\quad + \lim_{\epsilon \to 0} \langle \varphi_f | V_f (E - H_i)^{-1} V_i | \varphi_0 \rangle + \ldots \\ &= \text{first Born term } B^{(1)} \\ &\quad + \text{second Born term } B^{(2)} + \ldots \end{aligned} \tag{1}$$

Evaluation of terms containing the resolvent operator $R = (E - H)^{-1}$ is a prerequisite of the beyond-first Born treatment, and the difficulties involved are the main hindrance to development in the area of cross-section calculations. These difficulties are connected to the highly singular nature of the expectation value of the resolvent

$$B^{(2)} = \lim_{\epsilon \to 0} \int \frac{\langle \varphi_f | V_f | \varphi_i \rangle \langle \varphi_i | V_i | \varphi_0 \rangle}{E - E_i \pm i\epsilon} dE_i \tag{2}$$

In the simplest cases (like the hydrogen atom) the summation/integration over the infinity of intermediate states φ_i can be handled implicitly by converting the problem to the solution of a differential equation, and analytical results can be obtained. A very illustrative and pedagogical example of such a procedure has recently been presented by Tang et al.[2] Here we would like to show in an instructive method that also makes direct summation possible, provided one takes proper care of the analytical structure of the singular resolvent operator.

The straightforward approach of replacing the integration over the continuum of intermediate states by the summation over their discrete approximation does not preserve the analytical structure of the exact expression. In particular, the imaginary part of such an approximation will be equal to zero, even for the infinite basis set expansion; in this case quantity does not carry over into quality:

$$\begin{aligned} B^{(2)}_{\text{discretized}} &= \sum_{i=1}^{N} \frac{\langle \varphi_f | V_f | \varphi_i \rangle \langle \varphi_i | V_i | \varphi_0 \rangle}{E - E_i} \xrightarrow{N \to \infty} B^{(2)}; \\ \text{Im} B^{(2)}_{\text{discretized}} &= 0 \end{aligned} \tag{3}$$

It has been demonstrated recently that the complex coordinate method offers a practical and analytically correct alternative in evaluation of the expectation values of the resolvent,[3] and can be applied to the higher-order transition amplitudes.[4,5] This is because the discrete-type approximation to the dilated expectation value

$$\begin{aligned} B^{(2)}_{\text{discretized}}(\theta) &= \sum_{i=1}^{N} \frac{\langle \varphi_f^*(\theta) | V_f(\theta) | \varphi_i(\theta) \rangle \langle \varphi_i^*(\theta) | V_i(\theta) | \varphi_0(\theta) \rangle}{\mathbf{E} - \varepsilon_i} \\ &\xrightarrow{N \to \infty} B^{(2)}; \qquad \text{Im} B^{(2)}_{\text{discretized}}(\theta) \neq 0 \end{aligned} \tag{4}$$

converges to the exact expression under the basis set enlargement. The important point is that under the complex transformation defined as

$$\begin{aligned} U(\theta) f(r) &= e^{3/2} f(e^{\theta}); \\ H(\theta) &= U(\theta) H U^{-1}(\theta); \qquad \theta = \alpha + i\beta \end{aligned} \tag{5}$$

Journal of Computational Chemistry, Vol. 9, No. 5, 578–580 (1988)

CCC 0192-8651/88/050578-03$04.00

Two-photon absorption of atomic hydrogen from two light beams

J. H. Tung

Department of Physics, Chung Kung University, Tainan, Taiwan, China

A. Z. Tang, G. J. Salamo, and F. T. Chan

Physics Department, University of Arkansas, Fayetteville, Arkansas 72701

Received September 20, 1985; accepted January 28, 1986

Within the framework of nonrelativistic quantum mechanics, the analysis of the two-photon absorption by atomic hydrogen is generalized to the case of two incident beams with arbitrary direction and polarization (including circular polarization). In the dipole approximation, the second-order matrix elements responsible for two-photon absorption are transformed into a finite sum consisting of the product of a radial part and an angular part. Exact calculation of the angular part predicts that, for the s–s transition only, transparency is obtained regardless of the frequencies of the two beams with perpendicular polarizations. In addition, circularly polarized light is found to be more efficient (up to a factor of 1.5) for the s–d two-photon transition. The radial parts of the matrix elements are accurately evaluated by using the Coulomb Green's function technique and an implicit technique of Dalgarno and Lewis. Their calculation indicates that "zeros" exist in the two-photon absorption spectrum, thereby predicting that absorption is not possible at certain frequencies. It should be noted that in the calculated spectrum, near or at resonance points, the linewidths of the intermediate levels must be included in order to obtain accurate results.

1. INTRODUCTION

With the continuous development of laser techniques, two-photon spectroscopy has become a powerful tool for the study of excited states of atoms and molecules.[1] For example, Doppler broadening can be eliminated by using counter-propagating, equal-frequency laser beams. In some situations, however, it is advantageous to use *unequal-frequency* photons,[2] as the two-photon absorption rate usually can be increased many orders of magnitude by making use of resonant enhancement with an intermediate state.[3] As another example, Hunter[4] has recently shown that the two-photon Hanle effect, in which two-photon absorption plays an important role, is more powerful than the usual one-photon Hanle effect in providing a high-precision tool for the determination of atomic lifetime and collisional parameters. On the theoretical side, to the best of our knowledge, existing calculations on the two-photon absorption processes of atomic hydrogen are limited to the consideration of using only one incident beam (i.e., absorption of two fixed, equal-frequency photons)[5] or two incident beams[6–8] but with the same direction of polarization. Furthermore, Refs. 6–8 deal only with s–s transition.

In this paper, we generalized the analysis of the two-photon absorption of atomic hydrogen to the case of two incident beams with arbitrary direction and polarization (including circular polarization). Meanwhile, no restriction on the equal-frequency photons is made in our calculations. Atomic units will be used unless otherwise stated.

2. THEORY

When a hydrogen atom interacts with two electromagnetic waves, many different processes such as ionization, scattering, absorption, and emission may occur. In this paper we restricted our investigation to the two-photon absorption process. In the following discussion, we use $(n_2l_2m_2)$ and $(n_1l_1m_1)$ to denote the upper and lower energy states, respectively, of a hydrogen atom, while (nlm) is used to denote all possible intermediate states including both bound and free states. In addition, as shown in Fig. 1, $\mathbf{k}'$ and $\mathbf{k}''$ are used to denote the propagation vectors of two electromagnetic waves, while α is the angle between these two vectors, which are located for convenience in the horizontal y–z plane. Also shown in the figure are ϕ' and ϕ'', which are the angles that the polarization of these two light waves makes with the vertical x axis.

For the purpose of discussion in this paper, we will express the fields of two incident beams as

$$\mathbf{E}' = \hat{\epsilon}' E_0' \cos(\omega' t - \mathbf{k}' \cdot \mathbf{r})$$

and

$$\mathbf{E}'' = \hat{\epsilon}'' E_0'' \cos(\omega'' t - \mathbf{k}'' \cdot \mathbf{r} + \phi).$$

With these definitions, the transition rate of the hydrogen atom from the initial state $(n_1l_1m_1)$ to the final state $(n_2l_2m_2)$ through the two-photon absorption may be derived by a straightforward application of second-order perturbation theory in quantum mechanics. The result is

$$W^{n_2l_2m_2}_{n_1l_1m_1}(\omega') = \frac{\pi E_0'^2 E_0''^2}{8} \left| \sum_{n,l,m} \left[\frac{\langle n_2l_2m_2|\hat{\epsilon}'' \cdot \mathbf{r}|nlm\rangle \langle nlm|\hat{\epsilon}' \cdot \mathbf{r}|n_1l_1m_1\rangle}{\omega_{nn_1} - \omega'} + \frac{\langle n_2l_2m_2|\hat{\epsilon}' \cdot \mathbf{r}|nlm\rangle \langle nlm|\hat{\epsilon}'' \cdot \mathbf{r}|n_1l_1m_1\rangle}{\omega_{nn_1} - \omega''} \right] \right|^2 \times g(\omega' + \omega''), \quad (1)$$

0740-3224/86/060837-12$02.00

Lifetime of excited atomic states

J. D. Cresser,* A. Z. Tang, G. J. Salamo, and F. T. Chan
Physics Department, University of Arkansas, Fayetteville, Arkansas 72701
(Received 26 December 1984; revised manuscript received 26 July 1985)

In this paper we derive an expression for the lifetime of excited atomic states taking account of contributions due to nonresonant two-photon transitions. Explicit integration of the two-photon emission spectrum is not required. The results are applied to the case of the hydrogen atom.

I. INTRODUCTION

Although two-photon emission in atomic systems is a subject much studied since the original work of Goeppert-Mayer,[1] there still remain certain aspects of this process which have not been satisfactorily dealt with. This is the case in situations in which an atom in an excited state can decay to its ground state by two-photon emission while passing through an intermediate atomic state having an energy higher than the initial state (nonresonant two-photon emission) or through an intermediate state with an energy lower than that of the initial state (resonant two-photon emission). An obvious example of such a situation is that of the two-photon decay of the $3s$ (or $3d$) level of hydrogen in which nonresonant emission is mediated by the higher-lying intermediate np states ($n \geq 4$) and the lower-lying intermediate $2p$ state. The former process, being nonresonant, is very unlikely compared to the latter, but still has interesting potentially observable effects arising from quantum interference between the two different routes by which the atom can arrive in its ground state.[2,3]

A somewhat more basic aspect of this kind of two-photon decay was addressed by Florescu,[3] namely the problem of actually calculating the lifetime of such an excited state. The interest in this problem is related to the fact that for a metastable level (i.e., one for which there is no resonant lower-lying intermediate state) this lifetime can be calculated by simply integrating the two-photon emission spectrum over the frequencies of the emitted photons, taking account of the conservation of energy. Thus, for hydrogen (in atomic units)

$$A^{2E_1}_{n_i l\to 1s} = \int_0^{(E_{n_i}-E_1)/4\pi} A_{n_i l\to 1s}(\nu')\,d\nu' \tag{1a}$$

$$= \int_0^{(E_{n_i}-E_1)/4\pi} \frac{2^{10}\pi^6}{C^6}(\nu')^3(\nu'')^3\frac{1}{2l+1}\sum_m \left|\left| \sum_{n=2} \left[\frac{\langle 1s\,|\,\hat{\epsilon}'\cdot\mathbf{r}\,|\,n\rangle\langle n\,|\,\hat{\epsilon}''\cdot\mathbf{r}\,|\,n_i lm\rangle}{E_n - E_{n_i} + E_{\nu'}} + \frac{\langle 1s\,|\,\hat{\epsilon}''\cdot\mathbf{r}\,|\,n\rangle\langle n\,|\,\hat{\epsilon}'\cdot\mathbf{r}\,|\,n_i lm\rangle}{E_n - E_{n_i} + E_{\nu''}} \right] \right|\right|^2_{\text{ave}} d\nu' , \tag{1b}$$

where ν' and ν'' are the frequencies of the two photons (with unit polarization vectors $\hat{\epsilon}'$ and $\hat{\epsilon}''$, respectively) emitted with

$$\nu' + \nu'' = (E_{n_i} - E_1)/2\pi = \nu_{n_i 1} = \omega_{n_i 1}/2\pi . \tag{2}$$

The sums over n in Eq. (1b), the second-order matrix elements, run over all hydrogen wave functions, including both continuum and bound states, and could be evaluated exactly via the implicit technique[2] or the Coulomb Green's function in momentum space.[3]

In the absence of any resonant intermediate states, e.g., $n_i = 2$, the expressions in Eqs. (1a) and (1b) remain finite. However, if in the sums in Eq. (1b) there appears a resonant intermediate state, e.g., if $n_i = 3$, the corresponding denominators in the summation will vanish. That is, the perturbation theory expression breaks down. In order to perform the integration in Eq. (1) in this case, Florescu[3] adopted a procedure in which the energy of the intermediate state was assigned a complex energy, the imaginary part of this complex energy being the natural linewidth of this level. As shown in Ref. 3, such a procedure applied to, say, the $3s$ and $3d$ levels in hydrogen, yields, after numerically integrating the emission spectrum over frequency, the usually quoted value for the one-photon lifetime of the initially excited state.[4] The conclusion that was drawn was that the contribution to the lifetime of the excited state due to nonresonant two-photon decay is negligibly small, as already mentioned above, and in agreement with intuitive expectations.

The general validity of this procedure is, of course, open to question. In fact, Florescu[5] has raised the point that the lifetimes of both the initial and resonant intermediate states should be properly taken into account, and

Dynamic multipole polarizability of atomic hydrogen

A. Z. Tang and F. T. Chan
Physics Department, University of Arkansas, Fayetteville, Arkansas 72701
(Received 25 October 1985; revised manuscript received 9 December 1985)

Using an integral representation involving the radial Coulomb Green's function an analytic closed-form expression is derived for the dynamic multipole polarizability of atomic hydrogen in an arbitrary state. The application of the general expression to practical problems is discussed. Comparison is also made with other theoretical models.

I. INTRODUCTION

The exact evaluation of the dynamic 2^l-multipole polarizability of atomic hydrogen in an arbitrary $(n_i l_i m_i)$ state,

$$\beta_l^{n_i l_i m_i}(\omega)=\sum_{\substack{n'(\neq n_i)\\ l',m'}}\!\!\!\!\!\!\int \frac{|\langle\psi_{n_i l_i m_i}|\, r^l P_l(\cos\theta)\,|\psi_{n'l'm'}\rangle|^2}{E_{n'}-E_{n_i}-\omega}, \quad (1)$$

is of considerable interest in atomic physics. In Eq. (1), ω is the angular frequency of the electromagnetic field and E and ψ are the energy eigenvalue and eigenfunction of atomic hydrogen. $\sum\!\!\!\!\!\!\int$ represents a sum (excluding $n'=n_i$) over all discrete states and an integral over all continuous states.

The dynamic polarizability is an important quantity which describes the distortion of the electronic and charge distribution of an atom (or a molecule) in the presence of an oscillating electric field. It is directly related to the van der Waals constants,[1–4] the dynamic dipole shielding factor,[5] the Rayleigh scattering cross sections,[6] the Verdet constants,[7] the mean excitation energies,[8] and the frequency dependence of the refraction index.[9]

The problem of evaluating the dynamic polarizability in various forms has been studied by approximate or analytical methods by Karplus and Kolker,[9] Chan and Dalgarno,[10] Adamov, Kagan, and Orlov,[11] Vetchinkin and Khristenko,[12] Adamov, Balmakov, and Rebane,[13] Adamov, Orlov, and Rebane,[14] Deal and Young,[15] Shimamura,[16] and Au.[17] However, all these theoretical calculations are limited to the consideration of the dipole case, $l=1$, or of the spherical symmetric $n_i s$ state. The purpose of this paper is to derive a compact and analytic closed-form expression for Eq. (1) for the most general case of $l\geq 1$ and arbitrary $(n_i l_i m_i)$. Instead of using the Coulomb Green's function in three-dimensional momentum space,[17] we employ the one-dimensional radial Coulomb Green's function[18] in the derivation. The algebra involved is rather simple compared with that of other approaches.

Atomic units will be used unless otherwise stated.

II. ANALYTICAL EXPRESSION FOR $\beta_l^{n_i l_i m_i}(\omega)$

After calculating the angular part in Eq. (1), we have

$$\beta_l^{n_i l_i m_i}(\omega)=\sum_{l'=|l-l_i|}^{l+l_i}\left\{(2l_i+1)(2l'+1)\begin{bmatrix} l_i & l & l'\\ 0 & 0 & 0\end{bmatrix}^2\begin{bmatrix} l_i & l & l'\\ -m_i & 0 & m_i\end{bmatrix}^2 \times\int_0^\infty dr\,dr'(rr')^{l+2}R_{n_i l_i}(r)R_{n_i l_i}(r')\sum_{\substack{n'(\neq n_i)\\ (n'>l')}}\!\!\!\!\!\!\int \frac{R_{n'l'}(r)R^*_{n'l'}(r')}{E_{n'}-(E_{n_i}+\omega)}\right\}, \quad (2)$$

where $\begin{pmatrix} l_1 & l_2 & l_3\\ m_1 & m_2 & m_3\end{pmatrix}$ refers to the 3-j symbol.[19] In order to use the closure relation, we add and subtract a term with $n'=n_i$ inside $\sum\!\!\!\!\!\!\int$ in Eq. (2). Hence

$$\beta_l^{n_i l_i m_i}(\omega)=\sum_{l'=|l-l_i|}^{l+l_i}\left\{(2l_i+1)(2l'+1)\begin{bmatrix} l_i & l & l'\\ 0 & 0 & 0\end{bmatrix}^2\begin{bmatrix} l_i & l & l'\\ -m_i & 0 & m_i\end{bmatrix}^2 \times\left[\int_0^\infty\!\!\int dr\,dr'(rr')^{l+2}R_{n_i l_i}(r)R_{n_i l_i}(r')g_{l'}(r,r';E_{n_i}+\omega)+\frac{\epsilon_{n_i l'}}{\omega}\left[\int_0^\infty r^{l+2}R_{n_i l_i}(r)R_{n_i l'}(r)dr\right]^2\right]\right\}, \quad (3)$$

Simple example in second-order perturbation theory

A. Z. Tang, M. Lieber, and F. T. Chan
Physics Department, University of Arkansas, Fayetteville, Arkansas 72701

(Received 19 March 1984; accepted for publication 29 May 1984)

A common problem faced by teachers of quantum mechanics is to find a good example to illustrate perturbation theory in the second order. Probably the most popular example is that of the quadratic Stark effect in hydrogen or, what is essentially the same thing, the (static) dipole polarizability of hydrogen. In the former case, to be definite, the hydrogen atom is perturbed by a uniform external field $\mathscr{E} = \mathscr{E}\hat{z}$. The perturbation term in the Hamiltonian is

$$H' = -e\mathscr{E}z. \tag{1}$$

The Stark shift in the ground state energy is then given by second-order perturbation theory as

$$E_1 = E_1^0 + e^2\mathscr{E}^2 \sum_{\substack{n\neq 1\\ l,m}} \frac{|\langle 1,0,0|z|n,l,m\rangle|^2}{E_1^0 - E_n^0}, \tag{2}$$

where $|nlm\rangle$ is the unperturbed hydrogen state vector and E_n^0 the corresponding energy. The sum in Eq. (2) runs over the infinity of intermediate states other than the ground state, including the continuum, and its evaluation thus presents formidable problems for classroom presentation. One method requires the introduction of parabolic coordinates.[1] A simpler method was recently published in this journal.[2] Probably the simplest published treatment is that in the final edition of Schiff's textbook,[3] which is a version of the powerful but not well-known method of Dalgarno and Lewis,[4–6] which converts the infinite sum in Eq. (2) to a differential equation. Schiff integrates the differential equation by an expansion in power series, which he shows terminates after a few terms. The teacher can, of course, just produce this solution *ex nihilo*, but we have discovered what we believe to be a better alternative, which avoids solving the equation at all.

We begin by deriving the necessary differential equation. In the summation in Eq. (2), only the $l = 1, m = 0$ intermediate states contribute nonvanishing matrix elements, in accordance with the usual parity selection rules. If we write $z = r\cos\theta$ we can do the angular integral directly:

$$\iint Y_{10}^*(\theta,\phi)\cos\theta Y_{00}(\theta,\phi)\sin\theta\, d\theta\, d\phi = \frac{1}{\sqrt{3}}, \tag{3}$$

where we have used the spherical harmonics

$$Y_{00}(\theta,\phi) = (4\pi)^{-1/2}$$

and

$$Y_{10}(\theta,\phi) = (3/4\pi)^{1/2}\cos\theta.$$

Thus,

$$\sum_{\substack{n\neq 1\\ l,m}} \frac{|\langle 100|z|nlm\rangle|^2}{E_1^0 - E_n^0} = \frac{1}{3}\sum_{n\neq 1} \frac{|\langle R_{10}|r|R_{n1}\rangle|^2}{E_1^0 - E_n^0} = \frac{1}{3}\Sigma. \tag{4}$$

To calculate the sum Σ we define an auxiliary function $u(r)$ [which is $rf(r)$ in Schiff[2]]:

$$u(r) = \sum_{n\neq 1}\left[\left(rR_{n1}(r)\int_0^\infty R_{10}(r')R_{n1}(r')r'^3\, dr'\right) \times (E_1^0 - E_n^0)^{-1}\right], \tag{5}$$

where the $R_{nl}(r)$ are the radial factors of the hydrogen wave functions, satisfying, for $l = 1$ (we use units $m = \hbar = e = 1$):

$$\frac{1}{2}\frac{d^2}{dr^2}(rR_{n1}) + \left(\frac{1}{r} - \frac{1}{r^2}\right)(rR_{n1}) = -E_n^0(rR_{n1}) = [(E_1^0 - E_n^0) - E_1^0](rR_{n1}). \tag{6}$$

Using (6) we can show immediately that $u(r)$ satisfies

$$\left[E_1^0 + \frac{1}{2}\frac{d^2}{dr^2} + \left(\frac{1}{r} - \frac{1}{r^2}\right)\right]u(r) = \sum_{n\neq 1}^{\infty} rR_{n1}(r)\int_0^\infty R_{10}(r')R_{n1}(r')r'^3\, dr'.$$

Then, interchanging the order of summation and integration, and application of the closure relation for the $l = 1$ radial functions:

$$\sum_{n\neq 1}^{\infty} rR_{n1}(r)r'R_{n1}(r') = \delta(r - r')$$

gives us the differential equation satisfied by u:

$$\left[E_1^0 + \frac{1}{2}\frac{d^2}{dr^2} + \left(\frac{1}{r} - \frac{1}{r^2}\right)\right]u = r^2R_{10}(r) \tag{7}$$

which is equivalent to Schiff's Eq. (33.4). If we can find $u(r)$ then it is evident that

$$\Sigma = \int_0^\infty u(r)R_{10}(r)r^2\, dr = 2\int_0^\infty u(r)r^2e^{-r}\, dr. \tag{8}$$

Thus the summation reduces to the solution of Eq. (7) followed by the evaluation of the integral (8). However, the use of Laplace transforms avoids both steps.

We note that if we define the Laplace transform of $u(r)$:

$$v(p) = \int_0^\infty u(r)e^{-pr}\, dr \tag{9}$$

then

$$\Sigma = 2\left(\frac{d^2v}{dp^2}\right)_{p=1}. \tag{10}$$

Noting that $E_1^0 = -1/2$ in our units and rewriting Eq. (7) in the form

$$\left(\frac{r^2}{2}\frac{d^2}{dr^2} - \frac{r^2}{2} + r - 1\right)u = r^4R_{10} = 2r^4e^{-r}, \tag{11}$$

we find the Laplace transform of Eq. (11) is

$$\frac{1}{2}(p^2 - 1)\frac{d^2v}{dp^2} + (2p - 1)\frac{dv}{dp} = 48(1 + p)^{-5}, \tag{12}$$

Two-photon decay of hydrogenic atoms

J. H. Tung, X. M. Ye, G. J. Salamo, and F. T. Chan
Physics Department, University of Arkansas, Fayetteville, Arkansas 72701
(Received 9 December 1982; revised manuscript received 13 July 1983)

The two-photon decay mode of hydrogenic atoms from an arbitrary state (n_1,l_1,m_1) to an arbitrary state (n_2,l_2,m_2) is studied within the framework of nonrelativistic quantum mechanics. In the dipole approximation, these decay rates, which involve infinite summation over intermediate states, are derived exactly via a general second-order matrix element obtained by Kelsey and Macek and an implicit technique introduced by Dalgarno and Lewis. The results are expressed in terms of hypergeometric functions. For transitions $n_1s\rightarrow n_2s$, our results reduce to those of Klarsfeld whose starting point is the Coulomb Green's function. For transitions to the ground state, an alternative expression involving a simple one-dimensional integral is presented. The decay rate of the $2s$ metastable state of atomic hydrogen is calculated as an illustration of the method. The result, $1/\tau=8.2284\ \text{sec}^{-1}$, agrees with Klarsfeld. For transitions of $n_1s\rightarrow 1s$ and $n_1d\rightarrow 1s$ $(n_1\geq 3)$, the transition rates exhibit interesting and unexpected structures. In particular, "zeros" are found in the two-photon emission spectrum indicating that two-photon emission is not possible at certain frequencies. Physically, these "zeros" are the result of destructive interference between the radiating dipole terms associated with the sum over intermediate states. In addition to the emission spectrum the expected coincidence signal between two detectors monitoring the two photons simultaneously emitted during a two-photon transition is calculated as a function of the angle between the detectors. The angular distribution for the $n_1d\rightarrow 1s$ transitions is shown to be significantly different from the $n_1s\rightarrow 1s$ transitions. Finally, a possible experiment is suggested to test the results presented in this paper.

I. INTRODUCTION

The possibility of a two-photon process, which proceeds via intermediate states, was first pointed out by Mayer[1] in 1931. Breit and Teller[2] applied this theory to the case of the $2s\rightarrow 1s$ transition in atomic hydrogen and found that double photon emission is the most probable radiative decay mode, and is therefore the principal cause of the decay mechanism of the interstellar $2s$ hydrogen atoms. They also found that the mean lifetime τ corresponding to this mode of decay can be bracketed by the relation $6.5<1/\tau<8.7\ \text{sec}^{-1}$. Later, more detailed calculations[3,4] were carried out which involved term-by-term numerical evaluation of the infinite summation over intermediate states in the second-order matrix elements responsible for the decay. In particular, Shapiro and Breit[4] found that the decay rate for the metastable $2s$ state of a hydrogenlike atom of atomic number Z, $1/\tau$, is equal to $8.226Z^6\ \text{sec}^{-1}$, which corresponds to a lifetime of 1.9 msec for the case of He^+. However, these conclusions could be modified[5,6] due to the possible existence of a nuclear or electronic dipole moment which would produce a nonzero one-photon decay mode for the metastable hydrogenlike atom. Therefore, a careful study of the properties of this state is useful in the search for new fundamental interactions.

In connection with this interest and in view of experimental success in two-photon-absorption and ionization experiments, a series of theoretical papers[7–20] has appeared on how to perform exactly, within the framework of nonrelativistic quantum mechanics, the infinite sums in the second-order matrix elements responsible for various multiphoton processes. For the decay transition, the numerical result of the two-photon decay rate of metastable hydrogenic atoms, viz., $1/\tau=(8.2283\pm 0.0001)Z^6\ \text{sec}^{-1}$, obtained by Klarsfeld[14] is believed to be the most accurate one.[6,19] Recent calculations,[21,22] including all relativistic and retardation effects and all combinations of photon multipoles, give a very small correction in the case of low-Z hydrogenlike atoms. In addition, the two-photon decay rates of the singlet and triplet metastable states of heliumlike ions have also been calculated using variation procedures by Drake, Victor, and Dalgarno.[23]

In a recent paper[24] Kelsey and Macek used the implicit technique[7,8] to obtain a simple reformulation of a closed-form expression for a general second-order matrix element for hydrogen. While equivalent expressions have been derived[13,25,26] employing various representations[27–29] of the Coulomb Green's function, the mathematics involved is quite cumbersome. Although the work of Kelsey and Macek is very important and useful, it has not received enough attention. One of the purposes of this paper is to show that the elegant results of Kelsey and Macek and the powerful implicit technique can be employed to study the two-photon decay mode of a hydrogenlike atom from an arbitrary initial state (n_1,l_1,m_1) to an arbitrary final state (n_2,l_2,m_2). As a result, the two-photon transition rate is expressed in terms of repeated parametric differentiations of hypergeometric functions. The results we have obtained are equivalent to those of Gazeau,[19] but the starting points are quite different. Gazeau used powerful group-theoretical techniques whereas we have used simple alge-

Influence of the linear Stark effect on electron exchange in the eikonal calculations

F. T. Chan and M. Lieber
Physics Department, University of Arkansas, Fayetteville, Arkansas 72701
(Received 28 July 1983)

The eikonal approximation taking into account the post-collisional Stark effect removes the shortcoming of the previous calculations of relative l capture cross sections. We find good agreement between the calculated σ_{2s} and σ_{2p} cross sections and the available experimental data in $p+\mathrm{H}(1s)$ collisions.

In a series of papers[1-6] an eikonal approach[7,8] to electron capture from $\mathrm{H}(1s)$ into fast multichanged projectile ions has been proposed. The results obtained are not only in better agreement with experimental findings for hydrogen and helium targets, but have a remarkable simplicity, comparable with that of the simplest first-order theory, the Oppenheimer-Brinkmann-Kramers (OBK) approximation. However, the successes of the eikonal approximation reported so far have been *only partial*, since there is an overestimate of the $l \neq 0$ cross section compared with the corresponding s cross section for the same principal shell.

In a recent interesting publication[9] Burgdörfer pointed out the importance of the Stark mixing between the degenerate excited states of the projectile escaping the field of the residual target ion and named the coupling between states of the same principal shell long after the primary charge transfer has taken place the "post-collision interaction" (PCI). Applying the PCI model to the OBK approximation for the primary capture processes, Burgdörfer found improved agreement of the relative l cross section and the alignment parameter with experimental data. The agreement only holds for *relative, but not for the absolute* substate cross sections. In this paper, we apply the PCI model together with the eikonal approximation to study the σ_{2s} and σ_{2p} capture cross sections in $p+\mathrm{H}(1s)$ collisions. Atomic units are used throughout.

Consider the capture of an electron initially bound in the $1s$ shell of a hydrogenic target with charge Z_t into a given n,l,m state of a bare projectile ion with charge Z_p. In the eikonal approach the transition amplitude can be written as[5]

$$A_{1s-nlm}(\vec{b}) = \frac{i2\pi Z_p}{v}\int d^2p_b\,[g^*_{nlm}(\vec{p}+\vec{v})\,G_{1s}(\vec{p})]_{p_z=p_{0z}}\,e^{-i\vec{b}\cdot\vec{p}_b}\ , \tag{1}$$

where $p_{0z} = -\frac{1}{2}v+\eta\epsilon$ with $\eta = 1/v$ and the energy defect $\epsilon = -Z_p^2/2n^2 + Z_t^2/2$. In Eq. (1), g_{nlm} and G_{nlm} are defined and given by Eqs. (14) and (21), respectively, in Ref. 5. The phase factor[10] $(-i)^l$ in g_{nlm}, which was dropped in Ref. 5, is very important and must be retained in the present study.

Following Burgdörfer,[9] the eikonal amplitudes within the PCI model are related to the usual eikonal amplitudes [Eq. (1)] by an evolution operator, namely,

$$A^{\mathrm{PCI}}_{2s}(\vec{b}) = \cos\phi A_{2s}(\vec{b}) + i\sin\phi A_{2p0}(\vec{b})\ , \tag{2a}$$

$$A^{\mathrm{PCI}}_{2p0}(\vec{b}) = \cos\phi A_{2p0}(\vec{b}) + i\sin\phi A_{2s}(\vec{b})\ , \tag{2b}$$

$$A^{\mathrm{PCI}}_{2p,\pm1}(\vec{b}) = A_{2p,\pm1}(\vec{b}) \tag{2c}$$

TABLE I. Calculated charge capture cross sections σ_{1s-2lm} (in 10^{-16} cm^2) for the reactions $\mathrm{H}^+ + \mathrm{H}(1s) \rightarrow \mathrm{H}(2lm) + \mathrm{H}^+$ as a function of energy. The results for eikonal both with and without the PCI model are tabulated. 5.088(−1) is an abbreviation for 5.088×10^{-1}.

Cross section (10^{-16} cm^2) \ Incident energy (keV)		30	50	70	100	150	200	500
Eikonal	σ_{2p}	5.088(−1)	1.331(−1)	4.268(−2)	1.034(−2)	1.617(−3)	3.771(−4)	2.022(−6)
	σ_{2s}	2.822(−1)	9.546(−2)	3.910(−2)	1.279(−2)	2.903(−3)	8.915(−4)	1.180(−5)
	$\frac{\sigma_{2p}}{\sigma_{2s}}$	1.803	1.394	1.092	0.808	0.557	0.423	0.171
Eikonal with PCI	σ_{2p}	2.013(−1)	6.183(−2)	2.106(−2)	5.309(−3)	8.527(−4)	2.012(−4)	1.099(−6)
	σ_{2s}	5.893(−1)	1.667(−1)	6.073(−2)	1.783(−2)	3.667(−2)	1.067(−3)	1.272(−5)
	$\frac{\sigma_{2p}}{\sigma_{2s}}$	0.341	0.371	0.347	0.298	0.233	0.189	0.087

Calculation of the differential cross section for electron capture in fast ion-atom collisions

T. S. Ho and J. Eichler*
Bereich Kern- und Strahlenphysik, Hahn-Meitner-Institut für Kernforschung Berlin GmbH, D-1000 Berlin 39, Federal Republic of Germany

M. Lieber and F. T. Chan
Department of Physics, University of Arkansas, Fayetteville, Arkansas 72701
(Received 16 September 1981)

The approach to electron capture developed by Chan and Eichler is combined with the optical eikonal approximation for describing the effect of the internuclear potential on the projectile trajectory. In this way, a closed-form expression is derived for the differential cross section for $1s \rightarrow nlm$ capture. Numerical calculations have been performed for the reaction $H^+ + H(1s) \rightarrow H + H^+$ at collision energies of 25, 60, and 125 keV. Good agreement is obtained with the recent data of Martin *et al.* by using trajectories undeflected by the internuclear potential at small deflection angles and Coulomb-deflected trajectories at large deflection angles.

I. INTRODUCTION

Measurements of differential capture cross sections present a much more stringent test of theory than experimental data on total cross sections. In earlier experiments[1] such measurements have been confined to collisions of protons with multielectron targets (He and Ar), and only very recently Martin *et al.*[2] have reported differential capture cross sections for the one-electron collision system $H^+ + H(1s)$ which offers the cleanest test for any theory. This may help to clarify the longstanding[3] problem of the role played by the internuclear potential[4,5] in theoretical approaches.

In the present work we adopt the eikonal approach developed by Chan and Eichler[6] (in the following denoted by CE in order to save the term "eikonal" for the optical description of the projectile trajectory). This approach, extended in further work,[7–9] has proven to be quite successful[6–9] in predicting total capture cross sections. Its results are expressed by simple formulas which are derived from the original ansatz without further approximations. The agreement with experiment (for collision velocities high enough with respect to typical electron orbital velocities in target and projectile) is based on the fact that the CE theory takes into account the interaction of the captured electron with both the projectile nucleus (in first order) and the target nucleus (in higher order) and thus approximately includes double and multiple scattering contributions. The physical content of the CE approach has been analyzed in more detail[10] by performing a term-by-term comparison with the Born expansion. It is worth mentioning at this point that exact second-Born calculations[11] at collision velocities close to, and a few times greater than, the electron orbital velocity yield capture cross sections which are up to an order of magnitude too large. This makes it clear that the third order and higher orders are needed[10] to bring the cross section down to the experimental value or to the value predicted by the nonperturbative CE theory.

In this paper we adopt the optical eikonal approximation[12] to describe the effect of the internuclear potential on the projectile trajectory and combine it with the CE approach[6] for calculating the transition amplitude for electron capture as a function of the impact parameter. In Sec. II we give a brief outline of the theory and in Sec. III apply the resulting formula to the collision system $H^+ + H(1s)$ in order to compare with the recent experimental results.

II. THEORY

Consider the capture of an electron initially bound in the $1s$ shell of a hydrogenic target with

PHYSICAL REVIEW A VOLUME 24, NUMBER 6 DECEMBER 1981

Eikonal calculation of electron-capture cross sections in collisions of H-atoms with fast projectiles

T. S. Ho, M. Lieber, and F. T. Chan
University of Arkansas, Fayetteville, Arkansas 72701
(Received 20 April 1981)

We have employed the eikonal method to calculate the cross section for the capture of an electron into an arbitrary *nl* subshell in collisions between hydrogen atoms and fast projectiles. The projectiles were protons, C^{6+}, O^{8+}, and Fe^{24+}. The energy ranges considered were 20–100 keV in the proton case and 40–200 keV per nucleon in the other cases. These projectiles were selected because of their importance in fusion plasmas. For the highly charged case of Fe^{24+} we found that our formulas, while exact, involved a high degree of cancellation and produced unreliable numerical results, so that a numerical integration of the penultimate formula was substituted. In the proton case, agreement with recent experimental data is excellent.

INTRODUCTION

Recently, a need to study certain charge-transfer reactions in controlled thermonuclear fusion research has been recognized.[1,2] For example, in fusion plasmas, one of the most promising methods of heating and fueling a Tokamak fusion plasma is by injection of fast neutral H^0 and D^0 atoms. However, there is usually a considerable amount of highly stripped impurity ions such as C, O, N, Si, Ar, Fe, Co, Cu, Nb, Mo, or W contained in the plasma. When the injected H^0 or D^0 atom collides with one of these impurity ions, it is quite probable that the injected particle will lose its electron, either by charge exchange or ionization. If this occurs on the outer edge of the plasma, the ionized H or D atom will be magnetically deflected out of the plasma, strike the container walls, and therefore produce more impurity atoms. On the other hand, the heated plasma may lose its energetic fuel particles (p,d, or t) via charge exchange. Furthermore, the optical spectroscopy of highly charged ions, e.g., iron, provides the means of localized diagnostics of the interior of the plasma which is important in fusion reactor modeling.[3,4] One of the speculations in the observed spectrum is the large rise of the Fe^{23+} light intensity during the high-power neutral-beam injection. The most consistent explanation of this phenomenon has been the enhanced recombination of the heliumlike Fe^{24+} through charge exchange with the neutral H^0 and D^0 atoms supplied by the beams. So we need to have a knowledge of cross sections of such charge-transfer reactions. In this paper, we carry out, using the eikonal approach,[5,6] a detailed study of electron capture from H (or D) by H^{1+}, C^{6+}, O^{8+}, and Fe^{24+} projectiles in the energy range 40–200 keV/amu. (In the laboratory, of course, it is the hydrogen atom which is usually considered as the stationary target and the ion which is the energetic projectile. That is the language adopted below. The cross sections are the same from either point of view, depending only on the relative velocity, but the total energy of the particle labeled "projectile" will naturally be very different in the two situations.) Reliable information on these three reactions[4] is particularly important and is urgently needed for the diagonsis of the role played by impurities in neutral-beam heating of fusion plasmas. Our confidence in the eikonal approach is based on the success already achieved[5,6] in describing a large body of experimental results. In the proton case excellent agreement with recent experimental data[7] is particularly impressive. In summary, we present in this paper calculations on the capture process listed below:

$$(1)\ H^+ + H(1s) \rightarrow H(2s) + H^+ ,$$

$$(2)\ C^{6+} + H(1s) \rightarrow C^{5+}(\Sigma, n, nl) + H^+ ,$$

$$(3)\ O^{8+} + H(1s) \rightarrow O^{7+}(\Sigma, n, nl) + H^+ ,$$

and

$$(4)\ Fe^{24+} + H(1s) \rightarrow Fe^{23+}(\Sigma, n, nl) + H^+ .$$

Here, we remark that (i) the energy ranges from 20 to 100 keV for process (1), while 40 to 200

PHYSICAL REVIEW A VOLUME 24, NUMBER 6 DECEMBER 1981

Eikonal approximation for charge transfer from a multielectron atom to fast projectiles

T. S. Ho, M. Lieber, and F. T. Chan
Physics Department, University of Arkansas, Fayetteville, Arkansas 72701

K. Omidvar
Laboratory for Planetary Atmospheres, NASA/Goddard Space Flight Center, Greenbelt, Maryland 20771
(Received 24 March 1981)

The eikonal approach developed previously for calculating electron-capture cross sections for bare projectiles colliding with hydrogenic targets is extended here to allow for multielectron targets. Both the impact and wave pictures are employed and their equivalence is discussed. As a first approximation, each atomic orbital is specified by the three hydrogenic quantum numbers, an effective nuclear charge Z_t, and an energy eigenvalue in the impact picture, or ionization potential in the wave picture. The Z_t' appearing in the eikonal phase factor is left undetermined because of incomplete information on the many-body target. However, analytic expressions are derived for the theoretical cross sections, and numerical values are calculated for simple choices of Z_t'. Those results are compared with existing experimental data for C, Ne, Ar, N_2, O_2, and He targets.

I. INTRODUCTION

Electron-capture processes in ion-atom collisions, e.g., $A^+ + B \rightarrow A + B^+$, are of great interest both in terms of basic theory and in various practical applications. In particular, a capture cross section from atomic oxygen or iron are essential in finding the charge equilibrium of a high-energy beam passing through different gases, or in finding the radiation of cosmic rays passing through interstellar matter.

It is well known that the Oppenheimer-Brinkman-Kramers (OBK) approximation[1] gives a roughly correct shape for the dependence of the total electron-capture cross sections upon the collision energy but considerably overestimates the observed data by as much as an order of magnitude. Many efforts have been devoted to obtain a simple semiempirical formula of the capture cross section by scaling down the OBK results through the comparison with the existing experimental measurements.[2] The physical significance of this scaling behavior was not quite understood until the very recent elegant and instructive illustration furnished by the study within the eikonal approximation.[3] This eikonal approach has been further studied since then and has been very successful in predicting the cross sections of the electron capture for the bare projectile—hydrogenic target systems.[4–8] Among them the cross sections of the capture (i) from nl initial state to $n'l'$ final state,[6] and (ii) from nlm initial state to $n'l'm'$ final state[8] have been obtained in closed form, a very astonishing consequence considering most of other approaches (other than OBK) are so complicated that one must have recourse to numerical methods.

In this paper, we generalize this eikonal approach to describe, in (i) the impact picture and (ii) the wave picture, the capture process of a single electron from a multielectron atom into a fast bare projectile. As a first approximation, each atomic orbital is specified by the three hydrogenic quantum numbers, an effective charge, and an energy value (more accurately, an energy eigenvalue in the impact picture or an ionization potential in the wave picture).

In Sec. II, two techniques in formulating the capture cross section are presented, i.e., (i) a straightforward extension from one of our recent papers[8] and (ii) a generating operator (a differential operator, or, for short, a differentiator) and a generating function (an exponential function) are introduced in manipulations. In Sec. III, a discussion on the equivalence of the wave and impact pictures is given. And finally, in Sec. IV, our calculations are compared with the existing experimental data for capture cross sections from C, Ne, Ar, N_2, O_2, and He.

PHYSICAL REVIEW A VOLUME 24, NUMBER 2 AUGUST 1981

Eikonal calculation of electron-capture cross sections from an arbitrary nlm shell of a hydrogenic target into an arbitrary $n'l'm'$ shell of a fast bare projectile

T. S. Ho, D. Umberger, R. L. Day, M. Lieber, and F. T. Chan
Department of Physics, University of Arkansas, Fayetteville, Arkansas 72701
(Received 9 February 1981)

Using techniques similar to those previously employed, we apply the eikonal approximation to the evaluation of the cross section for electron capture from an arbitrary nlm shell of a hydrogenic target atom into an arbitrary $n'l'm'$ of a fast hydrogenic projectile. The results are obtained in exact analytical closed form. Numerical results are presented for the case $H^+ + H(1s) \rightarrow H(n'l'm') + H^+$ when $n' = 2$ and 3. Comparison is made with the corresponding Oppenheimer-Brinkman-Kramers (OBK) results.

I. INTRODUCTION

Charge-transfer processes have been of interest since the early days of quantum mechanics. This interest has increased considerably in the past few years, the focus being on processes relevant to magnetically confined-fusion plasmas and astrophysical plasmas. Knowledge concerning the charge transfer from a hydrogenic atom to a bare ion is important not only with regard to these applications but also from a fundamental point of view since such a process is the simplest type of a rearrangement reaction.

An approach for treating electron capture into arbitrary principle shells of energetic projectiles based on the eikonal approximation was developed by Chan and Eichler.[1] They later amended their approach for capture into arbitrary n', l' sublevels of a fast projectile from the ground state[2] as well as from an arbitrary initial n, l sublevel[3] of a hydrogenic target. The results obtained agree well with experimental findings for hydrogen and helium targets. In this paper we extend the eikonal treatment to cover n, l, m contributions. There are at least two reasons why such a study is interesting. First of all, specification of these contributions allow for a sterner test of capture theories. Such a test is realizable since techniques for measuring charge exchange for $p + N_2 \rightarrow N_2^+ + H(n' = 3, l', m')$ have recently been developed[4] and a corresponding study of charge capture for $p + H$ collisions is now underway at Harvard University.[5] The present study is partly motivated by these experimental interests. Secondly, it is the most general case and it contains all the previous results[1-3] as special cases. In addition, it furnishes information not available from classical trajectory Monte Carlo calculations.[6]

In Sec. II, we use the eikonal approximation to calculate the cross section for the capture of an electron into an (n', l', m') state of an energetic projectile from a hydrogenic target initially in the (n, l, m) state. The result is obtained in closed form, and is exact within the eikonal approximation. In Sec. III, we discuss our results and present some theoretical data for the reaction $H^+ + H(1s) \rightarrow H(n' = 2, 3, l', m') + H^+$. The Oppenheimer-Brinkman-Kramers (OBK) results are obtained as a limiting case and are given in the Appendix.

II. THEORY

We consider the process in which an electron, initially in the n, l, m state of a hydrogenic target atom of charge Z_t, is captured into a given n', l', m' state of a bare projectile ion of charge Z_p. We assume that the time which the projectile spends in the vicinity of the target nucleus is small compared with the transition time of the electron. Let $\vec{r}$, $\vec{r}_t = \vec{r} + \alpha \vec{R}$, and $\vec{r}_p = \vec{r} - (1 - \alpha)\vec{R}$ denote the position of the electron with respect to the center of mass, the target nucleus, and the projectile nucleus, respectively, with $\alpha = M_p/(M_p + M_t)$. The projectile is supposed to move rectilinearly and that its trajectory is given by $\vec{R}(t) = \vec{b} + \vec{v}t$ ($\vec{b} \cdot \vec{v} = 0$, $|\vec{b}|$ being the classical impact parameter) with respect to the target nucleus. The cross section can then be written as[7]

$$\sigma_{nlm \rightarrow n'l'm'}(v) = \int |A_{nlm \rightarrow n'l'm'}(\vec{b}, v)|^2 d^2b \,, \tag{1}$$

where the exact eikonal transition amplitude is, in its "prior" form, given by

$$A_{nlm \rightarrow n'l'm'}(\vec{b}, v) = -i \int_{-\infty}^{\infty} \left\langle \Psi_{n'l'm'}^{(-)} \left| -\frac{Z_p}{r_p} \right| \psi_{nlm} \right\rangle dt \,, \tag{2}$$

with the time-dependent wave functions

$$\psi_{nlm} = \varphi_{nlm}(\vec{r}_t) \exp(-i\epsilon_p t) \exp(-i\alpha \vec{v} \cdot \vec{r} - \tfrac{1}{2} i \alpha^2 v^2 t) \tag{3}$$

and

ADVANCES IN ELECTRONICS AND ELECTRON PHYSICS, VOL. 49

Applications of the Glauber and Eikonal Approximations to Atomic Collisions

F. T. CHAN AND M. LIEBER

University of Arkansas, Fayetteville, Arkansas

G. FOSTER*

Joint Institute for Laboratory Astrophysics
University of Colorado and National Bureau of Standards
Boulder, Colorado

AND

W. WILLIAMSON, JR.

University of Toledo, Toledo, Ohio

* Present address: University of Connecticut at Torrington, Torrington, Connecticut 06790.

ISBN 0-12-014649-5

Elastic scattering of electrons by metastable 2s atomic hydrogen

T. S. Ho and F. T. Chan
Physics Department, University of Arkansas, Fayetteville, Arkansas 72701
(Received 22 August 1977)

The elastic scattering of electrons with incident energies from 20 to 500 eV from the metastable 2s state of atomic hydrogen is calculated by using the Born and Glauber approximations (including the exchange effect). The results for the angular distributions are compared with some other theoretical calculations. It is found that the Born and Glauber integrated elastic-scattering cross section is well represented by $\sigma^{B,G}_{elastic}(2s \to 2s; K_i) = (4162/105)(\Pi a_0^2/K_i^2)$ for $E_i \geq 20$ eV.

Although study of electron scattering by atoms initially prepared in an excited state (in particular the long-lived metastable states) has important applications in astrophysics, plasma physics, and various gaseous phenomena, relatively little work has been done even on the scattering from excited states of simple atoms. In addition, such an investigation is interesting in itself since "the comparison of the scattering from an excited state with that from the ground state yields useful information on the dynamics of the collision process."[1] Several theoretical calculations have been performed to study the elastic[1] and inelastic[2,3] scattering of electrons by metastable hydrogen. Although only one experiment[4] has been carried out to measure the electron-impact ionization cross section of atomic hydrogen in the metastable 2s state, more experimental works on electron scattering (elastic and inelastic) from metastable hydrogen are now under way at the Queens University at Belfast.

In this paper we analyze the elastic scattering of electrons by the 2s state of atomic hydrogen in the framework of Glauber theory[5-7] (including exchange effect). Results on the inelastic scattering will be presented in a forthcoming paper.

The Glauber direct scattering amplitude $F_D^G(\vec{q})$ describing the elastic scattering of an electron with velocity v_i by a metastable hydrogen atom is given by[5-7]

$$F_D^G(\vec{q}) = \frac{iK_i}{2\pi} \int \phi_{2s}^*(\vec{r}) \Gamma(\vec{b}; \vec{r}) \phi_{2s}(\vec{r}) e^{i\vec{q}\cdot\vec{b}} d^2b\, d\vec{r}, \tag{1}$$

where

$$\Gamma(\vec{b}; \vec{r}) = 1 - (|\vec{b} - \vec{s}|/b)^{2i\eta}, \tag{2}$$

and $\eta = 1/v_i = 1/K_i$ (in atomic units). In Eqs. (1) and (2), $\vec{b}$ and $\vec{s}$ are the respective projections of the position vectors of the incident electron and the bound electron onto the plane perpendicular to the Glauber path. The Glauber amplitude was evaluated by taking the Glauber path integral along the direction perpendicular to the momentum transfer $\vec{q}$. The Glauber direct-scattering amplitude $F_D^G(\vec{q})$ can be expressed in a closed and compact form in terms of a generating function[8]:

$$F_D^G(\vec{q}) = -\frac{1}{4}\left[\left(\frac{\partial}{\partial\lambda} + \frac{\partial^2}{\partial\lambda^2} + \frac{1}{4}\frac{\partial^3}{\partial\lambda^3}\right) I(\lambda; q)\right]_{\lambda=1}, \tag{3}$$

where the generating function $I(\lambda; q)$ is defined and given by

$$I(\lambda; q) = \frac{iK_i}{(2\pi)^2} \int \frac{e^{-\lambda r}}{r}\left[1 - \left(\frac{|\vec{b} - \vec{s}|}{b}\right)^{2i\eta}\right] e^{i\vec{q}\cdot\vec{b}} d^2b\, d\vec{r}$$

$$= \frac{8\pi\eta}{e^{\pi\eta} - e^{-\pi\eta}} \frac{1}{\lambda^2 q^2} \times \left(\frac{q}{\lambda}\right)^{2i\eta} {}_2F_1(1 - i\eta, 1 - i\eta; 1; -\lambda^2/q^2). \tag{4}$$

In Eq. (4), ${}_2F_1$ is the usual hypergeometric function. After some manipulation, one can reduce $I(\lambda; q)$ into a form suitable for high incident energy limit, $(\eta - 0)$:

$$I(\lambda; q) \approx I_0(\lambda; q) + i\eta I_1(\lambda; q) + O(\eta^2), \tag{5}$$

where

$$I_0(\lambda; q) = \frac{4}{\lambda^2(\lambda^2 + q^2)}, \tag{6}$$

$$I_1(\lambda; q) = \frac{8}{\lambda^2(\lambda^2 + q^2)} \ln\left[\frac{q}{\lambda}\left(1 + \frac{\lambda^2}{q^2}\right)\right]. \tag{7}$$

In the limit of $\eta - 0$, substituting Eq. (6) into Eq. (3), the Glauber direct-scattering amplitude $F_D^G(\vec{q})$ is found to be identical with the Born direct-scattering amplitude $F_D^B(\vec{q})$, namely,

$$F_D^B(\vec{q}) = \frac{2}{q^2}[1 - F_H(q)], \tag{8}$$

where

$$F_H(q) = \frac{1}{(1+q^2)^2}\left[1 - \frac{3 - q^2}{1 + q^2} + \frac{3(1 - q^2)}{(1+q^2)^2}\right]. \tag{9}$$

We remark that the first term in Eq. (9) is the Rutherford scattering of the electron by the nuclei whereas the second term represents the electron-

Comparison of the Born and Glauber generalized oscillator strengths for the $2s \rightarrow 3p$ transition of atomic hydrogen

F. T. Chan, C. H. Chang, and M. Lieber
Department of Physics, University of Arkansas, Fayetteville, Arkansas 72701

Y.-K. Kim
Argonne National Laboratory, Argonne, Illinois 60439

(Received 11 April 1977; revised manuscript received 14 February 1978)

Minima and maxima of the generalized oscillator strength for the $2s \rightarrow 3p$ transition of atomic hydrogen are found using the Glauber approximation. In contrast to the first-Born approximation, the *number* of extrema and their positions are found to vary with the energy of the incident particle, and the values at the minima do not vanish. There is qualitative agreement in the behavior of the first minimum with known experimental data on the resonance transitions of rare gases and mercury. For large incident energy, the transition amplitude in the Glauber approximation falls off with large momentum transfer more rapidly than predicted by a previous calculation based on the second-Born approximation.

I. INTRODUCTION

The cross sections for discrete excitations often show undulations in the angular distributions. In the first-Born approximation (FBA) these undulations can be attributed to minima in the corresponding generalized oscillator strength (GOS). The minima in the GOS arise from a combination of the oscillations in the wave functions of the target atoms as well as oscillations in the transition operator.[1-4] Calculations based on the FBA have been verified *qualitatively* in many experiments,[2,5,6] and at very high incident energies the location of the minima are in agreement with experiment.[5] However, even at infinite energy, the FBA fails at very large momentum transfers,[7] partly because the FBA does not account for scattering by the nucleus at all.

In the FBA, the GOS is expressed as a function of the momentum transfer $\vec{K}$ (we use atomic units) and it is independent of the incident energy. Hence, the positions of the minima and maxima in the GOS remain fixed as incident energy is varied. The minima in the Born GOS occur when the transition matrix element changes sign, and therefore the GOS vanishes at the minima.

Experimental data, however, differ from the FBA results in three aspects: (a) the "experimental" GOS does not vanish at the minimum, (b) the magnitude of the GOS at the minimum depends on the incident energy, and (c) the position of the first minimum (expressed in terms of K) is shifted toward smaller K at intermediate- to low-incident-electron energies (<500 eV). Owing to the low intensity for large-angle scattering, subsequent minima at higher K have not been observed in any experiment so far. Another failure of the FBA is that the GOS falls off too rapidly as $K \rightarrow \infty$.[7]

In this paper, we present a study in the Glauber approximation of the minima in the GOS and the asymptotic behavior in K of the $2s \rightarrow 3p$ excitation of the hydrogen atom by electron impact.

Physically, there are several mechanisms that could produce the observed difference between the experimental and FBA results. In inelastic scattering the orthogonality of wave functions for the initial and final atomic states causes the nuclear-potential contribution to vanish in the FBA. In the second Born approximation (SBA), however, the nuclear potential is retained via coupling to the elastic channel in intermediate states. A recent estimate[8] of a part of the SBA amplitudes shows that SBA can partly account for the nonvanishing minima, and the positions of the minima shift with the incident energy. Furthermore, the SBA correction falls off more slowly with K and dominates over the FBA term at large K.

Another mechanism that could result in nonzero values of the minima is spin-orbit splitting. When the experimental resolution is insufficient to resolve multiplets split by the spin-orbit coupling, then the experimental minima may not vanish because each level of the multiplets may have minima at different K. Then the unresolved experimental data would appear as if there were one nonvanishing minimum. For instance, for the $6\,^2S \rightarrow 6\,^2P$ transition of Au, the spin-orbit interaction shifts slightly the locations of the zero minima for the spin-orbit doublet (see Table I). On the other hand, the effects of electron correlation shift the location of the minima, but they are not likely to change the fact that the FBA produces a zero minimum because the minimum (at least the major one) is a result of the vanishing transition ampli-

Polarization fractions in Glauber theory for electron impact excitation of the $n = 3$ levels of atomic hydrogen

F. T. Chan and C. H. Chang
Physics Department, University of Arkansas, Fayetteville, Arkansas 72701
(Received 29 January 1976)

With the use of recently proposed analytic methods, Glauber scattering amplitudes for the excitation of the $3d$ substates of atomic hydrogen by electron impact are obtained in closed form. The individual $n = 3$ cross sections and the Balmer-α cross section predicted by the Glauber theory in the range $18 \leq E_i \leq 500$ eV are compared with experiments and with other calculations. The polarization fractions of $3p$-$2s$, $3d$-$2p$, and of the Balmer-α line are also calculated in the Glauber approximation, and comparison is made with the existing experimental data and with the Born predictions. The parameters (λ, χ) predicted by the Glauber approximation are also given.

I. INTRODUCTION

Although the scattering of a charged particle by a hydrogen atom has long been of interest to astrophysicists and atomic and molecular physicists, the data on the $3l$ excitation of atomic hydrogen by electron impact are rather scarce. To date, only two experimental measurements on the total cross section[1,2] and the total polarization fraction[1] have been reported for $n=3$ excitation. By modulating the exciting electron beam and separating the individual excitations on the basis of the different fluorescence decay rates of the three substates ($3s$, $3p$, and $3d$), Mahan, Gallagher, and Smith[3] recently measured the cross-section ratios $\sigma_{3s} : \sigma_{3p} : \sigma_{3d}$ as well as the cross section of the Balmer line σ_α. Furthermore, Eminyan *et al.*[4] have recently developed a delayed-coincidence technique to measure the angular correlations between the emitted photon and scattered electron in inelastic electron-atom collisions, and have reported results on e^--He collisions for $2\,^1P$ and $3\,^1P$ excitations. From the angular correlations they are able to deduce the ratio (λ) of the differential cross sections for exciting the degenerate magnetic sublevels of the substates and the relative phase (χ) of the corresponding excitation amplitudes. These collision parameters λ and χ, measured without the need of any normalization, have generally been hidden in most refined theoretical calculations of the collision and lost in experiments designed to measure cross sections and polarization fractions alone. Their measurement, therefore, is expected to provide a new and more conclusive test of electron-atom scattering theories. Such a detailed experimental study,[5] using the electron-photon coincidence technique, of the polarization and the excitation of the Balmer-α line is now under way at the University of Stirling. The present study is partly motivated by these experimental interests.

Previous Glauber calculations[6] for electron impact excitation of the $3l$ states of hydrogen atoms, using the direction perpendicular to $\vec{q}$ as the quantization z axis, have concentrated on the predicted differential and total cross sections.[7,8] However, for calculating the polarization fraction and the parameters (λ, χ) it is necessary to have the Glauber amplitudes calculated in the coordinate system,[6,9] quantized along the direction of the incident electron. To simplify the previous calculations[7,8] involving numerical evaluation of a relatively simple one-dimensional integral, we have used the recently proposed analytic methods[10,11] to obtain the closed-form Glauber amplitudes $[F_{3d,1s}(q, m_l)]$, which require no numerical integration. In Sec. II, we express the closed-form Glauber scattering amplitudes in terms of four generating functions. Two of these (for $1s$-$3s$ and $1s$-$3p$ excitation) are given by Thomas and Gerjuoy[11]; the detailed derivation of the other two (for $1s$-$3d$ excitation) is deferred to an appendix. In this appendix we also show that the two analytic methods[10,11] yield the same results. The expressions for polarization fraction and the parameters (λ, χ) are also given in this section. In Sec. III, we present and discuss the results of numerical calculations of the expressions obtained in Sec. II.

II. GLAUBER THEORY

The Glauber scattering amplitudes $F^{(\zeta)}_{3l,1s}(q, m_l)$ describing the excitation of the hydrogen atom from the ground state $\Psi_{1s}(\vec{r})$ to the final state $\Psi_{3lm}(\vec{r})$ by an incident charged particle $Z_i e$ with velocity v_i is given by

$$F^{(\zeta)}_{3l,1s}(q, m_l) = \frac{iK_i}{2\pi} \int \Psi^*_{3lm}(\vec{r}) \Gamma(\vec{b}; \vec{r}) \Psi_{1s}(\vec{r}) \times e^{i\vec{q}\cdot\vec{b}}\, d^2b\, d\vec{r}\,, \quad (1)$$

Glauber e^--H_2 elastic cross sections using the model of independent scattering centers

J. T. J. Huang
Department of Chemistry, University of Arkansas, Fayetteville, Arkansas 72701

F. T. Chan
Department of Physics, University of Arkansas, Fayetteville, Arkansas 72701

(Received 22 November 1976)

The elastic scattering of electrons from molecular hydrogen is calculated by using the Glauber approximation (including the exchange effect) within the framework of independent scattering centers. Our theoretical values for differential cross sections give reasonable agreement with experimental data at incident energies of 30, 50, 100, and 200 eV.

In spite of numerous applications of the Glauber approximation[1-3] to electron-atom scattering problems, there have been only a few attempts to apply it to the electron-molecule scattering. This is because of the multicentered nature of the target molecule and the complexity of possible excitation channels. The difficulty of the problem increases enormously and rapidly with the increasing number of particles in the system. Although Chen[4] has proposed a method for treating problems of multicenter targets and of composite incident particles, no actual calculations following his formulations have been reported yet. However, the complication of the electron-molecule collision can be reduced with simplified assumptions, and theoretical (effective potential) results for scattering of electrons by H_2, N_2, I_2, and U_2 have been published.[5-7] In this paper, we would like to show an even simpler approach: Glauber approximation with inclusion of exchange effect is used within the framework of independent scattering centers[8,9] to evaluate readily the elastic-scattering cross sections of the hydrogen molecule by electron impact.

The differential cross section for elastic e^--H_2 collision in the model of independent particle scat-

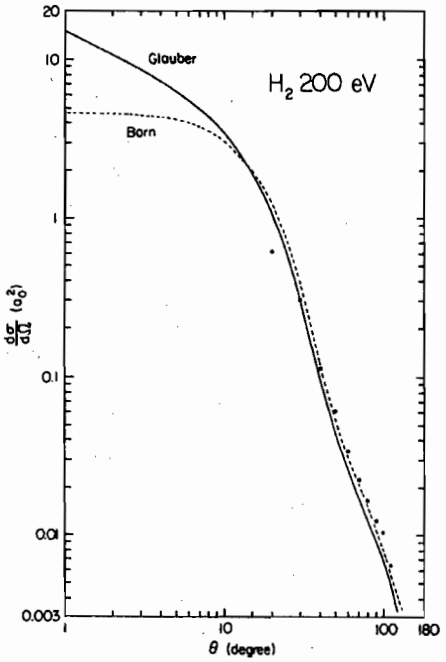

FIG. 1. Theoretical (— Glauber, --- Born) and experimental (●, Ref. 14) differential cross sections for e^--H_2 elastic scattering.

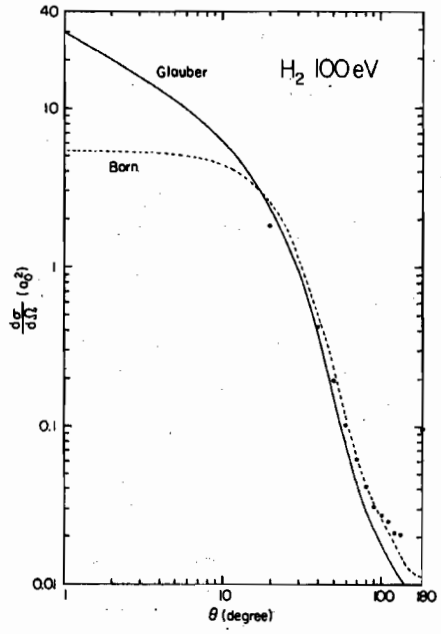

FIG. 2. Theoretical (— Glauber, --- Born) and experimental (●, Ref. 14) differential cross sections for e^--H_2 elastic scattering.

Bulletin of the American Physical Society, v 22, Issue 1, p 89-89, 1977

$\partial B_{z0}/\partial r$, where $\nu_{m\delta}(r,t) \triangleq \nu_{mo}\ \sigma_\delta(r,t)/\sigma_o(r)$ is roughly zero until the tube ages. Also, electric currents produce Joule heat within the photospheric-chromospheric tubes.

[1]K. McDonald, Bull. Am. Phys. Soc., 17 (1), 101-2 (1972).

SESSION JF: ELECTRONIC, ATOMIC, AND MOLECULAR COLLISION PROCESSES
Thursday morning, 10 February 1977
Parlor A (6th floor) at 9:00 A.M.
J.E. Bayfield, presiding

JF 1 Electron-Hydrogen Scattering in a Modified Eikonal Theory.* T.T. GIEN, Memorial U. of Newfoundland, St. Johns, Canada.-- A modified Glauber amplitude, in which a term of its eikonal expansion shown to contain a major defect is singled out and t eated in a substantially different manner than the rest of this amplitude, has been applied to studies of elastic scattering of electrons by a hydrogen atom at intermediate energies. The results are found in very good agreement with available experimental data recently acquired by absolute measurement. Discussions on the relationship between the defect of this eikonal term and the so-called straightline approximation used in the derivation of the Glauber amplitude are also given.

*Work supported in part by the National Research Council of Canada (Operating Grant A-3962).

JF 2 Electron Scattering by Li in Glauber Approximation.* C. H. CHANG and F. T. CHAN, U. of Arkansas, and Y.-K. KIM, Argonne National Laboratory.-- Differential cross sections for elastic scattering and for the excitation of the $2p^2P$, $3p^2P$, and $3s^2S$ states of Li have been calculated at 5.4, 10, 20, and 60 eV electron-impact energies in the frozen core Glauber approximation. It is found that the Glauber results are in reasonable agreement with the recent experimental measurements of Williams et al.[1] The polarization fraction of the resonance lines of Li is also calculated in the Glauber approximation. The theoretical results are in good agreement with the existing experimental data of Leep and Gallagher[2] in the incident energy range from 30-1000 eV.

*Work performed in part under the auspices of U.S. ERDA.

1. W. Williams, S. Trajmar, and D. Bozinis, J. Phys. B9, 1529 (1976).
2. D. Leep and A. Gallagher, Phys. Rev. A 10, 1082 (1974).

JF 3 Apparent Oscillator Strengths for Water Vapor.* R. H. HUEBNER and M. E. O'CONNOR,† Argonne National Laboratory, R. J. CELOTTA and S. R. MIELCZAREK, National Bureau of Standards.--Electron energy-loss spectra for H_2O were measured for 100, 300, and 400 eV electrons scattered close to the incident direction. Apparent oscillator strength distributions derived from these spectra are nearly identical for energy losses less than 15 eV. These results show excellent agreement with the composite of available photoabsorption data and provide an independent source of f values for the many discrete transitions in this region. For energy losses between 15 and 25 eV the three distributions differ by no more than ±30%, although they gradually rise above the vuv photoabsorption measurements. Previously reported electron-impact values in this spectral region are considerably smaller than both the optical data and our present results.

*Work supported in part by the U.S. ERDA.

†Undergraduate research participant from Clarke College, Dubuque, Iowa.

JF 4 Electron Drift Velocity in Methane. P. H. KLEBAN, U. of Minnesota* -- The drift velocity of electrons in gaseous methane (and several other polyatomics) shows a maximum as a function of electric field. This feature is apparently due to the interplay of elastic scattering at the Ramsauer minimum and inelastic scattering involving a vibrational transition (the inelastic threshold is very close to the Ramsauer minimum). These effects result in an electron velocity distribution that "streams" opposite to the field direction near the drift velocity maximum. We have solved the appropriate Boltzmann equation by computer using an iterative technique[1]. The solution is exact in a numerical sense. It converges when the final distribution is anisotropic and the inelastic scattering is large. Thus the assumptions made in previous analytic treatments can be avoided. Detailed numerical results will be presented.

* Supported by American Chemical Society Petroleum Research Fund 6066-AC6.

1 H. F. Budd, Phys. Rev. 158, 798 (1967); H. D. Rees, J. Phys. C. 5, 641 (1972).

JF 5 Feshbach Resonances in CH_3X(X=Cl,Br,I). Classification of Resonances and Prediction of Rydberg States.* D. SPENCE, Argonne National Laboratory.--Using an electron transmission spectrometer we locate Feshbach resonances in the alkyl halides. Combination of data from the acid halides and alkyl halides indicate that for structurally related molecules the energies of Feshbach resonances $E_{n\ell\ell'}(m)$ are related to the appropriate ionization potentials I(m) by the relationship. $E_{n\ell\ell'}(m) = A_{n\ell\ell'}I(m) + B_{n\ell\ell'}$ where $E_{n\ell\ell'}(m)$ is the nth resonance with excited electrons of angular momenta ℓ and ℓ' in species m, and $A_{n\ell\ell'}$ and $B_{n\ell\ell'}$ are constants independent of molecular species. This relationship enables easy identification or prediction of resonance energies in chemically related compounds. We show how low rydberg state energies may be obtained from Feshbach resonance spectra.

*Work performed under the auspices of the U.S. ERDA.

JF 6 Coincidence Study of Electrons Ejected at Surfaces by Metastable Helium Atoms. BAILEY DONNALLY and J. SHACKELFORD TOMS, Lake Forest College*--Allison, Dunning and Smith[1] suggested that the high yield of electrons when metastable helium atoms were incident on surfaces not atomically clean might be due to a two-step process in which two electrons are emitted. We have tested this idea by measuring time correlation of the electrons. Electrons ejected at a surface are transported to a channel electron multiplier by a magnetic field. Unless electrons emitted simultaneously came off at the same energy and the same angle, they would arrive at the detector at sufficiently different times to be resolved and measured by a time-to-amplitude converter. The system was tested by examining the multiple electron ejection occurring when 1 keV electrons strike MgO, and the single electrons ejected by 4.88 eV photons. For metastable helium on a surface, the fraction of the events in which two electrons were in coincidence is less than 10^{-3}. Therefore, the two-step, two-electron mechanism cannot account for the high secondary emission.

*Supported in part by the National Science Foundation.
[1]W. Allison, F. B. Dunning and A. C. H. Smith, J. Phys B 5, 1175 (1972).

JF 7 Reactions in a Fast Pulsed He Discharge. J. E. LAWLER, J. W. PARKER, L. W. ANDERSON, W. A. FITZSIMMONS,

Bulletin of the American Physical Society, v 21, Issue 1, p 50-50, 1976

TUESDAY MORNING, 3 FEBRUARY 1976
REGENT ROOM AT 9:00 A.M.
L. Spruch, presiding

ATOMIC COLLISIONS--HYPERFINE INTERACTIONS AND STRUCTURE

DF 1 Positronium Fine Structure Density Shifts in the Noble Gases* M.H. YAM, P.O. EGAN, W.E. FRIEZE, and V.W. HUGHES, Yale Univ.— The fine structure interval $\Delta\nu$ in the ground state of Ps formed in the noble gases has been measured using the microwave induced Zeeman resonance technique,[1] for gas densities D ranging from 1 to 3 atm. Using the measured value $\Delta\nu(D=0)=203.3849(12)$ GHz in nitrogen,[2] the linear fractional density shifts $a=(1/\Delta\nu)(\partial\Delta\nu(D)/\partial D)$ were found to be: $a(He)=(+1.6\pm0.3)\times10^{-5}$, $a(Ne)=(-1.9\pm0.4)\times10^{-5}$, $a(Ar)=(-6.2\pm0.3)\times10^{-5}$, $a(Kr)=(-6.6\pm0.5)\times10^{-5}$, $a(Xe)=(-7.3\pm1.7)\times10^{-5}(atm^{-1}\,0^{0}C)$. Comparing the Ps density shifts with those of H, we note: 1) The Ps shifts are an order of magnitude larger, 2) In Ne the Ps shift is negative but the H shift is positive, 3) In the heavy gases (Ar,Kr,Xe) the Ps shifts are approximately equal but the corresponding H shifts differ appreciably. Theoretical calculations of Ps density shifts are needed.

*Research supported in part by NSF under Grant #GP43847X.

[1]M. Deutsch and S.C. Brown, Phys. Rev. 85, 1047 (1952); [2]P.O. Egan, W.E. Frieze, V.W. Hughes and M.H. Yam, to be published in Phys. Lett. A.

DF 2 Glauber Cross Sections for Excitation of the 3l Levels of Hydrogen Atom by Electron Impact. F.T. CHAN and C.H. CHANG, University of Arkansas.--Using the integral reduction techniques of Thomas and Gerjuoy[1], the Glauber scattering amplitudes for the excitation of the 3l ($l = 0,1,2$) levels of atomic hydrogen by electron impact have been obtained in closed form. It is shown that the Glauber amplitudes can be written in terms of four generating functions: Two of these (for 3s, 3p) have already been derived by Thomas and Gerjuoy, the detailed reduction of the other two (for 3d) is given in this paper. Comparison is made with other theoretical models and with recent measurements.

[1]B.K. Thomas and E. Gerjuoy, J. Math. Phys. 12, 1576 (1971)

DF 3 Excitation of the $G^1\Sigma_g^+$ Level of H_2 by Electron Impact.* JAMES WATSON JR., BENJAMIN ASHMORE JR, and RICHARD J. ANDERSON, University of Arkansas, and SUNGGI CHUNG, University of Wisconsin--The optical excitation function of the $G^1\Sigma_g^+ \rightarrow B^1\Sigma_u$ transition of the H_2 spectrum has been determined for electron impact energies in the range 0-300 eV. Measurements of absolute optical cross sections have been carried out at 200 eV electron energy and 30 mtorr, H_2 gas pressure. Radiative lifetime measurements have also been carried out for the $G^1\Sigma_g^+$ state and yield a single mode decay with a decay constant of 38 nsec. The experimental measurements are used along with theoretical Franck-Condon factors to estimate the $G^1\Sigma_g^+$ direct excitation cross section.

*Research Supported by the Atmospheric Sciences Section, National Science Foundation.

DF 4 Radiative capture of keV electrons by ions.* C. M. LEE and R. H. PRATT, University of Pittsburgh--Radiative capture of electrons by atomic ions is an important process in plasmas. Such an radiative two-body recombination may be classified as 1) indirect capture through autoionizing states and 2) direct capture into the Rydberg series of the "electron + ion" system. We have studied direct radiative capture of electrons with kinetic energies greater than 1 KeV. The captured electrons is described as moving in a Hartree-Slater central potential. Applying quantum defect theory, the radiative capture and the tip bremsstrahlung processes may be treated together[1], because at atomic distances wave function shapes of energies close to the ionization threshold, are similar and vary slowly with the degree of excitation on ionization. As a result only two smoothly varying quantities, the quantum defect parameter and the cross sectic density, need to be calculated for each partial-wave channel. As an example, radiative capture of 1-100 keV electrons by Mo ions will be discussed, paying attention to the dependence on incident energy and degree of ionizatio .

* Supported in part by the National Science Foundation under Grant MPS74-03531A01.

[1] C.M. Lee and R.H. Pratt Phys. Rev. A12, 1825, (1975).

DF 5 On the Connection Between Atomic Photoeffect and Internal Conversion* SUNG DAHM OH and R. H. PRATT, Univ. of Pittsburgh.--It is shown that over an appreciable energy range K, L, and M shell photoeffect total cross sections are proportional to El internal conversion coefficients from the same subshell. In non-relativistic dipole approximation the ratio $\beta^{El}/\sigma = 3/8\pi(Z\alpha)^2$ independent of shell and subshell; numerically, for s waves, this ratio holds to 1 MeV. Screening effects enter only at low energies, reaching several per cent at the K shell threshold.

* Supported in part by the National Science Foundation under Grant MPS74-03531A01

DF 6 Radiative Corrections to Bremsstrahlung in the High Frequency Limit. J. MCENNAN, Univ. of Pittsburgh, M. GAVRILA, Univ. of Bucharest.—In a previous paper[1] the radiative corrections to atomic photoeffect were evaluated in lowest order in αZ (Sauter approximation). To the same order in αZ it has been shown that the phenomena of photoeffect and bremsstrahlung at the spectrum tip (tip-bremsstrahlung), in which all of the energy of the incident electron is emitted as radiation, are essentially inverse processes. Hence, cross sections for photoeffect and tip-bremsstrahlung, in this approximation, are simply related by detailed balancing. Angular distributions as well as polarization phenomena are identical for these processes. Thus, the results of ref.(1) can be applied directly to the radiative corrections to tip-bremsstrahlung. In addition to numerical results, analytic expressions for the non-relativistic and high energy limits of the radiative corrections to tip-bremsstrahlung are also considered.

[1]Bull. Am. Phys. Soc. 20, 91 (1975).

DF 7 Collisional Quenching of Metastable X-Ray Emitting States in a Fast Beam of He-Like Fluorine.* R. J. FORTNER and D. L. MATTHEWS, Lawrence Livermore Lab.--High resolution x-ray spectral measurements are used to determine the relative intensity of He-like fluorine x-ray transitions, $2\ ^3P_1 \rightarrow 1\ ^1S_0$ and $2\ ^1P_1 \rightarrow 1\ ^1S_0$, produced by fluorine collisions with Ne, Ar, and Kr gas targets at various pressures and in thin carbon foils and a thick carbon slab. The relative intensities are observed to be strong functions of both target density and incident charge Z. These effects are attributed to strong collisional quenching of both initial states by subsequent large impact parameter collisions. The data permit extraction for the first time of the total quenching cross sections (σ_Q) for fast fluorine ions in both states. A strong enhancement of the relative intensity of the $2\ ^3P_1$ is observed for F^{7+} projectiles. This strong en-

DM 12 Plasma Impurity Radiation. J. Rogerson, J. Davis, Naval Research Laboratory, and V. Jacobs, Science Applications, Inc.--An illustrative nonhydrodynamic model has been developed to described the optical emission from oxygen and iron impurities embedded in a Tokamak-like plasma. A system of rate equations has been solved assuming a time dependent coronal model (including the effects of dielectronic recombination) to yield the population densities of neighboring ground ionization stages. The model is first correlated with experimental data for oxygen and then is used to predict the radiative losses resulting from the iron impurities.

TUESDAY MORNING, 27 APRIL 1976
AMBASSADOR ROOM, SHOREHAM-AMERICANA AT 9:00 A.M.
R. Drachman, presiding

ELECTRON SCATTERING

DN 1. Low-Energy Elastic Scattering of Polarized Electrons by Polarized Hydrogen Atoms*. P.F. WAINWRIGHT, M.J. ALGUARD, G. BAUM,† V.W. HUGHES, J.S. LADISH, M.S. LUBELL, and W. Raith,† Yale Univ.—Measurements of the spin dependence in low-energy elastic scattering of electrons by atomic hydrogen are being carried out using polarized electrons and polarized hydrogen atoms in a crossed-beams configuration. Scattering of polarized electrons from polarized hydrogen atoms has been observed. The ratio of the singlet to triplet differential cross section is now being determined for 90° scattering at incident energies in the range from 10 eV to 30 eV. The polarized electron source, based upon the Fano effect in cesium,[1] produces an electron intensity of ~2 nA with a polarization of ~0.7. Polarization of the atomic hydrogen beam is achieved by high-field state selection in a six-pole magnet. A discussion of preliminary experimental results will be presented.

*Research supported by the NSF under Grant MPS75-02376 and by the ONR under Grant N00014-67-A-0097-0015.

†Present address Univ. of Bielefeld, Bielefeld, Germany.

[1]G. Baum, M.S. Lubell, and W. Raith, Phys. Rev. A 5, 1073 (1972).

DN 2 Cross Sections and Parameters (λ,χ) for the Excitation of n = 3 Levels of Atomic Hydrogen by Electron Impact and Polarization of the Resulting Radiation in Glauber Theory. F. T. CHAN and C. H. CHANG, University of Arkansas.--The Glauber scattering amplitudes for the excitation of the 3ℓ substates of atomic hydrogen by electron impact have been obtained in closed form. The individual n = 3 cross sections and the Balmer - α cross section predicted by the Glauber theory in the range $18 < E_i < 500$ eV have been compared with experiments and with other calculations. The polarization fractions of 3p-2s, 3d-2p, and of the Balmer - α line are also calculated in the Glauber approximation, and comparison is made with the existing experimental data and with the Born predictions. The parameter (λ,χ) predicted by the Glauber approximation are also given.

DN 3 Excitation of the n=2 State of Atomic Hydrogen by Electron Impact in the Distorted-Wave Approximation.* R. V. CALHOUN, D. H. MADISON, Drake U., and W. N. SHELTON, Florida State U.--The differential cross sections for excitation of the n=2 state of atomic hydrogen by the impact of electrons with energies of 54 to 100eV has been calculated in the distorted-wave approximation (DWBA) with exchange included. Cross sections for the $2s_{1/2}$, $2p_{1/2}$, and $2p_{3/2}$ were calculated and summed to give the n=2 angular distributions. The calculated angular distributions are compared to the experimental data of J. F. Williams and B. A. Willis.[1] The distorted-waves were calculated on the ground state hydrogen potential for both incoming and exit channels.

*Work supported by Research Corporation.

[1]J. F. Williams and B. A. Willis, J. Phys. B8, 1641 (1975).

DN 4 PWBA and DWBA Differential Cross Sections for Electron Impact Ionization of Helium.* D. H. MADISON and R. V. CALHOUN, Drake U. and W. N. SHELTON, Florida State U.--Double and triple differential cross sections for electron impact ionization of helium were calculated in the Plane Wave Born Approximation using atomic electron wave functions calculated as eigenfunctions of a Hartree-Fock potential. Similar cross sections were also obtained in the Distorted-Wave Approximation where all electron wave functions were calculated as eigenfunctions of the Hartree-Fock Potential. The PWBA calculations yield cross sections that are in good agreement with experimental doubly differential cross section data. For the triply differential cross sections, the PWBA calculations are not in satisfactory agreement with the data. The DWBA calculations, on the other hand, do give good agreement with available data. The DWBA calculations take almost two orders of magnitude more computer time than the PWBA calculations however.

*Work supported by the Research Corporation.

DN 5 A Useful Minimum Principle for $e^{\pm}$-Atom Scattering. *R. BLAU, L. ROSENBERG, and L. SPRUCH, NYU. — An upper variational bound (UVBd) on the scattering length A, when the target ground-state wavefunction ϕ is known, has long been available[1]. For ϕ imprecisely known, even a simple variational principle (VP) has up to now been unavailable due to the appearance of singular matrices[2]. An UVBd on the scattering length for a model problem defined in terms of a trial bound-state function ϕ_t is available only for the e^+-He case[3]. Representing A as $(\phi, T\phi)$ we define $A' \equiv (\phi_t, T\phi_t)$. We present an UVBd on A' which retains the simplicity of a VP, avoiding the necessity of inverting any singular matrices. It is applicable not only to e^+-atom scattering for any atom, but to e^--atom scattering as well.

*Work supported by ONR and NSF.

[1]L. Spruch and L. Rosenberg, Phys. Rev. 117, 143 (1960).

[2]R. Peterkop and L. Rabik, J. Phys. B, 4, 1440 (1971); B.A.P. Page, Journ. Phys. B 15, 2486 (1975).

[3]R.J. Drachman, J. Phys. B 5, L 30 (1972).

prognostication of the future of high energy physics to note that most of the Vietnam counterinsurgency recommendations of JASON were not only highly morally repugnant, but also tended to lie somewhere in the range between "highly impractical" and "patently absurd". One can only hope that those folks who brought us both the Electronic Battlefield and FNAL will not attempt to revitalize the moribund discipline of high energy physics by the same methods that they used so successfully to win the Vietnam war. To my knowledge, no member of HEPAP has suggested publicly that the productivity of postdocs could be increased by threatening to cut their ears off, but I would not be surprised if they were thinking about it.

SESSION DD: ATOMIC AND MOLECULAR PHYSICS

Tuesday afternoon, 21 December 1976
McCullough 134 at 2:00 P.M.
T.M. Miller, presiding

DD 1 Glauber e^- - H_2 Elastic Scattering Amplitude. F. T. Chan and J. T. J. Huang, University of Arkansas, Fayetteville. --The elastic scattering of electrons from molecular hydrogen is analyzed by using the Glauber approximation (including the exchange effect) within the framework of independent scattering centres. Our theoretical values for differential cross sections over the angular range 15^0 - 135^0 at incident energies of 30, 50, 100, and 200 eV are compared with recent experimental data of Lloyd et al.[1]

[1]C.R. Lloyd, P.J.O. Teuber, E. Weigold, and B.R. Lewis, Phys. Rev. 10A, 175 (1934).

DD 2 Collision-Broadened Linewidths of H_2S.* GOPAL D. TEJWANI and EDWARD S. YEUNG†, Ames Laboratory and Iowa State U. -- Self-broadened and foreign-gas (N_2 and O_2) broadened linewidths of H_2S at 300°K for a wide range of quantum numbers J and K_a, for both type A and type B bands, have been calculated using the Anderson-Tsao-Curnutte theory of line broadening. Computed values for self-broadened linewidths are in good agreement with the experimental results of Helminger and De Lucia. Air-broadened linewidths of H_2S at 200°K have also been calculated, so that the temperature dependence can be established.
*Supported by US ERDA under contract No. W-7405-eng-82.

†Alfred P. Sloan Research Fellow

DD 3 Production and Detection of OH in a Crossed Molecular Beam System.* D. R. MILLER and P. POULSEN, U. of California, San Diego--A barium chemi-ionization detector has been used to detect OH product in a crossed molecular beam study of the reaction $O + H_2O = OH + OH$. With ground state $O(^3p)$ the reaction is endoergic by 0.73 eV and the product OH is coned into a small solid angle of the laboratory system. We report on results of our first three experiments which suggest a threshold center-of-mass total energy (translational and vibrational) of about 0.92 eV. While the data is not adequate enough to quantitatively describe the importance of vibrational excitation of the H_2O to the total reaction cross-section, changes in the system components will be described which will permit such details to be extracted.
*Supported by NSF Grant ENG 71-02434

DD 4 The Effects of Spin-Orbit Coupling on $2p\sigma$ - $2p\pi$ Rotational Transitions.* R. ANHOLT, W.E.MEYERHOF, Stanford U., A.SALIN, Univ. de Bordeaux I.-- In near symmetric collisions with atomic charges $Z < 20$, the 1s electrons of the lighter collision partner are promoted in the $2p\sigma$ molecular orbital(MO) and any vacancy present in the $2p\pi$ MO may, through rotational coupling, jump to the $2p\sigma$ MO and end up as a K vacancy in either collision partner. Calculations of rotational coupling cross sections agree well with observed K vacancy production cross sections.[1] We have investigated the effects of the spin-orbit splitting between the $2p\sigma$ and $2p\pi(2p_{\frac{1}{2}}$ and $2p_{\frac{3}{2}})$MOs in higher-Z collisions. A general, approximate correction function is calculated which depends on a scaling parameter $\xi = \Delta E/(\hbar^2 k v^2)$ where ΔE is the $2p_{\frac{1}{2}}$ - $2p_{\frac{3}{2}}$ energy splitting, v is the ion velocity, and $k = 1/40\ Z_1Z_2(Z_1 + Z_2)^{\frac{1}{2}}e^2/a_0^3$. The function can be used to correct the nonrelativistic calculations of Taulberg et. al.[1] It varies from 1 ($\xi = 0$) to 1.15 ($\xi = 1$) then decreases rapidly to 0.03($\xi = 3$). The impact parameter dependence of the transition probability is also discussed.
*Partly supported by NSF.
[1]K.Taulberg, J.S. Briggs, and J. Vaaben, J. Phys. B9,1351 (1976).

DD 5 Electron Bremsstrahlung from Proton-Bombarded Beryllium. W. T. OGIER and TINA J. TANAKA, Pomona College--Observation of a weak continuous x-ray spectrum from light element targets bombarded with 1.6 MeV protons was reported in 1966 and attributed to bremsstrahlung radiation from stopping electrons first as they are accelerated by the proton and second as they stop.[1] Due to a computing error the intensities reported then were too low. We have recently remeasured the x-ray spectrum produced by 1.6 MeV protons on beryllium using a flow proportional counter with improved energy calibration, and we have recomputed the results of the theory,[1] which used classical bremsstrahlung formulas and ignored atomic binding forces. Intensities observed are 10^{-7} and 3×10^{-8} quanta/proton-sr-eV at quantum energies of 800 and 1500 eV respectively. Theoretical yields are less than a third as great, possibly because the theory ignores beryllium ions stripped after acceleration.

[1]W. T. Ogier, R. D. Carlson, and Jayne Knoche, Phys. Rev. 142, 50 (1966).

DD 6 Proton transitions in hydrogen bonds in terms of a first order perturbation model. W. G. Cooper, University of Houston Downtown. --A first order perturbation formalism is presented for analyzing the hydrogen bond proton transfer reaction given by

$$O\cdots H\text{-}N \longrightarrow O\text{-}H\cdots N.$$

Cross derivative terms in the kinetic energy operator are neglected and a piecewise-constant rectangular shaped potential surface is employed for the hydrogen bonding system. The full potential is separated such that the components responsible for reaction are defined and "sandwiched" between initial and final states to yield an expression for the proton transition rate. Analysis provides a physical model of energy transfer between modes, vibrational enhancement, and increased reactivity of newly opened reactive channels.

DD 7 Inhomogeneity Corrections to the Thomas-Fermi-Dirac Model of the Noble Gas Diatoms. CHIA C. SHIH and YEA H. UANG, Department of Physics and Astronomy, U. of Tenn.--Total and potential energies for interacting close shell noble gas diatoms are calculated according to the Thomas-Fermi-Dirac formula with the modified Weizsäcker inhomogeneity correction (TFDW)[1]. Taking the electron density of the Hartree-Fock (HF) molecular orbital calculation as input,[2] the inhomogeneity corrections are small compared to the total energies at all available distances for He_2, Ne_2, and Ar_2. Both the total and the potential energies are in good agreement with the HF results. Taking instead the electron-gas-approximation (EGA) as input,[3] where the superposition of the atomic

Glauber e^- - Li elastic scattering amplitude

F. T. Chan and C. H. Chang
Physics Department, University of Arkansas, Fayetteville, Arkansas 72701
(Received 8 December 1975)

The recently proposed analytic methods of Thomas and Chan, which reduce the Glauber amplitude for charged-particle–neutral-atom collisions to a one-dimensional integral representation involving modified Lommel functions, are used to study elastic e^- - Li scattering. The criterion for using the frozen-core approximation is discussed. The numerical results obtained using these two models are presented.

In recent years the Glauber approximation[1,2] (GA) has been widely used to study scattering of charged particles by neutral atoms and model atoms having one or two bound electrons.[3] For more complicated collisions, Franco[4] has proposed a method for obtaining a one-dimensional integral representation for the elastic and inelastic scattering of charged particles by arbitrary neutral atoms. However, Franco's final integral representation for these Glauber amplitudes involves the calculation and integration of the differences between strongly (exponentially) divergent functions, as well as the numerical calculation of δ functions whenever elastic scattering is considered.[5] To avoid these seemingly numerical problems, Thomas and Chan[5] have proposed another reduction procedure of the scattering amplitudes to a one-dimensional integral representation involving modified Lommel functions. Using this method, results for elastic and inelastic e^- + He collisions have also been reported.[5-7] On the other hand, Kumar and Srivastava[8] have been able to avoid the encounter with the divergent functions appearing in Franco's final expression[4] by stopping a step earlier, and have reported calculations for e^--Li elastic scattering. The price to be paid for this simplication is that their final expression is a two-dimensional integral representation. In this paper, we report calculations on the elastic e^--Li collision in GA using the integral reduction techniques of Thomas and Chan.[5] [Our notation follows that of this reference which will be referred to as TC; TC Eq. (4) means Eq. (4) of TC.]

The Glauber amplitude for elastic scattering of a charged structureless particle $Z_i e$ by ground-state Li atoms with wave function $\phi_i(\vec{r}_1, \vec{r}_2, \vec{r}_3)$ is given by

$$F(q) = \frac{iK_i}{2\pi} \int \phi_f^*(\vec{r}_1, \vec{r}_2, \vec{r}_3)\Gamma(\vec{b}; \vec{r}_1, \vec{r}_2, \vec{r}_3) \times \phi_i(\vec{r}_1, \vec{r}_2, \vec{r}_3) e^{i\vec{q}\cdot\vec{b}} d^2b\, d\vec{r}_1\, d\vec{r}_2\, d\vec{r}_3 , \tag{1}$$

where

$$\Gamma(\vec{b}; \vec{r}_1, \vec{r}_2, \vec{r}_3) = 1 - \left(\frac{|\vec{b} - \vec{s}_1|}{b}\right)^{2i\eta} \left(\frac{|\vec{b} - \vec{s}_2|}{b}\right)^{2i\eta} \left(\frac{|\vec{b} - \vec{s}_3|}{b}\right)^{2i\eta} , \tag{2}$$

and $\eta \equiv -Z_i/v_i$ (in atomic units). In Eqs. (1) and (2), $\vec{q} = \vec{K}_f - \vec{K}_i$ is the momentum transfer vector; $\vec{b}$, $\vec{s}_1$, $\vec{s}_2$, and $\vec{s}_3$ are the respective projections of the position vectors of the incident particle and bound electrons ($\vec{r}_1$, $\vec{r}_2$, and $\vec{r}_3$) onto the plane perpendicular to the direction of the Glauber path integration: $\vec{q}$, $\vec{b}$, $\vec{s}_1$, $\vec{s}_2$, and $\vec{s}_3$ are all coplanar. We shall show that the first term (independent of η) under the integral in Eq. (1), which leads to $\delta(\vec{q})$, is exactly cancelled by the same factor stemming from the second term (dependent on η) in the amplitude integral. Therefore, the $\delta(\vec{q})$ is explicitly removed. For the Li ground state, where the bound electrons are in $(1s)^2(2s)^1$ configuration, we use the variationally determined wave function given by Veselov *et al.*,[9] namely,

$$\begin{aligned}\phi_i^*\phi_i &= \frac{1}{3!} \left|\det(\Psi_{1s\uparrow}, \Psi_{1s\downarrow}, \Psi_{2s})\right|^2 \\ &= \Psi_{1s}^2(1)\Psi_{1s}^2(2)\Psi_{2s}^2(3) \\ &\quad - \Psi_{1s}^2(1)\Psi_{1s}(2)\Psi_{2s}(2)\Psi_{1s}(3)\Psi_{2s}(3) ,\end{aligned} \tag{3}$$

where

$$\Psi_{1s} = (\alpha^3/\pi)^{1/2} e^{-\alpha r} \tag{4a}$$

and

$$\Psi_{2s} = \left(\frac{3\beta^5}{\pi(\alpha^2 - \alpha\beta + \beta^2)}\right)^{1/2} \left(1 - \frac{\alpha + \beta}{3} r\right) e^{-\beta r} , \tag{4b}$$

with $\alpha = 2.694$ and $\beta = 0.767$. This wave function yields an energy of -7.414 a.u. in comparison with the experimental value of -7.4781 a.u. Substituting Eqs. (3) and (4) into Eq. (1), we find that the scattering amplitude $F(q)$ can be written in terms of a generating function; in particular,

Cross sections for excitation of the $n\,^1D$ states of helium by electron impact and polarization of the resulting radiation in Glauber theory

F. T. Chan and C. H. Chang
Physics Department, University of Arkansas, Fayetteville, Arkansas 72701
(Received 17 March 1975)

Recently developed analytic methods, which reduce the Glauber amplitude for charged-particle–neutral-atom collisions to a one-dimensional integral representation involving modified Lommel functions, are used to evaluate the cross sections for the direct excitation of $3\,^1D$ and $4\,^1D$ states of helium by electron impact with incident energies from 40 to 1000 eV. It is shown that the Glauber amplitudes can be written in terms of three generating functions: One of these has already been derived by Thomas and Chan; the detailed reduction of the other two is given in this paper. Comparison is made with the Born, Ochkur, and Woollings-McDowell approximations. The polarization fraction of the 6678-Å helium line emitted in $e^- + \mathrm{He}$ collisions is also calculated in the Glauber approximation. The agreement between theory and experiment is less than satisfactory in the entire energy region.

I. INTRODUCTION

Recently, collisional excitation of the $n\,^1D$ levels of helium has attracted considerable experimental interest since the subsequent radiation lines fall in the visible region of the spectrum and allow total-cross-section measurements. In the last decade, such electron-impact measurements have been made by several groups[1–4] with results which are inconsistant both qualitatively and quantitatively. For example, the results from Ref. 1 are larger than those from Refs. 2 and 3 by ~30–50% in the common energy range of measurements. Moreover, the energy dependences of the experimental cross sections do not agree among themselves. On the theoretical side, calculations have been performed with the Born approximation,[5,6] the Ochkur approximation,[7] and the Woollings-McDowell approximation.[8] But all these calculations give results which are in fairly large discrepancy with experimental values in the entire energy range (40–1000 eV). For example, the total cross section predicted from the Born approximation is smaller than data of Refs. 2 and 3 by ~55% for $3\,^1D$ excitation and by ~26% for $4\,^1D$ excitation even at 1000 eV. The situation is surprising since the Born approximation and the related approximations are expected to be valid in the high-energy region (incident energies $\geq$200 eV).

In this paper, we report results obtained from the Glauber approximation (GA),[9] which has recently been applied with partial success to elastic and inelastic scattering of electrons by atomic hydrogen[10–14] and helium[15–19] (the GA is reliable in predicting the magnitude but is incapable of finding the relative phase for the e^--He $1S$-nP excitation amplitude in the intermediate- and high-energy ranges). Furthermore, the present study is interesting in itself since it provides a nontrivial example in which the troublesome $\delta(\vec{q})$ function can and should be removed even for $\vec{q} \neq 0$ (inelastic collision).

We have organized this paper as follows: In Sec. II, we derive the Glauber scattering amplitudes in terms of three generating functions. One of these is given by Thomas and Chan[17]; the detailed derivation of the other two is deferred to an appendix. In Sec. III we derive the expression for the polarization fraction of the 6678-Å helium line in the Glauber approximation; in Sec. IV, we present and discuss the results of numerical calculations of the expressions obtained in Secs. II and III.

II. EXCITATION CROSS SECTIONS

The Glauber scattering amplitudes $F^{(\zeta)}_{n\,^1D,\,1\,^1S}(\vec{q})$ describing the excitation of the He from the ground state $\Psi_{1\,^1S}(\vec{r}_1, \vec{r}_2)$ to the final state $\Psi_{n\,^1D}(\vec{r}_1, \vec{r}_2)$ by an incident charged particle $Z_i e$ with velocity v_i is given by

$$F^{(\zeta)}_{n\,^1D,\,1\,^1S}(\vec{q}) = \frac{iK_i}{2\pi} \int \Psi^*_{n\,^1D}(\vec{r}_1, \vec{r}_2)\,\Gamma(b; \vec{r}_1, \vec{r}_2) \times \Psi_{1\,^1S}(\vec{r}_1, \vec{r}_2) e^{i\vec{q}\cdot\vec{b}}\, d^2b\, d\vec{r}_1\, d\vec{r}_2 , \quad (1)$$

where

$$\Gamma(b; \vec{r}_1, \vec{r}_2) = 1 - (|\vec{b} - \vec{s}_1|/b)^{2i\eta} (|\vec{b} - \vec{s}_2|/b)^{2i\eta} \quad (2)$$

and

$$\eta \equiv -Z_i/v_i \quad \text{(in a.u.)}.$$

In Eqs. (1) and (2), $\vec{b}$, $\vec{s}_1$, and $\vec{s}_2$ are the respective projections of the position vectors of the incident particle and the bound electrons ($\vec{r}_1$ and $\vec{r}_2$) onto the plane perpendicular to the direction of the Glauber path integration. The superscript (ζ) rep-

Glauber cross sections for excitation of the $2\,^1P$ level of helium by proton impact

F. T. Chan and C. H. Chang
Physics Department, University of Arkansas, Fayetteville, Arkansas 72701
(Received 4 November 1974)

The Glauber approximation is applied to excitation of $2\,^1P$ level of helium by proton impact with incident energies from 25 to 1000 keV. The theoretical results for the total excitation cross sections are in good agreement with the experimental data of Park and Schowengerdt and of Hippler and Schartner. Comparison is made with other theoretical models.

In a series of recent papers,[1-4] new reduction techniques for the Glauber e^--He elastic and inelastic scattering amplitudes are proposed. The results obtained using these methods for the predicted differential and integrated cross sections and for the polarization of radiation resulting from collisions are generally in good agreement with the experimental findings. The relative success of these analytic methods for electron scattering leads naturally to the question of its applicability to the proton-helium collision. Since the differential cross section for proton-helium scattering is more sharply peaked in the forward direction than for electron-helium collision, the Glauber approximation is expected to be more suitable in the former case. In this paper, we focus our attention on the excitation of helium atom to the $2\,^1P$ level from its ground state by proton impact, since extensive experimental[5,6] and theoretical[7-15] studies are available in literature.

In the center-of-mass system, the Glauber scattering amplitude $F_{fi}^{(\xi)}(\vec{q})$ describing the excitation of the He atom from the ground state $\Psi_{1S}(\vec{r}_1,\vec{r}_2)$ to the final state $\Psi_{2\,1P}(\vec{r}_1,\vec{r}_2)$ by an incident proton with velocity v_i is given by

$$F_{2P,1S}^{(\xi)}(\vec{q})=\frac{ik_i}{2\pi}\int \Psi_{2\,1P}^{*}(\vec{r}_1,\vec{r}_2)\Gamma(b;\vec{r}_1,\vec{r}_2)\times\Psi_{1\,1S}(\vec{r}_1,\vec{r}_2)e^{i\vec{q}\cdot\vec{b}}\,d^2b\,d\vec{r}_1\,d\vec{r}_2\,, \quad (1)$$

where

$$\Gamma(b;\vec{r}_1,\vec{r}_2)=1-(|\vec{b}-\vec{s}_1|/b)^{2i\eta}(|\vec{b}-\vec{s}_2|/b)^{2i\eta} \quad (2)$$

and

$$\eta=-1/v_i$$

(in atomic units). In Eqs. (1) and (2), $\vec{b}$, $\vec{s}_1$, and $\vec{s}_2$ are the respective projections of the position vectors of the incident proton and the bound electrons ($\vec{r}_1$ and $\vec{r}_2$) onto the plane perpendicular to the direction of the Glauber path integration. The upper index (ξ) denotes the $\vec{q}$-dependent center-of-mass coordinate system, whose z axis lies along $\hat{\xi}$ and is perpendicular to $\vec{q}$. The $1\,^1S$-$2\,^1P_m$ Glauber amplitudes are formally identical to those of corresponding electron scattering and are given by Eqs. (5), (6), and (20) of Ref. 3:

$$F_{2P,1S}^{(\xi)}(\vec{q},m_L=0)=0 \quad (3a)$$

and

$$F_{2P,1S}^{(\xi)}(\vec{q},m_L=\pm1)=\pm e^{\mp i\phi_q}h_{2P,1S}(q), \quad (3b)$$

where

$$h_{2P,1S}(q)=i\sqrt{\tfrac{3}{2}}\times0.8483\times0.37831\times128k_i\eta\sum_{n=1}^{4}c(n)\frac{\partial^2}{\partial\lambda_1\partial\lambda_2}\times\Big\{\Gamma(1+i\eta)\Gamma(2-i\eta)q^{2i\eta-3}\lambda_2^{-2}\lambda_1^{-2i\eta-2}[-(1+i\eta)_2F_1(2-i\eta,1-i\eta;2;-\lambda_1^2/q^2)+{}_2F_1(2-i\eta,1-i\eta;1;-\lambda_1^2/q^2)]$$
$$-(2i\eta)^2\int_0^\infty b^6\,db J_1(qb)[(1+i\eta)(i\lambda_1 b)^{-2i\eta-3}\mathfrak{L}_{2i\eta,1}(i\lambda_1 b)-i\eta(i\lambda_1 b)^{-2i\eta-2}\mathfrak{L}_{2i\eta-1,0}(i\lambda_1 b)]\times(i\lambda_2 b)^{-2i\eta-2}\mathfrak{L}_{2i\eta-1,0}(i\lambda_2 b)\Big\}_{\substack{\lambda_1=\lambda_1(n)\\ \lambda_2=\lambda_2(n)}}, \quad (3c)$$

with $c(n)=1$, 0.799, 0.799, 0.799^2; $\lambda_1(n)=1.895$, 3.095, 1.895, 3.095; $\lambda_2(n)=3.41$, 3.41, 4.61, 4.61; for $n=1,2,3,4$. In Eq. (3c), Γ, J_1, ${}_2F_1$, and $\mathfrak{L}_{\mu,\nu}$ are the usual gamma, Bessel, hypergeometric, and modified Lommel functions,[1] respectively.

Equations (3a)–(3c) differ from the expressions (5), (6), and (20) of Ref. 3 by the phase $\pm i$ (when $m_L=\pm1$) since we here use the same convention as those of Ref. 16.

The differential cross sections in the center-of-

Excitation cross sections of $e^-+He \rightarrow e^-+He(3\,^1P,4\,^1P)$ and the polarization of the 5016-Å helium line resulting from e^--He scattering in Glauber theory

F. T. Chan and S. T. Chen
Physics Department, University of Arkansas, Fayetteville, Arkansas 72701
(Received 29 April 1974; revised manuscript received 17 June 1974)

The recently derived generating function $I_p(\lambda_1, \lambda_2; q)$ in the Glauber amplitude for $2\,^1P$ excitation of He by electron impact is used to evaluate the cross sections for the $3\,^1P$ and $4\,^1P$ excitations of He by electron impact with incident energies from 50 to 1000 eV. Comparison is made with the Bethe approximation, the Born approximation, and the classical theory of Gryzinski. The theoretical results for the total excitation cross sections are in reasonable agreement with the experimental data. The positions of the peak values for the total cross section for both cases are found to be around 100 eV, which are consistent with the existing experimental findings. The n^{-3} rule is also briefly discussed. The polarization fraction of the 5016-Å helium line emitted in $e^- + He$ collisions is also calculated in the Glauber approximation. The theoretical results for the polarization fraction are in reasonable agreement with the existing experimental data in the energy range $50 < E_a < 1000$ eV.

I. INTRODUCTION

Recently, a large amount of experimental data[1-7] have become available on the total cross sections for the excitation of helium from its ground state to the $3\,^1P$ and $4\,^1P$ levels by electron impact. There appears to be good agreement between all the photon measurements so that the positions of the peak cross sections are around 100 eV, although there is considerable variation in peak height. On the theoretical side, calculations have been performed with the Born approximation,[8,9] the Bethe approximation,[10] and classical theory.[11] For energies greater than 200 eV, all these theoretical models produce results which are in reasonable agreement with the existing experimental data. However, the positions for the peak cross section predicted from these methods are in poor agreement with the experiments.

We want to do two things in this paper. First, we show that the generating function $I_p(\lambda_1, \lambda_2; q)$ recently derived[12] in the Glauber amplitude for the $2\,^1P$ excitation can be employed without much further effort to evaluate the cross sections for the $3\,^1P$ and $4\,^1P$ excitation of helium by electron impact. Second, we show that the properly computed polarization fraction $P(E_a)$ in Glauber theory does yield a reasonably good fit to the observed $P(E_a)$ in the range $50 < E_a < 1000$.

II. EXCITATION CROSS SECTIONS

The Glauber scattering amplitude $F_{fi}(\vec{q})$ describing the excitation of the He from the ground state $\Psi_{1\,^1S}(\vec{r}_1, \vec{r}_2)$ to the final state $\Psi_{n\,^1P}(\vec{r}_1, \vec{r}_2)$ by an incident charged particle $Z_i e$ with velocity v_i is given by

$$F_{fi}(\vec{q}) = (iK_i/2\pi) \int \Psi^*_{n\,^1P}(\vec{r}_1, \vec{r}_2)\Gamma(\vec{b}; \vec{r}_1, \vec{r}_2) \times \Psi_{1\,^1S}(\vec{r}_1, \vec{r}_2) e^{i\vec{q}\cdot\vec{b}} d^2b\, d\vec{r}_1 d\vec{r}_2, \quad (1)$$

where

$$\Gamma(\vec{b}; \vec{r}_1, \vec{r}_2) = 1 - (|\vec{b} - \vec{s}_1|/b)^{2i\eta}(|\vec{b} - \vec{s}_2|/b)^{2i\eta} \quad (2)$$

and

$$\eta \equiv -z_i/v_i \quad \text{(in atomic units)}.$$

In Eqs. (1) and (2), $\vec{b}$, $\vec{s}_1$, and $\vec{s}_2$ are the respective projections of the position vectors of the incident particle and the bound electrons ($\vec{r}_1$ and $\vec{r}_2$) onto the plane perpendicular to the direction of the Glauber path integration. The approximate ground-state wave function chosen (in atomic units) is the one described by Byron and Joachain,[13]

$$\Psi_{1\,^1S}(\vec{r}_1, \vec{r}_2) = (1.6966/\pi)(e^{-1.41r_1} + 0.799\,e^{-2.61r_1}) \times (e^{-1.41r_2} + 0.799\,e^{-2.61r_2}). \quad (3)$$

A. $1\,^1S$-$3\,^1P$ excitation

For the $3\,^1P$ state of He, we use the variationally determined wave function given by Goldberg and Clogston,[14] namely,

$$\Psi_{3\,^1P}(\vec{r}_1, \vec{r}_2) = (N_{3P}/\sqrt{3\pi})[e^{-2r_1}(c - r_2)r_2 e^{-\mu r_2} \times Y_{1m}(\theta_2, \phi_2) + e^{-2r_2}(c - r_1) \times r_1 e^{-\mu r_1} Y_{1m}(\theta_1, \phi_1)], \quad (4)$$

with

Glauber cross sections for excitation of the $2\,^1P$ state of helium by electron impact

F. T. Chan and S. T. Chen
Physics Department, University of Arkansas, Fayetteville, Arkansas 72701
(Received 4 February 1974)

Recently developed analytic methods, which reduce the Glauber amplitude for charged-particle–neutral-atom collisions to a one-dimensional integral representation involving modified Lommel functions, are used to evaluate the cross sections for the direct excitation of the $2\,^1P$ state of helium by electron impact with incident energies from 55.5 to 900 eV. The theoretical results for the differential and total excitation cross sections are in good agreement with the experimental data. In particular, the Glauber theory predicts a peak value for the total excitation cross sections around 80 eV which is consistent with the existing experimental findings, whereas other theoretical models give monotonically increasing values with decreasing energy below 100 eV.

I. INTRODUCTION

Recently, the Glauber approximation[1] (GA) for scattering amplitudes has been applied with considerable success to elastic and inelastic scattering of electrons by atomic hydrogen[2-4] and by helium.[5-8] For e^--He scattering, calculations have been performed only for cases where the final states of helium atom are spherically symmetric, e.g., elastic scattering and direct excitation of helium to $2\,^1S$ state. The purpose of this paper is to show that the analytic methods[6] for reducing the GA to a one-dimensional integral representation involving modified Lommel functions can be employed to evaluate the cross sections for direct excitation of helium to nonspherical symmetric states by electron impact. In this paper, we focus our attention on the $2\,^1P$ excitation of the helium atom where discrepancies exist between the other theoretical models and the experimental data.

II. CROSS SECTION EXPRESSIONS

The Glauber scattering amplitude $F_{fi}(\vec{q})$ describing the excitation of the He atom from the ground state $\Psi_{1s}(\vec{r}_1, \vec{r}_2)$ to the final state $\Psi_{2^1P}(\vec{r}_1, \vec{r}_2)$ by an incident charged particle $Z_i e$ with velocity v_i is given by

$$F_{fi}(\vec{q}) = \frac{ik_i}{2\pi} \int \Psi^*_{2^1P}(\vec{r}_1, \vec{r}_2)\Gamma(b; \vec{r}_1, \vec{r}_2) \times \Psi_{1^1S}(\vec{r}_1, \vec{r}_2) e^{i\vec{q}\cdot\vec{b}}\, d^2b\, d\vec{r}_1\, d\vec{r}_2 \,, \tag{1}$$

where

$$\Gamma(b; \vec{r}_1, \vec{r}_2) = 1 - \left(\frac{|\vec{b} - \vec{s}_1|}{b}\right)^{2i\eta} \left(\frac{|\vec{b} - \vec{s}_2|}{b}\right)^{2i\eta} \tag{2}$$

and

$$\eta \equiv -Z_i/v_i$$

(in atomic units). In Eqs. (1) and (2), $\vec{b}$, $\vec{s}_1$, and $\vec{s}_2$ are the respective projections of the position vectors of the incident particle and the bound electrons ($\vec{r}_1$ and $\vec{r}_2$) onto the plane perpendicular to the direction of the Glauber path integration. The approximate atomic wave functions chosen (in atomic units) are the orthogonal set described by van den Boc[9] and by Flannery[10]:

$$\Psi_{1s}(\vec{r}_1, \vec{r}_2) = (1.6966/\pi)(e^{-1.41r_1} + 0.799e^{-2.61r_1}) \times (e^{-1.41r_2} + 0.799^{-2.61r_2}) \tag{3}$$

and

$$\Psi_{2^1P}(\vec{r}_1, \vec{r}_2) = (0.37831/\pi)[r_1 e^{-0.485r_1} Y_{lm}(\hat{r}_1) e^{-2r_2} + r_2 e^{-0.485r_2} Y_{lm}(\hat{r}_2) e^{-2r_1}]. \tag{4}$$

In the case of excitation to the $m = 0$ state, one sees that by introducing the cylindrical coordinates for $\vec{r}_1$ and $\vec{r}_2$, $F(\vec{q})$ vanishes from Eq. (1), since the integrand under the integral is an odd function of z.

For excitation to either $m = +1$ or $m = -1$, the values of $|F_{fi}(\vec{q})|^2$ are equal. Let us calculate the excitation to $m = -1$ only. Substituting expressions (3) and (4) for $m = -1$ into Eq. (1), we obtain the amplitude $F(\vec{q})$ in terms of the generating function $I(\lambda_1, \lambda_2; q)$,

$$F_{fi}(\vec{q}) = \sqrt{\tfrac{3}{2}} \times 0.8483 \times 0.37831 \times K_i \left[\left(\frac{\partial^2 I}{\partial\lambda_1 \partial\lambda_2}\right)_{\substack{\lambda_1 = 1.895 \\ \lambda_2 = 3.41}} + 0.799 \left(\frac{\partial^2 I}{\partial\lambda_1 \partial\lambda_2}\right)_{\substack{\lambda_1 = 3.095 \\ \lambda_2 = 3.41}} + 0.799 \left(\frac{\partial^2 I}{\partial\lambda_1 \partial\lambda_2}\right)_{\substack{\lambda_1 = 1.895 \\ \lambda_2 = 4.61}} + 0.799^2 \left(\frac{\partial^2 I}{\partial\lambda_1 \partial\lambda_2}\right)_{\substack{\lambda_1 = 3.095 \\ \lambda_2 = 4.61}} \right], \tag{5}$$

Glauber Cross Sections for Excitation of the 2 ^1S State of Helium by Electron and Positron Impact

F. T. Chan and S. T. Chen
Physics Department, University of Arkansas, Fayetteville, Arkansas 72701
(Received 14 May 1973)

The recently proposed analytic methods, which reduce the Glauber amplitude for charged-particle–neutral-atom collisions to a one-dimensional integral representation involving modified Lommel functions, are used to evaluate the cross sections for the direct excitation of the 2 ^1S state of helium by electron and positron impact. Comparison is made with the Coulomb-projected Born approximation of Hidalgo and Geltman and the truncated eigenfunction-expansion method of Berrington, Bransden, and Coleman.

In a recent paper,[1] new reduction techniques for the Glauber e^--He elastic scattering amplitudes are proposed. The results obtained using these methods are in good agreement with those obtained by Franco[2] from a three-dimensional integral representation. The purpose of this note is to show that the generating function $I(\lambda_1, \lambda_2; q)$ obtained in Ref. 1 can be used to calculate the cross sections for direct excitation of helium by electron and positron impact.

The scattering amplitude $F_{fi}(\vec{q})$, where the He atom is excited from the ground state $\Psi_{1s}(\vec{r}_1, \vec{r}_2)$ to the final state $\Psi_{2^1S}(\vec{r}_1, \vec{r}_2)$ by an incident charged particle $Z_i e$ with velocity v_i, is given according to the Glauber theory by

$$F_{fi}(\vec{q}) = \frac{ik_i}{2\pi} \int \Psi^*_{2^1S}(\vec{r}_1, \vec{r}_2)\Gamma(\vec{b}; \vec{r}_1, \vec{r}_2) \times \Psi_{1s}(\vec{r}_1, \vec{r}_2) e^{i\vec{q}\cdot\vec{b}} d^2b\, d\vec{r}_1\, d\vec{r}_2, \quad (1)$$

where

$$\Gamma(\vec{b}; \vec{r}_1, \vec{r}_2) = 1 - \left(\frac{|\vec{b} - \vec{s}_1|}{b}\right)^{2i\eta} \left(\frac{|\vec{b} - \vec{s}_2|}{b}\right)^{2i\eta} \quad (2)$$

and

$$\eta \equiv -Z_i/v_i \text{ (in atomic unit).}$$

In Eqs. (1) and (2), $\vec{b}$, $\vec{s}_1$, $\vec{s}_2$ are the respective projections of the position vectors of the incident particle and the bound electrons ($\vec{r}_1$ and $\vec{r}_2$) onto the plane perpendicular to the direction of the Glauber path integration. The approximate atomic wave functions we choose (in atomic units) are the orthonomal set used by van den Bos[3] for calculations on proton-helium scattering and Hidalgo and Geltman[4] for calculations on e^--helium collisions:

$$\Psi_{1s}(\vec{r}_1, \vec{r}_2) = \frac{2.605^2}{4\pi} (e^{-1.41r_1 - 1.41r_2} + 0.799e^{-2.61r_1 - 1.41r_2} + 0.799e^{-1.41r_1 - 2.61r_2} + 0.799^2 e^{-2.61r_1 - 2.61r_2}) \quad (3)$$

and

$$\Psi_{2^1S}(\vec{r}_1, \vec{r}_2) = \frac{0.6451}{\pi(1 + 0.06996^2)^{1/2}} (e^{-2r_1 - 1.136r_2} + e^{-1.136r_1 - 2r_2} - 0.2806r_1 e^{-0.464r_1 - 2r_2} - 0.2806r_2 e^{-2r_1 - 0.464r_2}). \quad (4)$$

Substituting Eqs. (3) and (4) into Eq. (1), we obtain the amplitude $F(\vec{q})$ in terms of the generating function $I(\lambda_1, \lambda_2; q)$,

$$F(\vec{q}) = 1.092ik_i \Bigg[\left(\frac{\partial^2 I}{\partial\lambda_1\partial\lambda_2}\right)_{\substack{\lambda_1=3.41 \\ \lambda_2=2.546}} + 0.799 \left(\frac{\partial^2 I}{\partial\lambda_1\partial\lambda_2}\right)_{\substack{\lambda_1=4.61 \\ \lambda_2=2.546}} + 0.799 \left(\frac{\partial^2 I}{\partial\lambda_1\partial\lambda_2}\right)_{\substack{\lambda_1=3.41 \\ \lambda_2=3.746}} + 0.6384 \left(\frac{\partial^2 I}{\partial\lambda_1\partial\lambda_2}\right)_{\substack{\lambda_1=4.61 \\ \lambda_2=3.746}}$$
$$+ 0.2806 \left(\frac{\partial^3 I}{\partial\lambda_1^2\partial\lambda_2}\right)_{\substack{\lambda_1=1.874 \\ \lambda_2=3.41}} + 0.2242 \left(\frac{\partial^3 I}{\partial\lambda_1^2\partial\lambda_2}\right)_{\substack{\lambda_1=3.074 \\ \lambda_2=3.41}} + 0.2242 \left(\frac{\partial^3 I}{\partial\lambda_1^2\partial\lambda_2}\right)_{\substack{\lambda_1=1.874 \\ \lambda_2=4.61}}$$
$$+ 0.1792 \left(\frac{\partial^3 I}{\partial\lambda_1^2\partial\lambda_2}\right)_{\substack{\lambda_1=3.074 \\ \lambda_2=4.61}} \Bigg], \quad (5)$$

PHYSICAL REVIEW A VOLUME 8, NUMBER 1 JULY 1973

Glauber e^- + He Elastic Scattering Amplitude: A Useful Integral Representation*

Brian K. Thomas
Department of Physics, University of Pittsburgh, Pittsburgh, Pennsylvania 15260
F. T. Chan
Department of Physics, University of Arkansas, Fayetteville, Arkansas 72701
(Received 15 March 1973)

New analytic methods for reducing the Glauber amplitude for charged particle–neutral atom collisions to a one-dimensional integral representation involving modified Lommel functions are proposed. To illustrate these new methods, the reduction of the Glauber amplitude for e^- + He elastic scattering, using a simple Hylleraas wave function for the He ground state, is described in detail, and the resulting integral for the amplitude is evaluated numerically. The Glauber-approximation-predicted elastic scattering amplitude previously calculated by Franco from a three-dimensional integral representation, with a more complex Hartree-Fock wave function for the ground state, is also recalculated using these new procedures; these results are in good agreement with those obtained by Franco. Thus, the utility and practicality of these new techniques are demonstrated. The application of these procedures to more general charged particle–neutral atom collisions is discussed.

I. INTRODUCTION

Recent applications of the Glauber approximation[1] (GA) to charged particle–neutral atom collisions have been restricted to atoms and model atoms having one or two bound electrons. The GA-predicted differential and total (integrated over scattering angle) cross sections for electron[2] and proton[3] collisions with atomic hydrogen, without rearrangement or ionization, have been calculated from one-dimensional integral representations of the amplitude; moreover, these amplitudes and integrated cross sections can be obtained in closed form.[4,5] Glauber calculations of elastic[6] and inelastic[7] scattering of electrons by ground-state helium atoms have been performed using three- and two-dimensional integral representations, respectively, for the amplitudes. However, electron–lithium atom collisions have been considered in the Glauber approximation only after making a frozen-core approximation,[8] thereby reducing the lithium atom to an effective one-electron system.

Although Franco[9] has proposed a method for obtaining a one-dimensional integral representation for the elastic and inelastic scattering of charged particles by arbitrary neutral atoms—excluding rearrangement (i.e., exchange or charge transfer) and ionization—there are no reported calculations actually using Franco's expressions. Moreover, Franco's final integral representation for these Glauber amplitudes appears to present several *seemingly* serious numerical problems, which generally include the calculation and integration of the differences between strongly (exponentially) divergent functions, as well as the numerical calculation of δ functions whenever elastic scattering is considered. We have, therefore, reexamined the GA-predicted amplitude for structureless charged-particle collisions with arbitrary neutral atoms. In this paper we propose certain new analytic procedures for evaluating the Glauber amplitude; these procedures again lead to a one-dimensional integral representation for the amplitude, which can be computed numerically with relative ease and without the sort of difficulties seemingly inherent in Franco's procedure. To illustrate these procedures we consider only the case of elastic scattering of electrons by helium atoms, using the simplest possible Hylleraas wave function for the ground state. We are able to establish a rather loose criterion for the easy and convenient use of Franco's procedures in this simple case, at least—provided the aforementioned δ function first is removed. The generalization of these procedures to inelastic collisions with He, or to collisions with more complex atoms is, aside from the application of our new analytic techniques, very much along the lines which Franco[9] suggests in general. We shall discuss in some detail how to apply our new analytic methods in the more general case.

The contents of this paper now can be summarized as follows. In Sec. II we describe the reduction of the e^- + He elastic Glauber amplitude to a one-dimensional integral involving a Bessel function of the first kind and functions $\mathfrak{L}_{\mu,\nu}$, which we shall call "modified Lommel functions." In Sec. III we present the results of our numerical calculation of the amplitude obtained in Sec. II. We also describe the rough limits within which we feel Franco's procedures may be conveniently used to evaluate this amplitude. Moreover, we have also recalculated, via our new procedures,